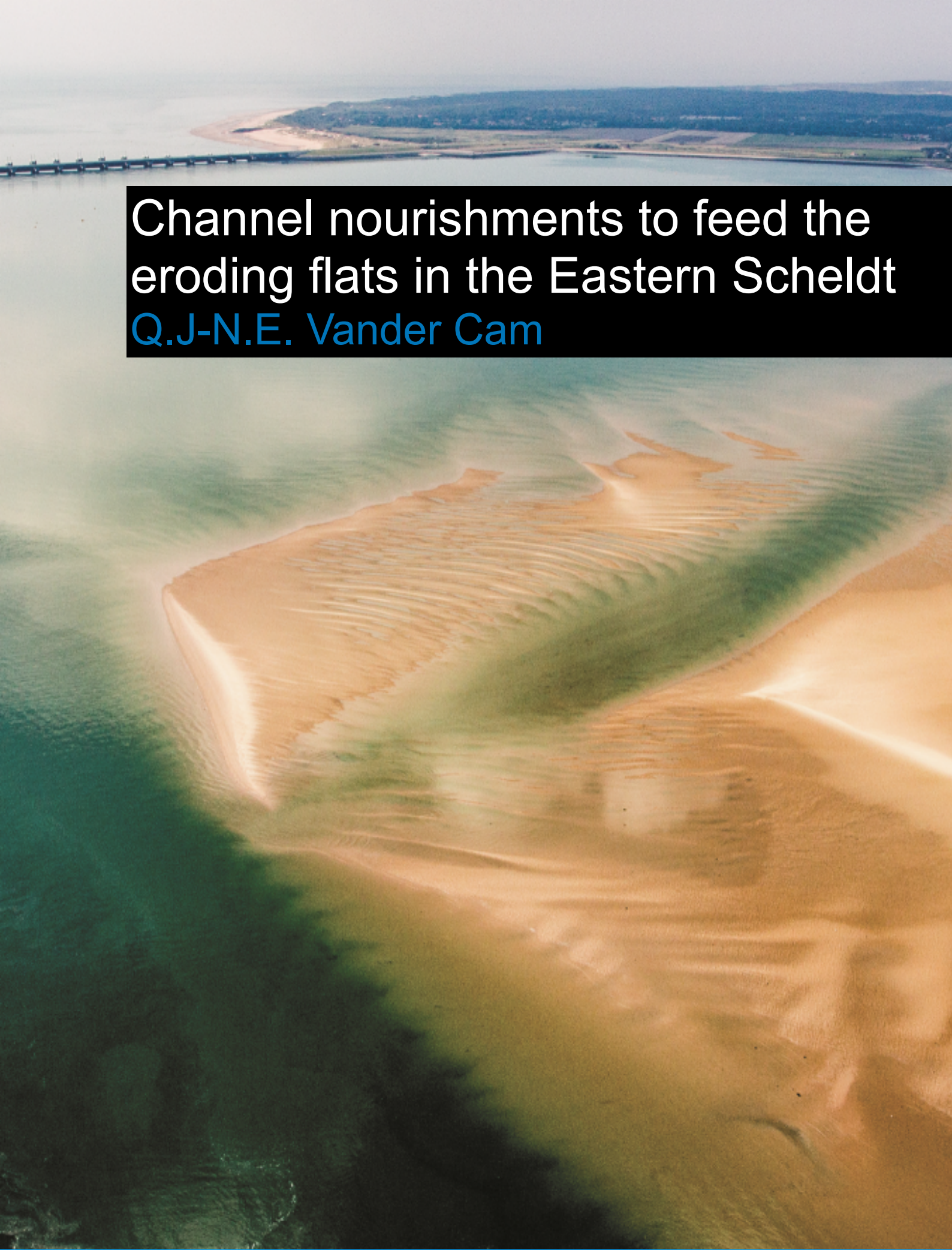

Channel nourishments to feed the eroding flats in the Eastern Scheldt

Q.J-N.E. Vander Cam

TU Delft

Channel nourishments to feed the eroding flats in the Eastern Scheldt

by

Quentin Vander Cam

to obtain the degree of Master of Science
at the Delft University of Technology,
to be presented publicly on the 16th of june 2021.

Student number: 4370562

Project duration:	June 1, 2020 – June 16, 2021	
Thesis committee:	Prof. dr. ir. Z.B Wang,	TU Delft and Deltares, chair
	Dr. T. Zitman,	TU Delft
	Dr. M.Z. Voorendt,	TU Delft
	Dr. D.C. Maan,	TU Delft, daily supervisor
	Dr. P.L.M. de Vet,	TU Delft and Deltares

An electronic version of this thesis is available at http://repository.tudelft.nl/.

TU Delft

Preface

This master thesis represents the final work in order to obtain my Master of Science degree in Hydraulic Engineering in which I specialised in Coastal Engineering at the Delft University of Technology. The research subject was issued by Rijkswaterstaat, the province of Zeeland, waterboard Scheldestromen and Delta Platfrom. These parties have come together to issue a series of graduate projects that have one factor in common, the sediment starvation in the Eastern Scheldt. During a meeting with all these parties where I got to present an introduction to my research, I understood the importance of my work and it inspired me to do the best I can. I greatly enjoyed working on this subject because of its current importance and its link with nature preservation.

I would like to take this opportunity to show my gratitude to some people, for their guidance and every-day support, which proved to be extremely welcome in this strange COVID-19 period.

Firstly, I would like to show my gratitude to my graduating committee: Zheng Bing Wang, Tjerk Zitman, Mark Voorrendt, Cynthia Maan and Lodewijk de Vet. Their guidance helped me during the whole process to stay critical and helped me to develop my scientific and reporting skills. I appreciate the discussions we had during the progress meetings and it gave me energy to see how passionate you all are about the subject.

Secondly, I want to specifically thank my daily supervisor Cynthia Maan with whom I have skyped almost every other week. Your experience with Delft 3D and knowledge of intertidal areas proved to be of great help during the whole process.

Last but not least I would like to thank my family, girlfriend and friends, who supported me in every way possible. Making you proud is what kept me motivated during the harder periods. I also thank my roommates for always cooking delicious meals when I had no time to cook and providing the well-needed distraction. Looking back at my period as a student in Delft will always put a smile on my face.

Quentin Vander Cam Delft, June 2021

Abstract

The tidal channels in the Eastern Scheldt basin, are out of equilibrium due to the reduced tidal prism as a consequence of the construction of the Storm Surge Barrier in 1986. An estimated 500 million cubic meters of sediment is required in order to reduce the cross-sectional areas of the tidal channels such that the system reaches a new equilibrium. This phenomenon is referred to as sediment starvation. The sediment starvation has been causing severe erosion of the intertidal areas which are the only available sources of sediment to feed the tidal channels because the storm surge barrier practically blocks sediment import into the estuary. The intertidal areas form the habitats for the benthic community, foraging ground for wader birds, and rest area for aquatic animals. In addition to their ecological value, the intertidal areas are valuable wave dampers and therefore important for flood protection of the hinterland. Their erosion thus harms the ecosystems as well as the flood safety of the hinterland.

Mitigation measures have been carried out in the form of directly nourishing the intertidal areas (Roggenplaat, Galgenplaat, and Oesterdam). These nourishments have had detrimental effects on the ecology that remained for a period of 5 years after the implementation. Nourishing the channels, hence reducing the cross-sectional area of the channels, can feed the intertidal areas gradually, thus preserving or increasing the ecological value of the intertidal area. Nourishing the channels can succeed according to the theory on channel-shoal interaction and the experience from the Western Scheldt; however, this has not been studied yet for the Eastern Scheldt.

In this study, the effects of a nourishment in a tidal channel have been evaluated for different nourishing methods, volumes and locations in the Eastern Scheldt Estuary. The objective of this research is to answer the following research question: Is a tidal channel nourishment in the Eastern Scheldt a feasible way of supplying the channel's surrounding intertidal areas?

To answer this question, we applied a 2DH numerical model (ScalOost) that runs in the Delft 3D software. For this research, the forcing consists out of tidal elevations as well as a wind climate. For reasons of simplicity and to limit larger computational time, wind waves are excluded from the model's forcing. The numerical model is capable of simulating the hydrodynamic effects and the morphodynamic evolution of a tidal channel nourishment. For four channels, the effect of nourishing on the velocity magnitude is studied for different ways of nourishing (elevating or narrowing the channel). The model results show that the considered nourishments cause a local increase of the velocity magnitude and an additional flow on the surrounding intertidal area during flood. According to the analyses of the computed hydrodynamics, the Krabbenkreek and the Brabantsche Vaarwater channels show the most potential considering the velocity magnitude increases and velocity direction changes. Therefore, these two cases were analysed separately in form of two case studies with an in-depth hydro- and morphodynamic analysis for various nourishment designs.

For the Krabbenkreek, a nourishment of 2 million cubic meters increases the maximal flow velocities in the order of 0.15 m/s, such that the critical velocity for sand transport (0.45 m/s) was exceeded over a larger part of the channel; to approximately 750 meters further landwards. The period in which the critical velocity is exceeded, increased by 15 to 60 minutes per tidal cycle. The results of the morphodynamic simulations indicate that 2.5% of the initial nourishment erodes over the first year, of which 80% settles above the MLW-line. Bearing in mind the model's limitations, it is concluded that a tidal channel nourishment in the Krabbenkreek feeds the intertidal area at a slow pace such that the ecology is not adversely affected.

The Brabantsche Vaarwater and its two main bends were used to study the effect of secondary flow on sediment transport and eventually on the behavior of a nourishment. Historic data, as well as theoretical analysis, indicate that in both bends, the centrifugal effect is dominant over the Coriolis effect for generating secondary flow. Model results confirmed this observation, yet the dominance of the centrifugal effect is larger in the second bend. As outer bends tend to erode and inner bends to accrete, the outer bends were nourished (750 & 920 $* 10^3$ cubic meters) in order to use the secondary flow to transport

sediment towards the inner bend and eventually onto the intertidal area. The simulation results show that for both bends, 3% of the initial nourishment erodes after the first year of which 80% accreted on both the inner and outer bend. The morphodynamic simulation results do not confirm the dominance of the centrifugal forces on sediment transport, as larger accretion rates than those simulated on the inner bends were expected. Although the results were not as expected, the nourishments did increase the velocities which increased the suspended sediment concentration in the channel and as simulation results show, sedimentation in sheltered areas.

A tidal channel nourishment in the Eastern Scheldt has been proven to be a potentially successful way of indirectly nourishing the channel's surrounding intertidal areas. However, the accretion rates were predicted in the order of 2% per year, whereas this would be 100% if directly nourished. Furthermore, the impact of a tidal channel nourishment on the sediment starvation in the whole basin is small considering the proposed volumes in this research only represent 0.4% of the actual sediment demand. Nourishing a tidal channel should be considered in view of maintaining ecological values.

Contents

1

Introduction

1.1. Motivation for this research

The Eastern Scheldt is a semi-closed tidal basin in the southwestern part of The Netherlands (Figure 1.1). After the severe flood in 1953, the Netherlands started with the Delta Works which consisted of protecting the coast against storms in the future by means of large dams. The Storm Surge Barrier in the Eastern Scheldt is one of these works and construction started in 1969 and was delivered in 1986. The barrier was the largest structure ever built in terms of its scale and dimensions, the barrier is regarded as a landmark worldwide in hydraulic engineering. In Figure 1.1, the other delta works are indicated. Initially, the barrier was supposed to be a fully closed dam like the other works but because of the potential loss of the ecological value of the estuary, a permeable barrier was constructed (van der Werf et al., 2015). The barrier is closed once a year for testing purposes and if the water level is expected to exceed +3 m NAP. The Eastern Scheldt has a high ecological value, especially the tidal flats. They are important for birds (such as waders) as foraging grounds and need to be 50-80% of the time dry so the birds can find food and rest (van der Werf et al., 2015).

Figure 1.1: Overview of the Delta Works with the Eastern Scheldt domain indicated in red

According to Van Zanten and Adriaanse (2008), the area of the intertidal area in the Eastern Scheldt

is diminishing by 50 ha per year which has a big impact on the ecology. This large erosion pattern is referred to as sediment starvation. It occurs when the cross-sectional area of a channel is too large with respect to the tidal range, leading to severe erosion of surrounding areas in order to reduce the cross-sectional area. Even though the barrier is permeable, the cross-sectional area of the inlet decreased significantly from 80.000 m^2 to 16.000 m^2 (Eelkema et al., 2013) which affected the tidal range greatly. Shortly after the construction of the storm surge barrier, two back-barrier dams were constructed (Philipsdam and Oesterdam) in order to limit the length of the basin and thus restricting the decrease of the tidal range (Eelkema et al., 2013). The effect of these hydraulic works on the tidal range measured in the central part of the basin can be observed in Figure 1.2. The rate at which the intertidal areas are decreasing seems to have slowed down but it is still a large concern regarding ecological values and flood protection of the hinterland (van Maldegem and van Pagee, 2005). The subject of this report is the study and mitigation of sediment starvation in the Eastern Scheldt.

1.2. Problem Analysis

1.2.1. Events leading up to sediment starvation

Before the start of the Delta Works, the Eastern Scheldt used to be an estuary connected to two other estuaries: The Haringvliet and The Grevelingen. These were closed off before the storm surge barrier was constructed creating two closed basins. These closures played an important role in the hydrodynamics and sediment transport inside the Eastern Scheldt (Eelkema, 2013). Long before any of the works, the Eastern Scheldt estuary was deepening itself and exporting sediment to the ebb-tidal delta (Kohsiek et al., 1987). This exporting character began after 1530 when Zuid-Beveland got flooded (area between Oosterschelde and Westerschelde on 1.1). The subsoil of Zuid-Beveland is mostly made out of a hard clay layer that does not erode easily. This lead the rest of the erodible basin to deepen itself and export sediment (Eelkema, 2013). Before the construction of the barrier, the ebb-tidal delta has been accumulating sediment, especially the deep delta (deeper than 10m) (Aarninkhof and van Kessel, 1999). The length scale of the Eastern Scheldt estuary is relatively long compared to the tidal wavelength. This leads to a phase difference between the cross-shore and alongshore tidal velocities at the inlet of the estuary. This phase difference is the cause for a delta with many bifurcated channels (Aarninkhof and van Kessel, 1999). The Coriolis effect has influenced the orientation of the channels, the flood channels are bent to the south and the ebb channels are bent to the north, this feature is still visible. Since the construction of the barrier, the trend seems to have changed from sedimentation to erosion and the morphological activity has decreased significantly (Aarninkhof and van Kessel, 1999). The now created basin has not reached the morphological equilibrium yet and needs sediment to reach this state (Kohsiek et al., 1987). This together with the location of the barrier (which traps the ebb-tidal delta) are reasons found in the literature for the erosion of the intertidal areas and low morphological activity.

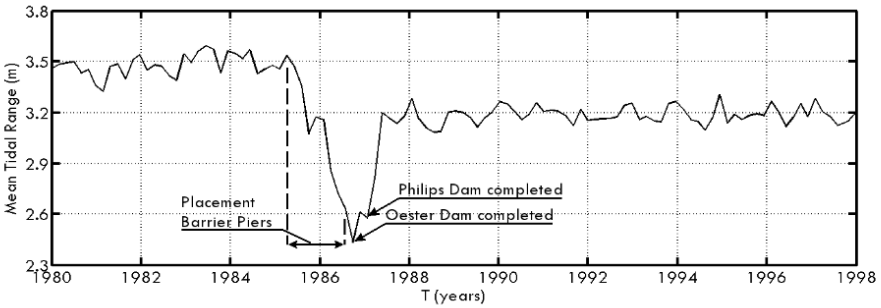

Figure 1.2: Tidal range in the centre of the basin (Eelkema et al., 2013)

1.2.2. Causes for the sediment starvation in the Eastern Scheldt

The sediment starvation leads to multiple issues, both ecological and flood safety-related. The sediment starvation is observable on the intertidal flats in the basin which are eroding at a quick pace. It is expected that in 2100 less than half of the original intertidal flats will remain (van der Werf et al., 2019). The intertidal flats have a large ecological value as they provide foraging ground for many wader species (birds)(van der Werf et al., 2019). Next to the ecological value, they act as wave breakers and reduce the energy attacking the shores attached to the basin.
During a literature study the following causes have been identified that lead to sediment starvation in the Eastern Scheldt:

- The construction of the Volkerak dam in 1969 caused sediment export with an estimated total volume of 40 million m^3 (Eelkema, 2013). This could have been prevented by constructing the storm surge barrier sooner after finishing the Volkerak dam.
- Both due to the position of the barrier and the reduced inlet area, the storm surge barrier blocks most of the sediment import into the basin (Ten Brinke, 1993).
- The construction of the storm surge barrier itself caused the width of the tidal inlet to decrease which led to a reduction of the tidal prism of 0.4 million m^3 leading to a prism of 0.9 million m^3. The average tidal range decreased from 3.7 m before construction to 3.25 m after construction and the velocity from 1.2 m/s to 0.8 m/s (Ten Brinke et al., 1994). The area which is exposed to waves and currents is smaller due to a smaller tidal range. This has as a consequence that the intertidal areas will suffer more than before closure (Brand et al., 2016).
- The cross-section area of the channels inside the basin is too large given the reduced tidal prism leading to a sediment demand of the channels (van der Werf et al., 2015).
- The sediment deficit in channels is compensated by strong eroding intertidal flats. This erosion combined with sea-level rise reduces the emergence time of the flats, the emerged area reduces by 60 ha per year (De Ronde et al., 2013).
- The tidal currents transport sediment from the channels towards the tidal flats (Eelkema, 2013). Because of a reduction of the tidal currents the sedimentation of the flats has consequently reduced. The erosion of the tidal flats is mainly driven by wind waves which have the same energy as before the construction. This leads to a serious net erosion of the tidal flats, especially during storms (with strong S-W winds).
- Tidal power is generated in the barrier. This hinders the tidal current and enhances sediment starvation inside the basin. (Guijt, 2018)
- The scour holes near the barrier could be the reason why the exchange of sediment between the ebb-tidal delta and the basin itself is so hard. The sediment flow towards the basin is trapped in the scour holes at flood and removed from the holes at ebb (Bosboom, 2019).

The main cause that leads to sediment starvation in the tidal basin is the new equilibrium state that the basin is working towards. The construction of the storm surge barrier caused the equilibrium situation of the basin to change. This is mostly due to the reduction of the tidal prism leading to a sediment deficit of +- 500 million m^3(Kohsiek et al., 1987).

1.2.3. Mitigation measures for sediment starvation found in the literature

To counter the sediment starvation, mitigation measures have been studied and some of them have been carried out in the form of pilot nourishments. Three nourishments have been carried out:

- The Galgenplaat nourishment was completed in 2008 and consisted out of a circular shape with a radius of approximately 225 m and 1 m high resulting in 130.000 m^3 of sand. The idea behind the circular nourishment is that natural processes such as wind and waves spread the nourishment. In addition, the ecosystem is only disturbed on the nourished area (Ecoshape, 2012) compared to a more classical nourishment. After 3 years of monitoring, the results showed that the nourishment did not spread as expected. It is argued that this is due to the location of the nourishment

(relatively high), the relatively large grain size, as well as the ”bounding’ wall around the nourishment, hindering sediment transport (Ecoshape, 2012). Applying the nourishment killed all the benthic life present on the nourishment area which took 2-3 years to recolonize (Ecoshape, 2012).

- The Oesterdam hook-shaped nourishment was completed in 2013 and consisted out of 350.000 m^3 of sand in combination with 4 artificial oyster reefs to dissipate energy and preserve the nourishment (Boersema et al., 2018). This was done in order to protect the Oesterdam from the wave impact and postpone reinforcement works of the Oesterdam by 25 years. Furthermore, the goal was to feed the already present but eroding intertidal area with the sediment from the nourishment. The nourishment did feed the intertidal area but only to a limited extent such that the erosion on the intertidal area stopped. In three years’ time, approximately 10% of the nourished volume disappeared into the larger system (Boersema et al., 2018). This type of nourishment had a large positive impact on the ecology creating a sheltered area that serves as foraging grounds for various bird species.

- The Roggenplaat nourishment is the largest nourishment so far in the Eastern Scheldt which consisted out of 1.300.000 m^3 of sand and was completed in 2019. The goal of this large nourishment is mainly to preserve the ecological value of this intertidal area in the reference year 2010 for the following 25 years as well as to reduce the wave attack on the dike of Schouwen (Ysebaert, 2016). The design of the nourishment is location-specific and consists out of 7 well-determined zones. These zones have been determined by a thorough hydrodynamical study as well as a morphodynamical study. Furthermore, the lessons learned from previous pilot nourishments have been processed into this design.

Next to the carried-out mitigation measures, Rijkswaterstaat has studied multiple measures in 2008 that intuitively reduce the sediment starvation issues. The measures either lead to an increase in the water volume flowing through the channels or increase the amount of sand in the channels.
The first measure is to optimize the flow pattern by reducing the resistance to the inflowing volume. This can be done in three ways:

- Smoothen the pillars will increase the flow capacity by 5% (van Zanten and Adriaanse, 2008).

- Change the slope of the sill on both sides of the barrier will increase the flow capacity by 15 to 30% (van Zanten and Adriaanse, 2008).

- Implementing a new opening in the Mattenhaven will lead to an increase of 20% in flow capacity (van Zanten and Adriaanse, 2008).

The result of the combination of these measures is an increase of maximal 800ha of the intertidal area. Because these measures do not stop the sediment starvation it is only a temporary measure and is not preferred.
Another possible measure one could think of is the closure of one of the three main channels. By doing this the velocity could increase in the remaining open channels. The effect has been studied in a hydrodynamic model by Lievense(2006), the positive effect has only been observed near the barrier (Roggenplaat and Neeltje Jans). In the rest of the basin, negative effects have been observed (van Zanten and Adriaanse, 2008).

If an opening could be created in the Philipsdam the area of the water body increases by 8300 ha (Jörissen, 2003). Modeling has been done with an opening of 600 m^3, because of the geometry and characteristics of the basin a phase difference of 2.5hours was observed (see Figure 1.3)(van Zanten and Adriaanse, 2008). Because of this phase difference, the two tides counteract each other leading to no or even a negative effect on the sediment starvation of the Eastern Scheldt.

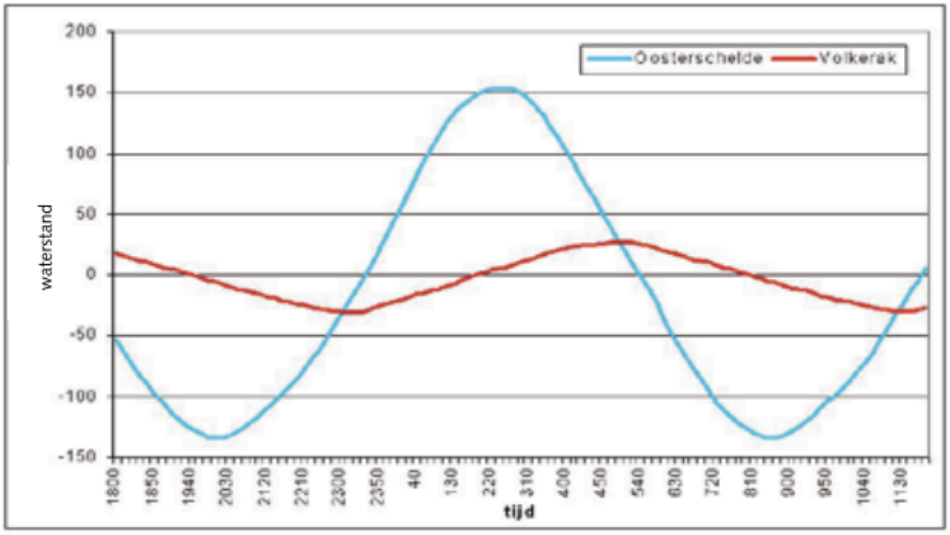

Figure 1.3: Tidal range difference (van Zanten and Adriaanse, 2008)

The last possible measure discussed in the report is to complete an old plan. This plan consisted of linking the Eastern Scheldt with the western Scheldt by means of a canal, the ”Overschelde”. This would initially lead to a decrease of the low water line between 5 and 8 cm (Svasek Hydraulics, 2004) and a small increase in the tidal prism. Because this measure is not contributing to solving the sediment starvation issue but only postponing the outcome it is not considered an effective measure.

1.2.4. Problem Statement

The intertidal area in The Eastern Scheldt basin is suffering severe erosion. This is because the tidal prism and the cross-sectional area of the tidal channels are out of equilibrium. To bring the system into a new equilibrium, an estimated volume of sand of 500 million m^3 is required. A significant amount of research has been carried out on possible measures to remedy the sediment starvation in The Eastern Scheldt. Some measures have been carried out in the form of pilot nourishments, while others have not been carried out and require more research. Due to the complexity of The Eastern Scheldt system, mitigation measures against sediment starvation are location-specific. Nourishing the channels can work according to the theory on channel-shoal interaction and the experience from the Western Scheldt but this has not been studied yet for the Eastern Scheldt.

1.3. Research objective

In the literature three options to solve the problem present themselves as being the following:

1. Supply the tidal flats in a regular manner. This is a short-term solution and has been researched and applied already and proven to be successful. The largest nourishment so far is the one on the Roggenplaat (a tidal flat in the basin) of 1.3 million m^3. With this nourishment, the tidal flat will fulfill the needs of the different species until 2035 (van der Werf et al., 2019).

2. Apply the principle of ”Building with nature” which consists out of letting nature do the work. Something similar to the Zandmotor in Kijkduin, The Netherlands, could be applied in the basin. One or more huge nourishments could be applied in specific locations where the tidal currents, wind-induced waves, and wind can be used to redistribute the sediment and reach the new equilibrium situation in a sustainable way.

3. The last option is to increase the tidal velocities inside the basin (Eelkema, 2013).

For this research, a combination of solution 2 and 3 is chosen to lead to the following research objective:

The objective of this master thesis is to study the effectiveness of tidal channel nourishments in The Eastern Scheldt and thus to increase the tidal velocities.

By nourishing one or more tidal channels, the sediment starvation can locally be satisfied. By doing this, the channels would not need sediment from the tidal flats anymore. On the contrary, they will supply the tidal flats with sediment. This is only possible if the tidal current in the channels is strong enough. Through the cross-channel circulation, the sediment is deposited on the tidal flats.

The result of this thesis can lead to a suggestion of a new way of applying nourishments in the Eastern Scheldt basin, with a view on the long term and preservation of nature. In a more direct way, if the research turns out to be positive, this research could lead to a pilot nourishment as a final validation step and compare the modeling work done in this thesis to observed field data.

1.4. Research scope

To make this study as interesting and relevant as possible a scope needs to be defined to be able to dive into the specific subjects of interest.

- Although the wave climate and its forces will be analyzed, in view of time, waves will not be incorporated in the model until the very last calculations or not at all.
- In the morphodynamic part of this study the only sediment type that will be taken into account is sand.
- Sea level rise is not taken into account in this study in view of time. It might sometimes be mentioned but will not be taken into account in calculations
- The costs of a nourishment are not part of this study. When evaluating possibilities with the same outcome, the costs will play a role but will not be a leading factor.

1.5. Research question

From the findings in the literature study and the available tools I dispose of, the objective of this research has been determined. This objective has been determined by taking into account the available time and knowledge I dispose of to fulfill this thesis. In this section, the research question is given together with sub-questions. These sub-questions are meant as an aid to answer the main question in a step-wise manner.

"Is a tidal channel nourishment in the Eastern Scheldt, a feasible way of supplying the channel's surrounding intertidal areas?"

Sub questions

1. What are the current problems for the intertidal areas in the Eastern Scheldt and why is a human interference necessary?
2. How does a tidal channel nourishment affect the sediment transport between the channel and the surrounding intertidal flat?
3. What are the benefits and downsides of nourishing a tidal channel?
4. What are the effects of nourishing two specific tidal channels: The Krabbenkreek and the Brabantsche Vaarwater on the hydrodynamics and morphodynamics?
5. Can general conclusions be drawn from the two case studies?

1.6. Main research approach and reading guide

The study of a nourishment in a tidal channel is a complex process and needs to be approached in a systematic way. Throughout this study different steps are taken in order to answer the sub-questions above, these steps are listed below. Some of these steps are part of the general Building with Nature principle presented by de Vriend et al.

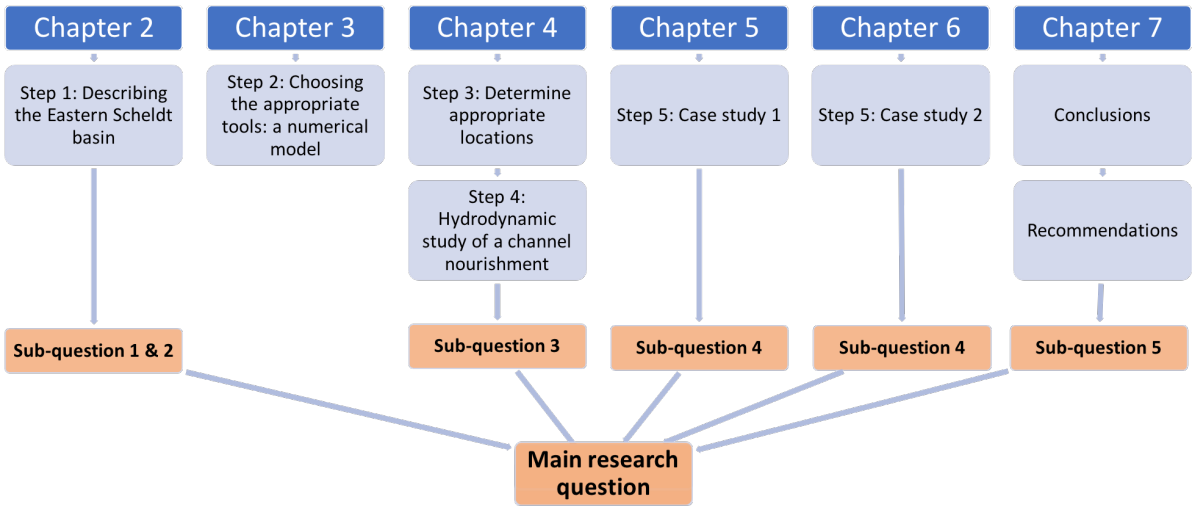

Figure 1.4: Reading guide

1. **Describing the Eastern Scheldt system**. In every design process, this is the first step and most crucial one, it creates the foundation of the research (de Vriend et al., 2014). In this step it is important to consider different sources of information such as historic data and academic research. This step is thus partly literature review and partly the researchers own thinking and analysing process. This step is elaborated in Chapter 2 and will answer sub-question one.

2. **Choosing the appropriate tools: a model**. Theoretical analysis (hand calculations) is an appropriate way to get familiar with the effects of large-scale changes in simplified systems. To be able to answer the research question correctly numeric calculations are necessary. This is due to the complexity of the Eastern Scheldt and because this study aims to analyze cases that resemble the reality as much as possible. Considering this study focuses on the physical processes in the basin and not on the modelling side, an existing model will be chosen to conduct this study. This step is elaborated in Chapter 3 and is necessary to answer the following sub-questions.

3. **Determine appropriate locations**. With the knowledge gained in step 1, potential locations can be identified. This choice will be based on geographical parameters such as location and geometry and disturbance of activities. The morphological history of the basin will also play a role in this decision. This is not a linear process but rather iterative until 4 potential locations are found. This step is elaborated in the first section of Chapter 4. The second research question is answered in this chapter.

4. **Channel analysis : Hydrodynamics**.No waves will be included in the model's forcing. As seen in the theory and literature, waves most likely enhance erosion and thus have a negative effect on the accretion on the intertidal area as a consequence of a channel nourishment. Only if the results turn out to be positive, the waves will be implemented in the research if time allows it. The research will be executed by running the model for different channel bathymetries by changing the bathymetry locally. The aim of this chapter, is to increase the local velocity magnitude as well as the direction in order to enhance transport from channel towards shoal. This increase in velocity magnitude can lead to an increase in sediment transport similar to pre-construction of the barrier (Figure 1.5). From these graphs can be seen that the flood period has decreased while the ebb period has increased. This step will be an iterative process and not all the results will be included in the report. This step is elaborated on in the second section of Chapter 4.

5. **Case study and final design: Morphodynamics**. In the final step, two cases from the previous step will be analyzed extensively. Firstly, the hydrodynamic processes will be analyzed. Secondly, the impact of a nourishment on sediment transport will be analyzed. The goal of this last step is

to propose a nourishment in a channel and specify all the characteristics necessary to make it successful. Here the research question will finally be answered. This last step is elaborated on for the two case studies in Chapter 5 and Chapter 6 respectively.

Data gathering and analysis The necessary data will be provided by Rijkswaterstaat while the necessary models will be provided by Deltares and the TU Delft. The necessary data to successfully complete this research is listed below.

- Bathymetry of the Eastern Scheldt and more specifically of the area of interest.
- Historic Lidar data of the basin, the longest period possible
- Current and elevations in the channels
- Grain size distribution and percentage of suspended sediment
- Density of the soil and density of the water.

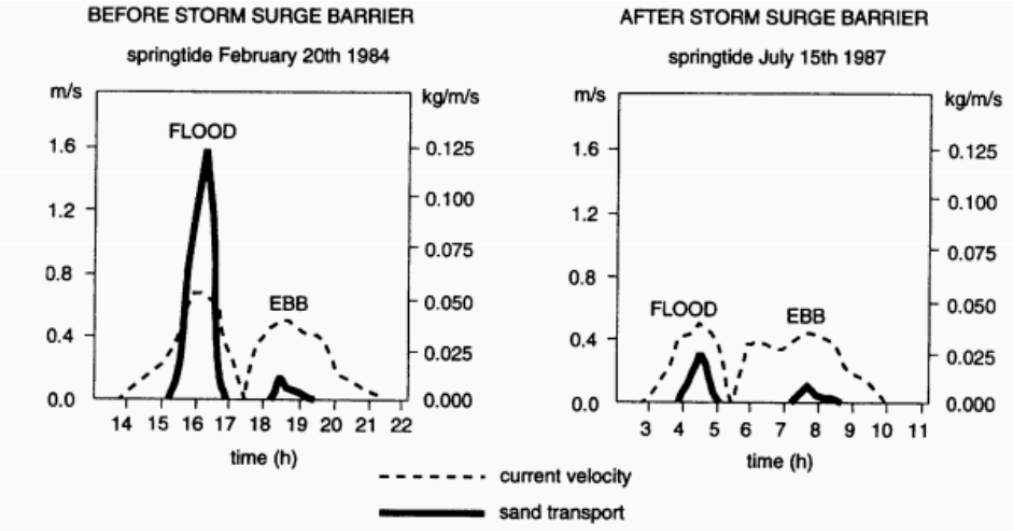

Figure 1.5: Sediment transport as a result of tidal velocities before and after construction of the Storm Surge Barrier (Quyen, 2010)

2

Description of the Eastern Scheldt tidal basin

Throughout the thesis, references are made about the ecology and theory such as the tide and waves. This chapter has as purpose to give the reader the necessary background information to enjoy and understand the thesis to its full extent. This chapter works out the first step of the methodology introduced in Section 1.6.

2.1. The Eastern Scheldt as a tidal basin - The sediment budget

The Eastern Scheldt is a semi-closed tidal basin located in the southwestern part of the Netherlands. The Eastern Scheldt tidal basin is made out of multiple elements: an inlet, channels, intertidal areas called tidal flats and an ebb-tidal delta. In Figure 2.1a , a typical tidal basin is schematized to illustrate the different elements. The inlet of the basin is in this case the barrier, made of hard structures removing any possible dynamics in the shape or location of the inlet. Basins can be classified from wave to tide-dominated. David and Hayes (1984), identified 5 classes which are various combinations of the mean wave height with the mean tidal range (Bosboom and Stive, 2015). With a mean tidal range of 3.2m and a mean wave height of 0.4m in the vicinity of the mouth of the basin (Quyen, 2010), this classifies the Eastern Scheldt basin as a tide-dominated basin. A tidal basin can either be flood dominant or ebb dominant depending on the asymmetries of the tide. A tidal basin is always working towards a morphological equilibrium between the ebb-delta and the tidal prism (Bosboom and Stive, 2015). The tidal prism is the volume of water flowing through the inlet per tidal cycle, 0.9 million m^3 in this case. This volume is characterised by the geometry and the tidal range of the basin (Eelkema, 2013). Multiple equilibrium relations have been derived which are all empirical. These formulas are particularly useful in early stage computations considering it is fairly easy to check the effect of changes in the elements of the basin. A list of the empirical relations is given below.

- With an open inlet there is a constant sediment exchange between the ebb-delta and the basin (intertidal area and channels). The following relation has been derived between the tidal prism and the volume of the ebb-delta:

$$V_{od} = C_{od} * P^{1.23} \tag{2.1}$$

  where V_{od} is the volume of sand, C_{od} is an empirical coefficient [$m^{-0.69}$] and P is the tidal prism (Bosboom and Stive, 2015).

- The cross-section of the entrance channel is a variable in most tidal basins and its character is usually quite dynamic, its equilibrium state can be expressed as follows:

$$A_{eq} = C * P^{q} \tag{2.2}$$

where A_{eq} is the volume of sand, P is the tidal prism and q and C are empirical coefficients [-, m^{2-3q}] (Bosboom and Stive, 2015).

- The most applicable relation in the case of the Eastern Scheldt is the equilibrium relation between the tidal channel and the tidal flats. The following relation is only valid if the intertidal area spans the entire basin which is the case for the Eastern Scheldt.

$$V_c = C_V * P^{3/2} \tag{2.3}$$

where V_c is the equilibrium total channel volume below MSL, P is the tidal prism and C_V is an empirical coefficient [$m^{-3/2}$] (Bosboom and Stive, 2015). In the literature, a range for the empirical coefficient is found to be: $73 - 80 * 10^{-6}$ (De Vriend et al., 2002). The actual tidal prism is known to be approximately 0.9 million m^3 which corresponds to an equilibrium channel volume of 2000 million m^3. To know how much sand is needed to bring it in equilibrium, the actual volume of the channels is required. Computing the equilibrium channel volume, with the tidal prism before the closure of the basin, the equilibrium channel volume is 3400 million m^3. With the knowledge that the basin was still an estuary that has been made into a semi-closed tidal basin by the closing of some channels, this value is highly overestimated. Furthermore, before the construction of the barrier, the channels were eroding and hence not yet near the volume of 3400 million m^3. The actual channel volume is estimated to be around 2700 million m^3 which leads to the conclusion that the channels need to fill up 700 million m^3 of sand according to the empirical relation. In Figure 2.1b, the three situations are given as dots on the empirical relation (blue line). As the blue arrow illustrates the sediment starvation in the basin, the channel volume needs to decrease a significant amount in order to reach the equilibrium. Koshiek et al derived, also empirically that the sediment starvation in the Eastern Scheldt amounts to roughly 500 million m^3 which is slightly less than what has been computed here. This empirical relation probably overestimates the sediment demand since Koshiek et al are often cited without questions. Nevertheless, this empirical relation shows that it reproduces large changes well and should only be used as a tool when analysing the effect of large scale changes.

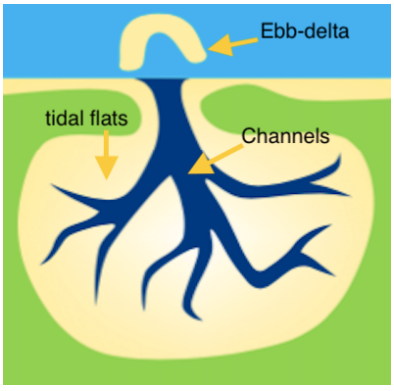

(a) Illustration of a typical tidal basin and its components (Bosboom and Stive, 2015)

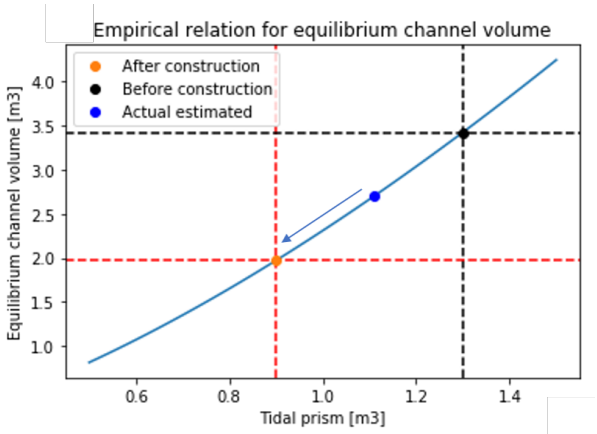

(b) The empirical relation between the equilibrium channel volume and tidal prism for the Eastern Scheldt. Volumes on the y axis are in $10^{12} m^3$ and volumes on the x-axis in $10^9 m^3$

Figure 2.1: On the left a schematic overview of a tidal basin and on the right the empirical relation between the channel volume and tidal prism

2.2. Geographical characteristics

The Eastern Scheldt has quite an interesting history that led the basin to look as it looks now, see Chapter 1. Here the basic characteristics of the basin are given which will be referred to in the remaining of the research.

- **intertidal area** The basin counts multiple intertidal areas which are depicted in Figure 2.2a. In this research, an intertidal area is considered to have elevations between the mean low water (MLW): -1.35 m NAP and the mean high water (MHW): +1.61 m NAP, see Appendix A.1. These areas differ in characteristics such as the sediment type, exposure to wave attack and if they are attached to the land or not. In Table A.2 (Appendix A.2), an overview of the intertidal areas with their characteristics is given. Some of the biggest intertidal areas are the Roggenplaat, Neeltje Jans and the Vondelingsplaat also called de Galgenplaat.

- **Salinity** Since the closure of the Volkerak dam, the fresh water supply was cut off. This measure had consequences for the salinity gradient in the basin which increased since then and is now more or less equal to the concentration at sea. The salinity is hovering around 1800 mg/l (Rijkswaterstaat, 2020).

- **Soil type** Because of the size and geometry of the basin, the hydrodynamic forcing differs significantly across the basin, leading to a diverse range of channels and flats. Some locations are fully exposed whereas others are sheltered, this leads to a diverse sediment distribution in the basin. The following sediment types can be found: coarse sand, fine sand, peat, clay and silt. The top layer is mostly coarse/fine sand (Dinoloket, 2020). For this study, only one type of sediment will be acknowledged: fine sand. The bottom of the basin mainly consists of fine sand ranging between 150 and 200 μm (Huisman and Luijendijk, 2009). During this study, the diameter might vary depending on the goal of the computation. It can also be a means of calibrating the model.

- **bathymetry** The latest available bathymetric data is from measurements in 2019 which is mostly LiDAR data and can be examined in Figure 2.2b. The basin has been less morphologically active in the last decade compared to the period after the construction of the barrier (Brand et al., 2016)

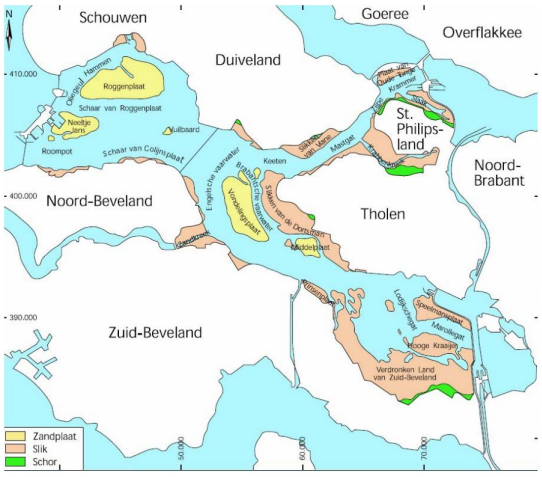

(a) Intertidal areas in the Eastern Scheldt basin (Van Maldegem, 2004)

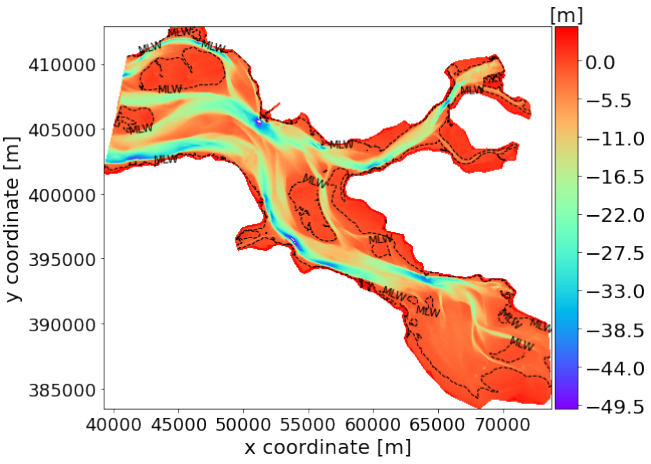

(b) Bathymetry data (LiDAR) of the Eastern Scheldt basin in 2019

Figure 2.2: On the right an overview of all the intertidal areas in the Eastern Scheldt basin can be found while on the right the bathymetry of the basin in the year 2019 is depicted

2.3. The ecology in the Eastern Scheldt

The Eastern Scheldt has a high ecological value that is put at risk as a result of the construction of the SSB. In this section, the kind of species that can be expected to be found in the basin as well as how they are affected by the barrier are inventoried. The ecology can be split up into three parts: the Benthos community, the wader birds, and the aquatic animals.

The Benthos community in the Eastern Scheldt mostly lives on the intertidal flats. The community exists out of different types of water snails such as mollusks and worms. They have experienced the construction of the barrier in a positive way, the biodiversity has increased as well as an increase in species

richness (Brand et al., 2016). This is due to a decrease in turbidity and suspended sediment. This positive effect is not expected to last long, if the intertidal flats continue to erode and become permanently submerged, the Bethos community will suffer significantly. Applying nourishments on the intertidal flats directly affects the Benthos community greatly. Following a pilot nourishment on the Galgenplaat, an intertidal flat in the basin, the species richness decreased significantly, see Figure 2.3(van der Werf et al., 2015). Next to the species richness, the density as well as the biomass decreased as a result of the nourishment. It took 3 years for the species to stabilize on the whole of the flat. However, it can be seen that the richness has decreased and has lost around 15 species.

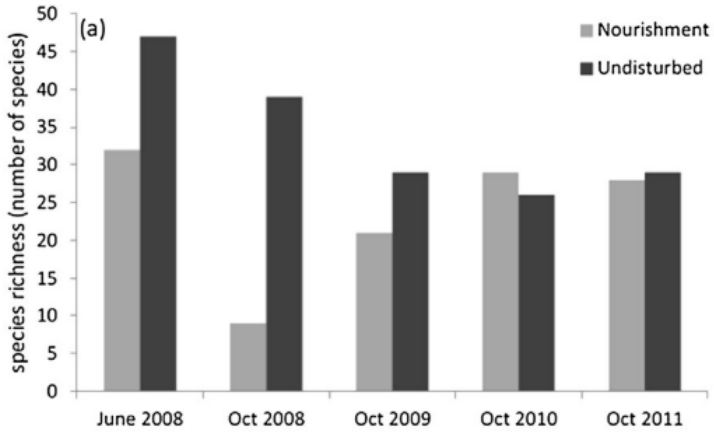

Figure 2.3: Benthos species richness, June 2008 is situation pre nourishment (van der Werf et al., 2015)

The threat the wader birds are under has received the most attention since the SSB was constructed. This is because they have a protected status while other species such as seals and fish do not have the protected status (Brand et al., 2016). The birds that use the intertidal flats vary from migratory birds in autumn and spring to wader birds such as the Oystercatcher. For migratory birds these intertidal flats are of vital importance, they use these flats as foraging grounds to fatten up before their migration (Schelling et al., 2014). The counting of the birds has started in 1987 and since then some breeding bird species showed a decline in numbers. On the other hand, the non-breeding birds did not seem to be affected initially, the biodiversity indices even slightly increased. Overall the breeding, as well as the non-breeding birds, showed an increase in numbers as well as species richness (Brand et al., 2016). As a result, no direct effect of the barrier can be measured on the abundance of numbers and species. The latter can be explained by all the hard work executed to create new breeding spaces since 1999 (Brand et al., 2016). Although the effect cannot be measured, the threat these birds face is real since the foraging grounds are disappearing slowly under the MLW-line.

The aquatic animals in the Eastern Scheldt can be split up into two classes: fish and seals.
The fish population that lives in the channels will not experience any change in their habitat only that it might become less deep. The fish that use the shallow areas on the intertidal flats will find these areas increase in depth. Different kinds of flatfish (such as plaice and turbot) and sea bass use these shallow areas to grow up (van Zanten and Adriaanse, 2008). These areas are particularly suitable for these young fish because of the relatively warm water which is favorable for their growth. These areas will eventually disappear if the intertidal areas are all under the MLW-line, thus putting these fish at risk. Because of the high fluctuations in the fish populations throughout the years and the only small contribution of Eastern Scheldt fish to the North Sea fish population, the effect of the SSB will barely be noticeable (van Zanten and Adriaanse, 2008).
In 2016/2017 there were 161 seals present in The Eastern Scheldt basin, accounting for 20% of the total dutch seal population (Arts et al., 2018). The seals are mostly found on the Roggenplaat but do not depend on the intertidal areas for food. The seals can migrate to other locations where nursing and resting is still possible (Brand et al., 2016). The amount of seals has been growing tremendously in the past 20 years (Figure 2.4). Therefore it is not expected that the seals have or will experience the sediment starvation in the Eastern Scheldt as negative.

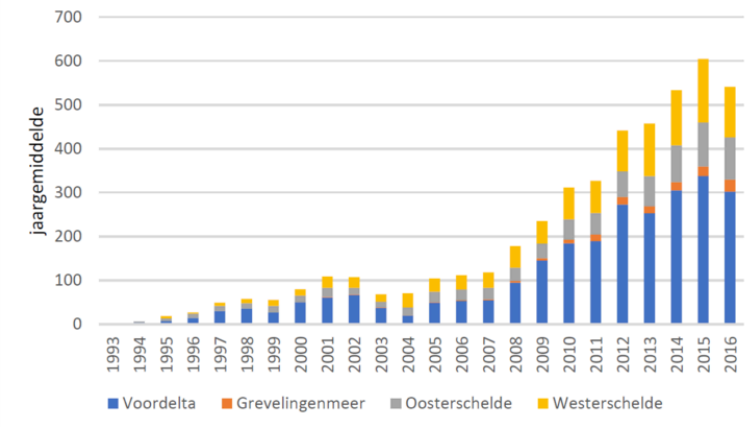

Figure 2.4: The seal population in The Netherlands (Arts et al., 2018)

2.4. Stakeholders

Next to the general physical characteristics, it is important to understand which parties have an interest in the system. Two large stakeholders can be identified: the shipping industry and the aquaculture industry. There are much more stakeholders than the ones that are handled in this section but these are the ones that might have the most influence regarding a nourishment. Other stakeholders are for example divers and water sports recreationists.

The Eastern Scheldt is not known for its importance as a shipping route but each year 45.000 ships sail across it, carrying around 25 million tons worth of goods (NatuurparkOosterschelde). The shipping routes are depicted in Figure 2.5a by the black dotted lines. Note that the weight of the lines differ which is an indicator of how busy the shipping route is, the thicker, the busier. The maximum draft of the ships allowed in the Eastern Scheldt is about 5 m (Binnenvaartkennis.nl). This information is really important in the scope of this study. This means that if a channel nourishment were to take place on one of these routes, the minimal depth that has to be guaranteed is -5 m NAP. The other aspect to take into account is how the nourishment will evolve over time. More specifically, the nourishment can not have as a result that some places in the channel will accumulate sediment and raises the bottom and become shallower than -5 m NAP.

Aquaculture is the artificial way of cultivating/breeding fish, shellfish and algae. This sector is becoming a more important sector regarding food provisioning and will probably within 10 years be at least as important as the traditional fishing methods (Deltares, 2014). The two main shellfish that are cultured here are the Pacific oysters and the blue mussels and cover an area of 1550 and 2250 ha respectively (Brand et al., 2016). As can be observed in Figure 2.5b, the aquaculture is well spread along the basin with a higher density in the southeast corner. The names on the map are in dutch but the four main colors that can be observed on the map stand for:

- grey stands for mussels
- light brown stands for oysters
- yellow stands for hanging mussel culture
- light blue stands for locations where oysters are transported to for their last growth phase

There is quite a clear distribution of oysters, mostly towards the basin ends and mussels more at the entry/middle section of the basin. In the past, there have been nourishments in the Eastern Scheldt which were all directly placed onto the intertidal area. During the design phase of these nourishments, a 'safe' distance with the aquaculture was guaranteed. The reason for this is that accumulation of sediment can be devastating for the production of shellfish. By nourishing the channel, the objective is to enhance transport from the channel towards the intertidal area. In the first place, this sediment will settle between the MLW and MHW-line. Since most of these cultures are also located between the MLW and MHW-line, it is beneficial to ultimately design a nourishment that is not likely to interfere with any type of aquaculture.

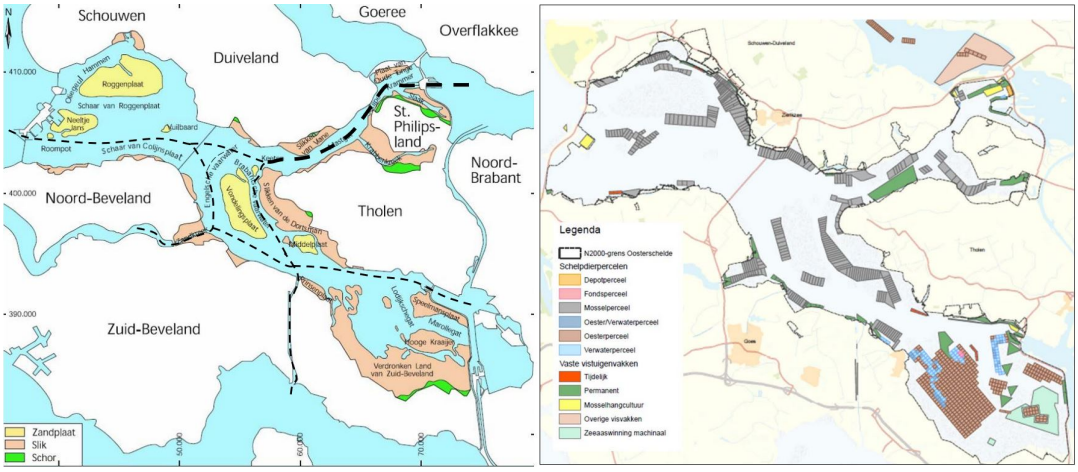

(a) Overview of the shipping routes inside the Eastern Scheldt basin (Van Maldegem, 2004)

(b) Overview of the aqua culture in the basin (Henkens et al., 2012)

Figure 2.5: Overview of the spatial distribution of the shipping routes and the aqua culture

2.5. Morphological history since completion Storm Surge Barrier

In the Introduction, a brief summary of the history of the Eastern Scheldt basin was given, from when it was an estuary up until now. To illustrate how the basin has been transforming under the influence of the barrier, the bathymetry has been measured. One data set 1983-2001 is based on LiDAR (Light Detection And Raging) has been processed and visualised by A.J.M. Geurts van Kessel, see Figure 2.6a. The other LiDAR data set is from 2007-2019 and has been analysed and visualised by me, see Figure 2.6b. The particularity of both figures is that only the bed changes on the intertidal areas are plotted, areas between MLW en MHW-line. Because these figures illustrate data that has been acquired by LiDAR at different moments in time, these figures should be used to recognize and analyse trends rather than details.

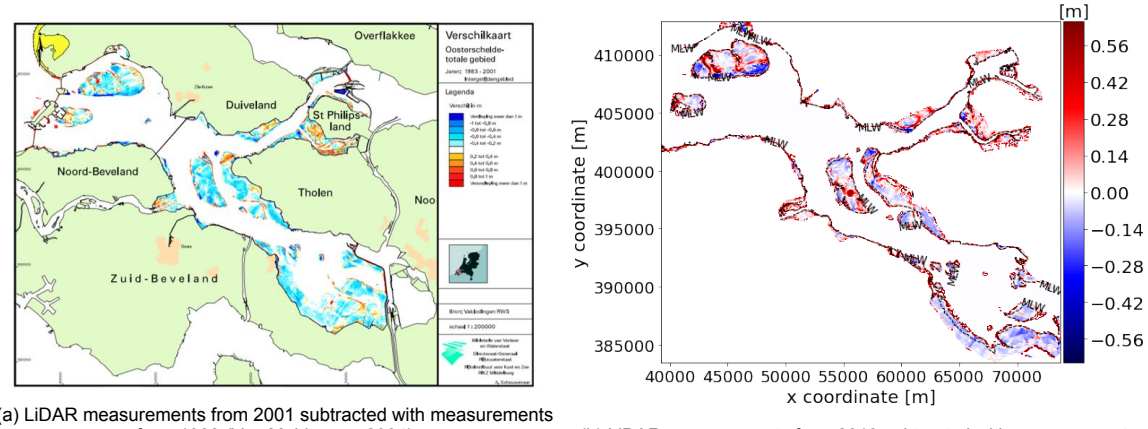

(a) LiDAR measurements from 2001 subtracted with measurements from 1983 (Van Maldegem, 2004)

(b) LiDAR measurements from 2019 subtracted with measurements from 2007

Figure 2.6: Visualisation of historic data from 1983 to 2001 and 2007 to 2019.

In both figures, the erosive trend on the intertidal areas is visible, indicated in blue, which is a typical characteristic for sediment starvation. Yet, in Figure 2.6a, the Krabbenkreek located in the upper east corner does not seem to follow the erosive trend. However, A.J.M. Geurts van Kessel argued that this accumulation of sediment is most likely due to measurement errors. When comparing this data to the more recent data, the same area still seems to accumulate more sediment than the other intertidal areas which confirms the trend observed with the older data. There are a lot of similarities between both figures with some exceptions. In Figure 2.6b, some nourishments are visible such as the circular one on the Galgenplaat which has been completed in 2008 and the hook-like nourishment which has

been completed in 2013 at the Oesterdam. In 2019, the Roggenplaat has been nourished which is not visible on the data, probably due to the measurements being taken before the implementation of the nourishment. Another difference that can be observed, is that the surface area of the Hoogekraaier has decreased significantly which is caused by the area reducing in height and becoming lower than MLW-line. In the first 15 years after the construction of the barrier, changes in the intertidal areas of approximately 1 m have been observed. This trend of 1 m change seems to have slowed down to 0.6m in the last 12 years which leads to believe that the basin is becoming less morphologically active as N.Brand et al (2016) concluded. Again, these numbers are only a guideline but changes larger than 0.1-0.2m can be assumed to be independent of measuring errors.

The hypothesis that the basin is becoming less morphologically active is confirmed by measurements displayed on Figure 2.7b. Here, the evolution of four different intertidal areas is depicted through time, from 1968 to 2013, based on height, area and volume. This data should be looked at critically since only 8 measurements are available with an interval of 5.5 years. Before the construction of the barrier, the intertidal areas were notably increasing in all three parameters. What can be observed is that after the construction of the barrier, the largest changes occurred and since 2005-2010 these changes have slowed down significantly. Neeltje Jans has experienced the least changes regarding height, area and volume whereas Hoogekraaier has experienced the most loss in area and volume as could also be observed from Figure 2.6a & 2.6b. These three parameters do not provide direct insight into the evolution of the hypsometry of the flats (de Vet, 2019). This is because this data is only based on two measurement points for each flat (de Vet, 2019). To better understand the evolution of the tidal flats and small-scale patterns more transects should be analysed, see the study performed by de Vet, P.L.M. (2019).

In Figure 2.7a, the bed level changes of the whole basin have been plotted. Because of the larger scale, the differences in the intertidal areas are almost no longer visible. The latter one illustrates that there is a large difference between bed level changes on the intertidal area and changes in the channels, these are approximately three times larger. The intertidal areas are indicated by means of a dotted line which represents the MLW-line. The changes in the channels are on the other hand visible and typical for sediment starvation. The channels are mostly colored red which means that sediment is accumulating. As we can see in Figure 2.6b, the intertidal areas mostly erode, this sediment then settles down in the deep channels as can be seen in Figure 2.7a. Although most of the basin is accumulating sediment, in some parts erosion still occurs which is hypothesised to be the result of local accelerations due to change in bathymetry. What can be concluded from this historic data analysis is that the basin is still suffering sediment starvation and undergoing lots of changes. Although the changes have slowed down, it has not yet reached the new morphological equilibrium.

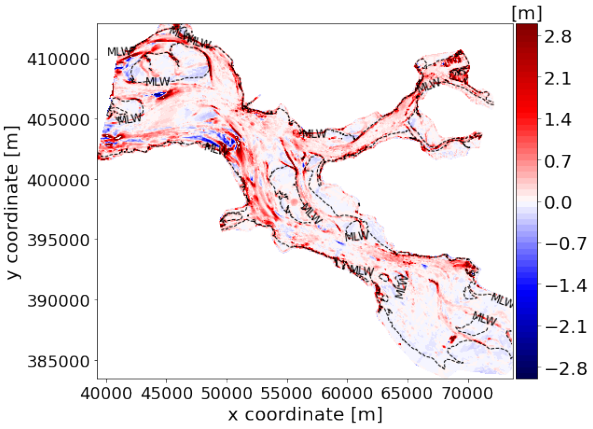

(a) LiDAR measurements from 2019 subtracted with measurements from 2007

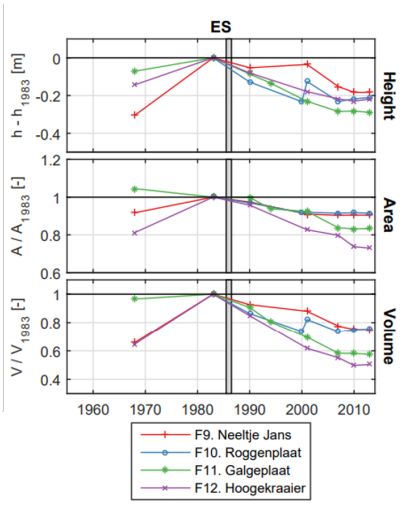

(b) Long-term changes of the average height, area and volume of 4 intertidal areas as derived from the Vaklodingen dataset. The grey box indicates the construction of the SSB. (de Vet, 2019)

Figure 2.7: Morphological evolution of the Eastern Scheldt basin spatially and specifically on some intertidal areas

2.6. Tidal channel nourishment in an estuary

Since 1922, the Western Scheldt has undergone many dredging activities, in order to maintain a certain depth allowing the access to ports located along the Western Scheldt (Cox, 2018). The dredging activities consisted out of 3 capital dredging activities and maintenance dredging. Most of the sediment was inserted back into the system, only 10% was extracted as construction material (Cox, 2018). The approach to dump the sediment back into the system has varied over the years. For the last large dredging activity, in 2010, a new way of disposing of the sediment was introduced. The aim of the new approach was to preserve the multi-channel system of the Western Scheldt, attain maximum ecological gain on the edges of intertidal flats and preserve the environmentally valuable surface area of the Western Scheldt (Depreiter et al., 2011). This approach proposed to dump the sediment directly in the channels in different forms: in scour holes, in secondary channels and in the vicinity of shoals/sand bars. The combination of the different methods resulted in the relocation of approximately 10 million m^3 of sand each year (de Vet et al., 2020).

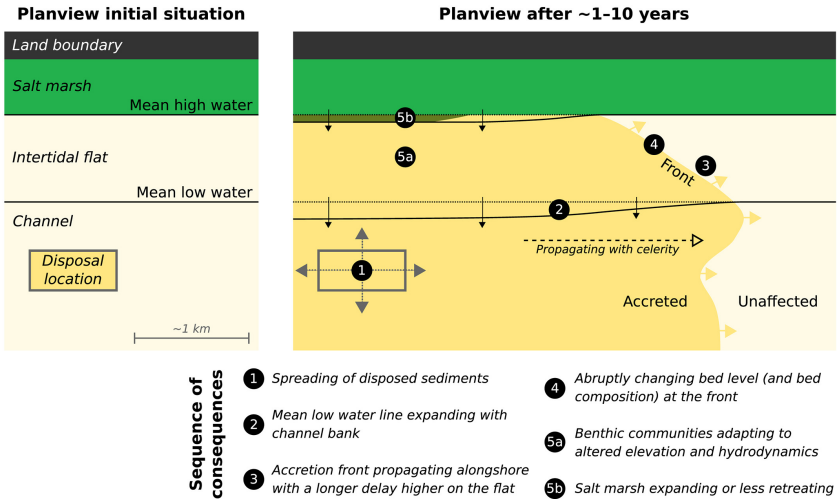

Figure 2.8: Conceptual diagram on the sequence of consequences of sediment disposals in channels for the eco-morphology of intertidal flats.(de Vet et al., 2020)

Tidal channel nourishments (disposals) have been applied in the Western Scheldt in the past 15-20 years. In the scope of this research, previous research and observations about tidal channel nourishments are valuable. In order to better understand how these sediment disposals interact with the intertidal area, the research and observations from (de Vet et al., 2020), are discussed next. In this study, the effect of disposing sediment on a specific location in a channel, adjacent to an intertidal area is studied over time by means of extensive data on morphology, bed composition, and ecology (measured in the Zuidgors area by Rijkswaterstaat). This study showed that the disposing of sediment in a tidal channel has a significant effect on the cross-section of the channel as well as the morphodynamics of the intertidal area. The adjacent intertidal area shows significant accretion which took place in different steps, each with their respective time scale. A schematic of the effect is depicted in Figure 2.8. For a more in-depth analysis and visualisation of the data (location and evolution of the cross-sections), please consult the following paper: ”sediment disposals in estuarine channels alter the eco-morphology of intertidal flats” by de Vet et al (2020). The adaptations around the MLW-line (step 2 on Figure 2.8), were an order of magnitude faster (years) than at higher elevations (decades). It was expected that the accretion on the intertidal area was caused by reduced hydrodynamic energy. On the contrary, the hydrodynamic energy increased (the tidal velocities) as a result of the change in bathymetry (as a result of the yearly disposals). Although the observations were desirable, erosion was observed in the first few years at some locations which can be explained by the time required for an accretion front to propagate along an intertidal flat. This is illustrated by step 3 in Figure 2.8, its celerity was measured to be smaller than 0.5 km/year in this case. The propagation front causes an abrupt change in bed level as well as in bed composition which changed from 150 μm to 50 μm (step 4 on Figure 2.8). It is argued that this can have two causes. Firstly, on intertidal areas in tide-dominated estuaries, grain sizes typically decrease with reduced current velocities toward higher elevations (Friedrichs, 2011). Secondly, when an erosive

intertidal flat becomes accretive, the newly accreted sediments determine the surface bed composition. The accreted sediment was finer than the sediment originally present in the bed which can be caused by either storms or seasonal variations. However, these changes persisted and were found to be induced by the disposals. The salt marsh and benthic life adaptation have the largest morphological time-lag (step 5a &b). It was observed that the edges of the salt marshes became less erosive and expanded locally. Finally, it was observed that the benthic communities showed a significant increase in abundance as a result of the bed elevation. To conclude, the data and the analysis shows that channel nourishments can be successful regarding maintaining the intertidal area and even elevating the intertidal area. Although these results can not be extrapolated towards the Eastern Scheldt, they offer a good perspective.

2.7. Physical processes

2.7.1. Tidal propagation

Since this research focuses on the hydrodynamic and morphodynamic changes of a basin with the tide as the main force, the tide needs further explanation. The tide is the result of the sum of gravitational forces between the earth, the moon, and the sun. The tide inside the Eastern Scheldt basin can be seen as a standing wave with the horizontal and vertical tide that are 90 degrees out of phase (Quyen, 2010). In most locations around the earth, the tide is semi-diurnal which implies that the period equals half a day (12h25min) (Bosboom and Stive, 2015). The principal lunar tide (M2), together with the principal solar tide (S2), are the main constituents of the semi-diurnal tide (Bosboom and Stive, 2015). This implies that two times per day, a flood wave enters the basin and an ebb wave exits the basin. The result of this is currents moving in and out of the basin leading to sediment transport (Figure 1.5).

In most tidal basins, the tidal currents for an ebb wave are different than the ones for a flood wave. This is the case for the Eastern Scheldt and is called tidal asymmetry. Without tidal asymmetry, the net sediment transport would usually be zero (Eelkema, 2013). If there is net sediment import the tide is called flood dominant and ebb dominant if there is net sediment export. The hydrodynamic feature behind this asymmetry is that the wave crest travels faster than the wave through (Speer and Aubrey, 1985). This is valid under the consideration of a long wave and neglecting friction (Bosboom and Stive, 2015). The tidal wave celerity then follows the following relation:

$$c = \sqrt{g * h} \tag{2.4}$$

Two types of asymmetry can be identified and will affect different types of sediment:

- Skewness: a smaller flood duration means a higher horizontal tide(current) which will lead to sediment import into the system mostly for coarse to medium grains (Bosboom and Stive, 2015).
- The second type of asymmetry is caused by the slack water. Slack water is a period of time when the horizontal tide is zero, the flow reverses from ebb to flood and vice versa. This effect is most dominant for finer grains because these grains need time and velocities near zero to settle down. If the high water slack is longer than low water slack, the duration of slack just before ebb is longer and more grains will settle which leads to net import (Bosboom and Stive, 2015).

The Eastern Scheldt has been exporting sediment until the construction of the SSB. This export of sediment was caused by the ebb-dominance in the tidal flow (Eelkema, 2013). At the start of construction, the basin had deep channels and wide intertidal areas. Because of the construction of the SSB, the tidal prism has reduced and the tidal currents have become flood dominant. The sediment exchange between the basin and the ebb-tidal delta has almost completely stopped since the construction of the barrier. As stated previously, the sediment transport from the ebb-tidal delta is being trapped by the large scour holes near the barrier. There is though, some net input of sediment of silt rich material of around 1 million m^3 (van Maldegem and de Jong, 2004).

2.7.2. Wind waves

Since the construction of the SSB, almost all waves coming from the sea are blocked by the barrier. All the remaining waves inside the basin, are either wind-generated or result from marine traffic. The wind blows primarily from the west, south-west with an average velocity of 8 m/s near the mouth and 6.5 m/s

in the East of the basin (Quyen, 2010). The characteristics of waves generated by wind, depend on the characteristics of the wind field as well as the fetch and local water depth (Bosboom and Stive, 2015). The fetch is the distance over which the wind can freely blow over the water surface and transform the wind energy into wave energy. Figure 2.9, illustrates the correlation between the wind speed and the wave height inside the basin. The data is from 2 different measuring stations in the Eastern Scheldt delivered by Rijkswaterstaat for the period 1/06/2020-28/06/2020. The fetch over which the wind can blow from the west is maximal 6 km. It can be observed that the wave height pattern follows the wind speed pattern. One large wind speed peak does not result in a corresponding wave height peak. The latter is due to the wind direction which was North-East at that moment in time. If any wave mitigation measures would be designed to counter the erosion of the intertidal areas it should thus focus on the south-west, west waves.

Wind causes shear stresses on the water surface which can be described by the quadratic friction law (Bosboom and Stive, 2015). The upper part of the water column is affected by this effect, if the area is shallow, this can have an effect on the sediment transport. During flood, part of the intertidal area in the Eastern Scheldt is submerged, creating shallow areas where these wind stresses can have a significant effect on sediment transport. It is likely that during lasting storms, considerable transport of both water and sediment takes place towards the east (Bosboom and Stive, 2015).
Wind can cause sediment transport in a more direct way, for instance, through eolian transport. This has most effect on the emerged land, the intertidal areas. The intertidal flats can be expected to have a slope oriented from southwest to northeast.

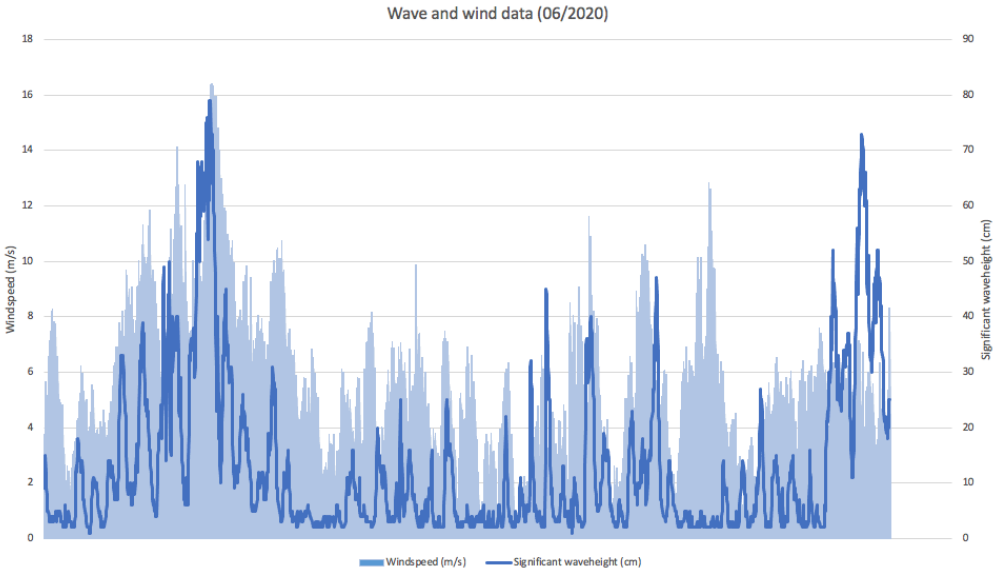

Figure 2.9: Wind and wave data plotted respectively for the month july in 2020 in the Eastern Scheldt (data courtesy of Rijkswaterstaat)

2.7.3. Velocities

The velocities in the basin are changing all the time due to the tidal forcing it experiences. The bathymetry also plays a large role in how the flow propagates into the basin. Figure 2.10 depicts the maximal depth-averaged velocities (numerical model simulation results) for flood and ebb respectively. It can be observed that the maximal flood velocities are 0.4 m/s larger than the maximal ebb velocities. As the water levels are larger during flood, more area is flooded as is depicted in Figure 2.10a which is as can be expected. Furthermore, the northeastern branch of the basin as well as the southeastern branch are slow areas where the maximal velocity does not seem to exceed 0.5 m/s.

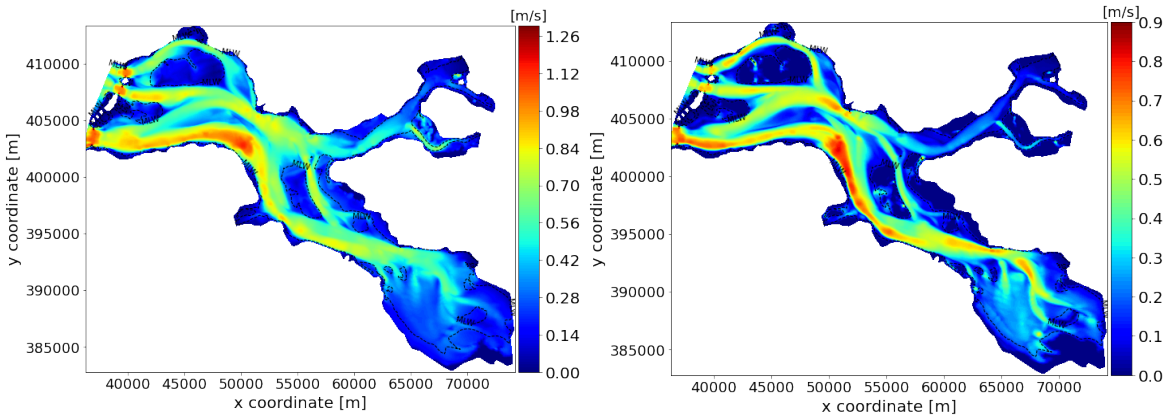

(a) Maximal depth averaged velocities during flood

(b) Maximal depth averaged velocities during ebb

Figure 2.10: Maximal depth averaged velocities for flood and ebb. These are results from numerical simulations of the base case

2.7.4. Sediment transport between a channel and the surrounding intertidal area

The essence of the thesis is to stimulate sediment transport from the tidal channels towards the intertidal areas. In Appendix A.3, the basic principles of sediment transport are discussed such as initiation of motion and fall velocity. In this section, the sediment interaction between the channels and intertidal specifically is discussed.

In order for sand transport to happen, initiation of motion is necessary, as discussed in Appendix A.3. In this case, with a diameter of 190 μm, the critical velocity is found to be 0.45 m/s. Sand is supplied to the tidal flats by the tidal channels. The latter is done via suspended sediment being transported onto the intertidal area by flood tidal currents (Wang et al., 2018), especially during the spring tide, where as much as four to five time more net sediment transport takes place (Kohsiek et al., 1987). Bed-load transport from the channel floor to the flats is almost absent (Kohsiek et al., 1988). When the flood tidal current is overflowing the intertidal area, the flow experiences depth-induced friction and the sand starts to settle, the coarsest grains first (Wang et al., 2018). Whether the finer grains will settle, is depending on the high water slack, the wave action on the intertidal area and the ebb tide.

During calm weather (small wave action), such as July and August for the Eastern Scheldt, accretion of the intertidal areas is expected. Tidal levees, consisting out of coarse sediment are created in this period, along the edges of the intertidal areas. During high wind periods, depending on the fetch, wind-generated waves lower these created tidal levees. In addition, the wind-generated waves bring the fine sediment on the shoals into suspension leading to either net erosion or unchanged bed (Postma, 1961).

A conceptual model for a sandy tidal-flat development over longer timescales is proposed by Wang et al (2018). The sediment supply from the channel is constant and the rate of deposition is dependent on the meteorological conditions (wind waves & water level). The net accretion/erosion rates of the flat over a longer period will thus be determined by the alternation of calm weather periods and high wind periods. Following this concept, the elevation of a tidal flat can be described as a stochastic process which over a longer interval, has a more or less constant level that depends on the average local wave conditions (Wang et al., 2018). When one of the factors determining this equilibrium level is changed by human interventions or SLR, a new equilibrium level is defined. This will either lead to net erosion or accretion over longer periods until the new equilibrium level is reached. Hereafter, the flats will store sand again and depending on the wave conditions, it will be eroded.

3

Numerical model

In this chapter, step 2 of the methodology is elaborated on. Firstly, a choice is made about which numerical model is suited for the research. Secondly, the model set-up is given and explained.Lastly, the model is validated by means of historic data.

3.1. Selection of a numerical model and grid

Multiple models of the Eastern Scheldt are available, these models are either 1D, 2D, or 3D. Examples of these models are the IMPLIC model, the WAQUA model, and the ScalOost model respectively. The major differences are the differences in accuracy and computation time. The disadvantage of the 3D model is the long computation time. The WAQUA model is a flow model that computes the water levels, currents, and particle transport (Svasek Hydraulics, 2004). This model is very precise but can not compute sediment transport. A Delft 3D version of this WAQUA model that takes sediment transport into account has been made and is called the ScalOost model. This model describes the Eastern Scheldt and up to 30km offshore (de Vet et al., 2017). The drawback of the ScalOost model is that it is less accurate than the WAQUA model, however, for this study, the inaccuracies that come with this model are accepted. This existing model could be improved in a later stage of the research.

For the study of the nourishment on the Roggenplaat, two grid sizes were considered, 10x10 m or 30x30 m. The smaller grid could not reproduce small-scale current effects better than the larger grid (Van der Werf et al., 2016). Considering computations times are up to 30 times larger with the smaller grid (Van der Werf et al., 2016), leads to the conclusion that for this research a grid smaller than 30x30 m will not be used.

3.2. The model setup

As stated in the previous section, the ScalOost model has been chosen to conduct the numerical calculations for this research. The model will be run in Delft 3D which is an integrated software made to run simulations for 2DH, 2DV, and 3D models. Delft 3D can carry out simulations of flows, sediment transports, waves, water quality, morphological developments, and ecology (Delatres). The ScalOost model is a 2DH model, considering that the physical processes of interest are orders of magnitude larger than the errors that come with the depth average simplification, the errors are argued to be acceptable(de Vet, 2019). In Figure 3.1, the domain of the ScalOost model is indicated on the right, the computational grid is originating from the Simona model and is depicted in Figure 3.1. The ScalOost model is a nested version of the DCSMv6-ZUNOv4-model which is indicated in blue in Figure 3.1. The 49 boundaries located in the North Sea are thus originating from this larger model.

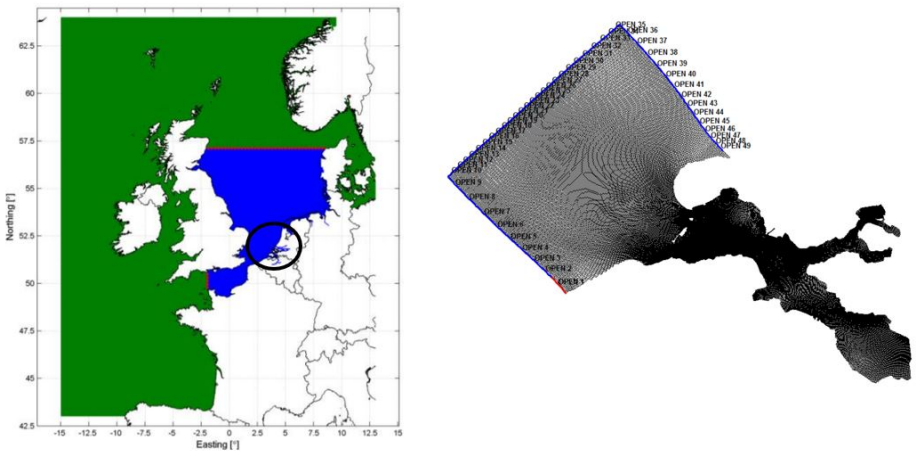

Figure 3.1: Left: DCSMv6 domain (Green), ZUNOv4 domain (Blue) (Zijl, 2016)|Right: Scaloost domain (Delft3d Gui)

The flow chart of the ScalOost model is depicted in Figure 3.2, here the different relations and necessary input to run the model are listed. Considering waves are not included in this study, the only modules that will be used are the Flow and Transport modules.

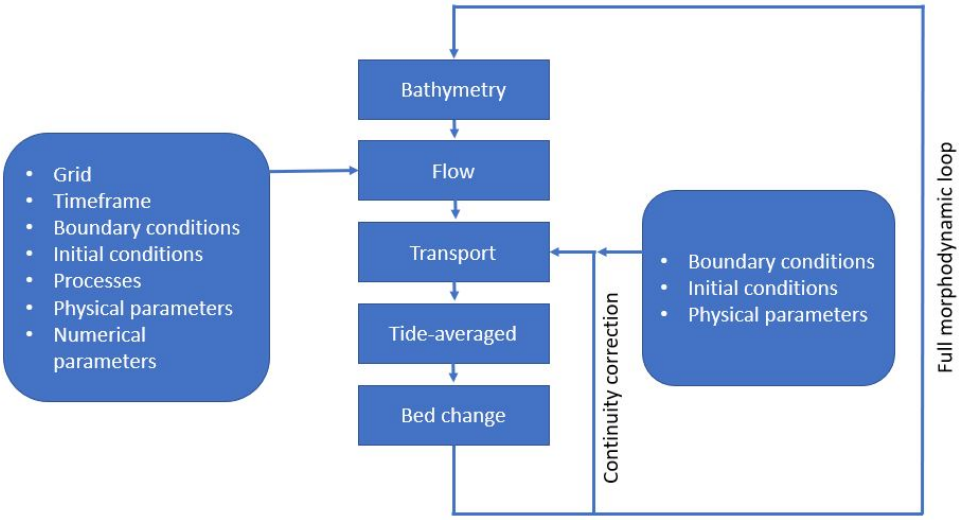

Figure 3.2: Flowchart for the ScalOost model used in this study

The characteristics of the various parameters in the Flow and Transport module that need explanation are listed below, the other parameters are listed in Table 3.1 with their respective values and units.

3.2.1. The Flow module

- The **bathymetry** that is used in the model has been measured by means of Vaklodingen in 2013 which is a combination of single beam measurements and LiDAR data (de Vet, 2019).

- The **grid's** resolution varies from 410x160 m in the North Sea to 45x45 m inside the basin (Zijl, 2016). There are multiple dry points and thin dams present in the model. The storm surge barrier is modeled as six porous plates which are calibrated by means of a permeability energy coefficient, the foundation is also taken into account in the model (Pezij, 2013)

- The model counts 49 **boundaries** that originate from the larger DCSMv6-ZUNOv4 model. These boundaries are time series of water level and velocity for the period: 01/08/2013-01/01/2015.
- **The initial conditions** consist out of an initial water level which is set to + 1.5 m NAP and an initial secondary flow which is set to 0 m/s.
- The **wind** is a time series of the year 2013 measurements with an interval of 10 min at the Rijkswaterstaat measuring station Stavenisse. The wind drag coefficient is linearly dependent on the wind speed, from 0.00063 for a wind speed of 0 m/s up to 0.00723 for a wind speed of 100 m/s.
- **Secondary flow** is the way of taking spiral flow into account in a 2D-depth average model such as this model. The formulas to compute this flow account for two sources, the centrifugal forces and the Coriolis forces. This is done by using the depth-averaged velocity and a radius of curvature (Delatres). In Chapter 6, a more in-depth study will be carried out when looking at the effect of bends and how these forces compare to each other.

3.2.2. The Transport module

- **Sediment transport** is split up into cohesive and non-cohesive sediment due to their different properties and behaviours. Settling in high concentration mixtures can be hindered for both sediment types. In order to account for this hindered settling effect, Richardson and Zaki (1954) are followed (Delatres).
  - **Non-cohesive** sediment transport is computed following the method of Van Rijn. From literature, the grain diameter has been found to be 190 μm (de Vet, 2019).
  - **Cohesive** sediment transport is computed following the method of Partheniades-Krone (Partheniades, 1965). The settling velocity of a cohesive sediment fraction is computed following the method described by Winterwerp. This method assumes a constant settling of the sediment fractions by setting the critical bed shear stress for sedimentation to 1000 N/m^2.
- The **morphological scale factor** can be seen as a tool to reduce computational time regarding morphological computations. Considering the timescale of morphological changes is several times longer than typical flow changes, it would take a relatively long time to see bed changes. This problem is solved by multiplying the erosion and deposition fluxes from the bed to the flow and vice versa by this factor at each computational time step (Delatres). Although a factor of 25 is given in Table3.1, this factor will not always have this value and will be experienced with.

Module	Parameter	Value	Unit	Description
Flow	Δt	0.125	min	Time step
	T	01/09/2013-15/09/2013	-	Simulation start-stop time
	α	0	s	Reflection parameter alpha
	g	9.813	m/s^2	Gravity
	ρ_w	1025	kg/m^3	Water density
	ρ_a	1	kg/m^3	Air density
	β_c	0.5	-	beta_c
	U&V	0.029 & 0.029	-	Manning roughness formula
	Vicouv	1	m^2/s	Horizontal eddy viscosity
	Dicouv	10	m^2/s	Horizontal eddy diffusivity
Transport	Cref	1600	kg/m^3	Reference density for hindered settling
	RhoSol	2650	kg/m^3	Specific density
	CDryB	1600	kg/m^3	Dry bed density
	D_{50}	190	microm	Median sediment diameter D50
	MorFac	25	-	Morphological scale factor
	MorStt	2160	min	Spin-up before morphological changes
	SedThr	0.1	m	Minimum depth for sediment calculation
	AksFac	1	-	Van Rijn's reference height factor
	Thresh	0.05	m	Threshold sediment thickness

Table 3.1: Overview of all the parameters and their value for the base case scenario

3.3. Model validation

In this section data is compared to the results of the model, this is done for both the hydrodynamics as well as for the sediment transport. First, the hydrodynamics are validated, then the sediment transport is validated.

3.3.1. Hydrodynamics

Ideally, both the tidal range and the velocities should be investigated in order to evaluate the reliability of the model results. Validating one is not enough because the two hydrodynamic characteristics are independent of each other. For example, the tidal range at the barrier is roughly 3 m and the corresponding velocity 1 m/s while a higher tidal range at the Hoogekraaier is near 3.5 m with corresponding lower velocities of 0.2 m/s. This is most likely the result of the length scale of the tidal wave and the length scale of the basin, as well as the bathymetry and shape of the basin. First, the water levels are validated, then the velocities are validated.

Pezij, M.(2015) validated the ScalOost model by analyzing the different tidal constituents (M2, M4, and S2), the tidal asymmetry, and the water levels for the year 2013. The results of this study are depicted in Figure 3.3. The results show that the data coincide with the simulation results to an acceptable extent. However, the model underestimates all three amplitudes by a little. Furthermore, the sudden increase in phase of the M4 component between the offshore station and Stavenisse (inside the basin), is a clear indicator that the tidal wave deforms when entering the basin.

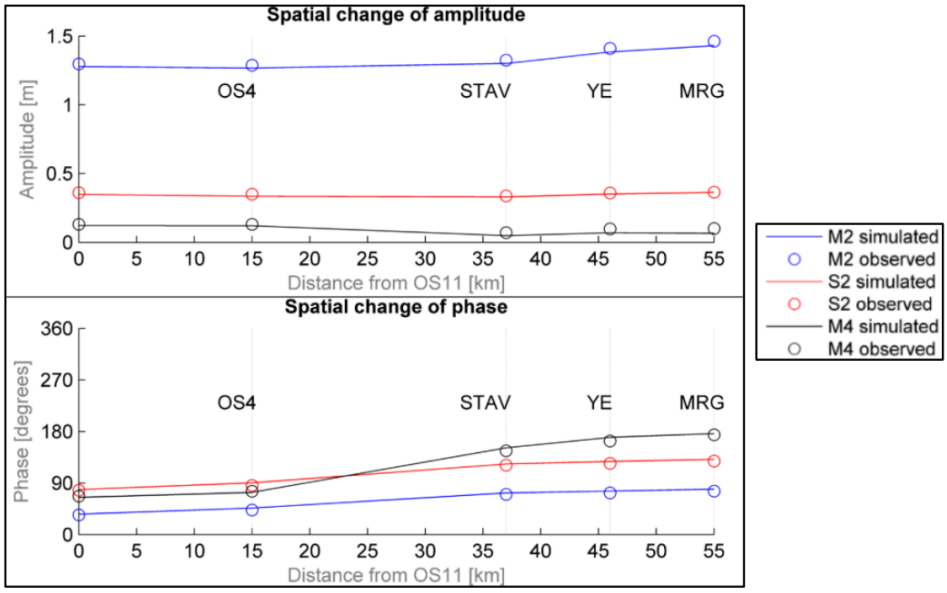

Figure 3.3: A comparison between the observed and simulated tidal amplitude and phase along observation points in the Eastern Scheldt (Pezij, M., 2015)

The water levels were validated using three statistical coefficients: the unbiased root mean square error, the bias, and the Nash-Sutcliffe coefficient (Pezij, M., 2015). The months of December and March are used as validation periods, representing stormy and calm conditions respectively. For more information about this method and the results please consult Pezijs's work. The results of this study are depicted in Figure 3.4. Multiple observations can be made about these results. Firstly, the difference in tidal signal between the two periods. The first period shows more fluctuations in the form of peaks whereas the second period represents a more calm and constant signal. Secondly, outside the basin, the large peak is reproduced accurately whereas the latter is not the case for the two observation points inside the basin. This is due to the SSB closing its gates during this storm which consequently led to a significant decrease of the water levels (Pezij, M., 2015). Thirdly, the low water levels are underestimated for both periods while the high water levels are predicted well. Fourthly, the phase is predicted well. The results

of the different statistical coefficients together with the results depicted in Figure 3.3 & 3.4 proved that the accuracy of the model is good with a slight underestimation of the low waters in the order 5-10 cm. This accuracy also rules for the year 2014, the modeled water levels didn't´t deviate more than 10 cm compared to the data that year(de Vet, 2019).

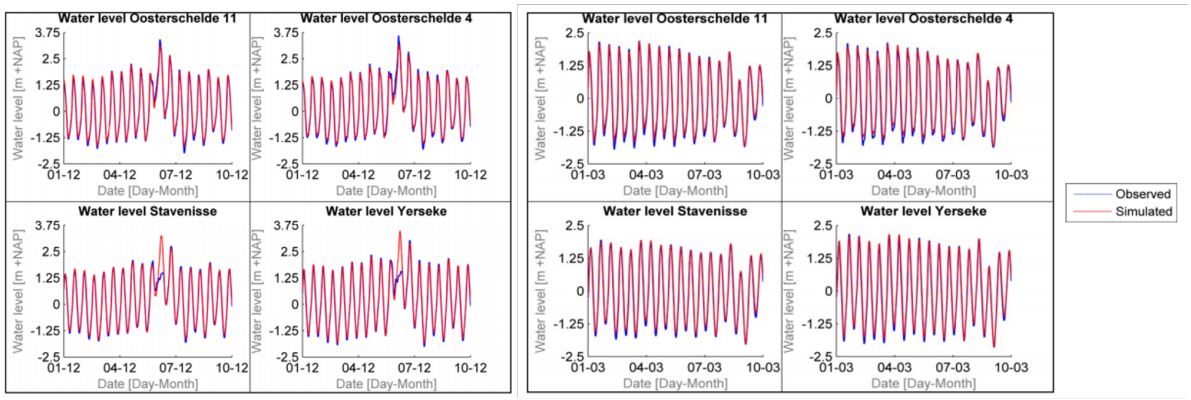

Figure 3.4: A comparison between the observed and simulated water levels along observation points in the Eastern Scheldt. The graph on the left represents the month December while the graph on the right represents the month March(Pezij, M., 2015)

Not much data is available to compare the modeled velocities with, however, there is one study (performed by de Vet, P.L.M. 2019), that has validated the ScalOost model for specifically the area around the Roggenplaat. For the purpose of studying the effect of a nourishment on the Roggenplaat, the velocity has been measured on 16 different locations dispersed over three transects in the months February/March in 2015. In Figure 3.5, the results of this study are depicted. Most locations present fair results with a small absolute bias of 3.5 cm/s and a RMS ranging between 3.5-7 cm/s which can be seen as an acceptable accuracy (de Vet, 2019). The ScalOost model is used indirectly to compute these velocities since the used model is a nest of the area around the Roggenplaat. Thus, the accuracy of the results presented in Figure 3.5 can be directly related to the accuracy of the ScalOost model.

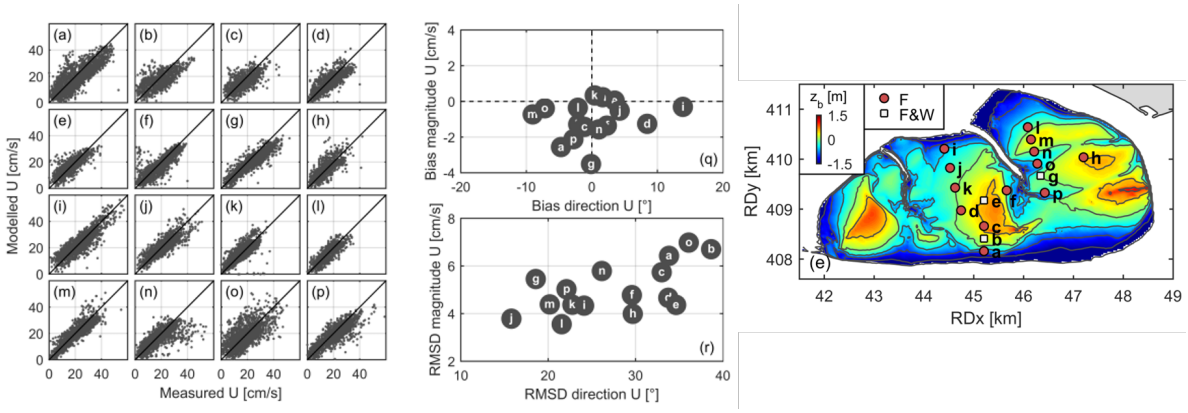

Figure 3.5: On the left, a comparison between the observed and simulated velocities for the measuring stations on the Roggenplaat in the Eastern Scheldt is depicted. The bias, as well as the RMSD are depicted in the middle and on the right the locations of the measuring points are depicted (de Vet, 2019)

3.3.2. Morphodynamics

The goal of this study is eventually to assess the potential of one or more tidal nourishments with the ScalOost model as a tool. In order to draw conclusions, the accuracy and limitations of the model regarding sediment transport must be studied. This will be done in this section by comparing model simulations to historic data. The model can then be calibrated in order to get results that fit the data the best by tweaking parameters such as sediment size or type. Multiple simulations with different parameters have been performed to this end. The parameters that resulted in the best outcome and for which the base simulation has been performed are given in Table 3.2. In Figure 3.6, a comparison

between the actual data and simulation results is presented. When comparing the results of a model with historical data, there are two factors that can be taken into account: the sediment transport patterns and the sediment transport magnitude. Because the model is used as a tool, the emphasis will be on the sediment transport patterns rather than on the exact magnitude. In Figure 3.6, 8 boxes are introduced which are used to discuss the different zones in the Eastern Scheldt.

Parameter	Value
Time	15 days
D_{50}	190 μm
Erodible layer	Uniform 5m
Morphfac	25
Hydrodynamic Spin-up	2160 min

Table 3.2: Model parameters base case

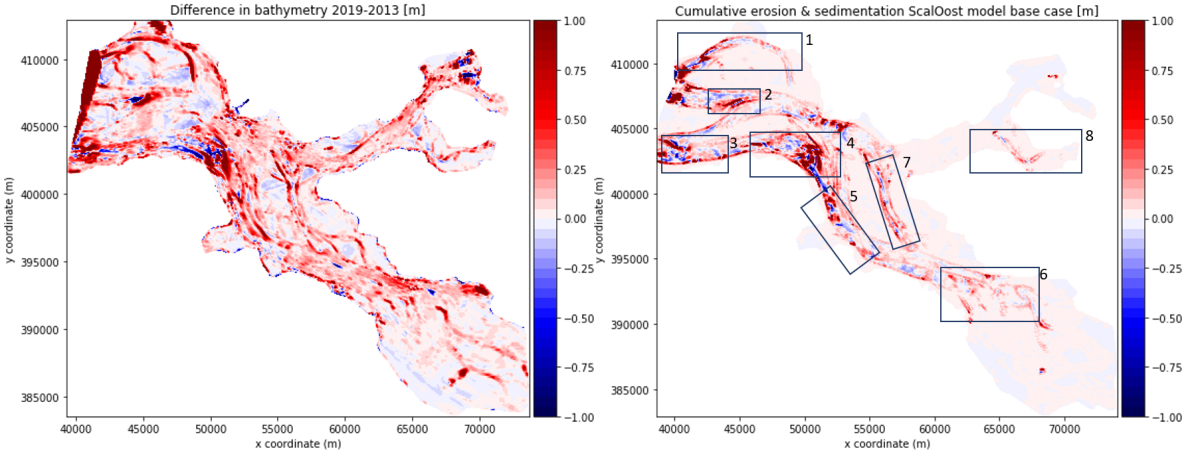

Figure 3.6: On the left, the difference in measured data (LiDAR) between 2013 and 2019. On the right, results of a simulation with the ScalOost model that is representative for 375 days (2013-2014). On the left figure, the red area at the top left is caused by the 2013 data not being complete there. The same scale has been used for both figures such that comparisons can be made. Al the values larger than 1 m or smaller than -1 m are regarded as 1 m and -1 m respectively

It can be observed that the model represents some patterns well while some transport patterns are not visible at all. On the intertidal area for example, there is no sign of net erosion/sedimentation after a one year simulation, while in reality, these zones are morphologically active. Locations 1, 2, 3, 6 and 7 coincide with the data when strictly looking at net erosion/sedimentation patterns. Although locations 4 and 5 present a high morphological activity which coincides well with the historic data, the larger sedimentation/erosion patterns are not simulated correctly. Where large erosion patterns are measured in the data, large sedimentation is observed in the simulation results. Lastly, location 8 only shows sedimentation/erosion in the first half of the channel compared to the entire channel in the data. Furthermore, the simulated sedimentation/erosion on the first half of the channel has an acceptable resemblance compared to the data.

The magnitude of the changes differ with a factor of approximately 2 whereas the duration of the simulation differs with a factor of 7. This result shows that the model overshoots the sedimentation/erosion for simulations with parameters depicted in Table 3.2. The differences between the simulation results and the historic data have multiple reasons which can all be concluded by the model being a simplification of the reality. Firstly, the wind forcing represents only 15 days of the year from the month of September which is a representation of a rather mild wind climate. During storms, the largest sedimentation/erosion patterns are observed. This leads to the second reason for the differences: waves are not taken into account as forcing by the model, only surface stresses caused by the wind. The latter is the reason that there are no bed changes at all in the intertidal areas. Lastly, the modeled sediment

type is sand whereas in reality the intertidal areas are also composed of finer sediment. Some simulations did incorporate fine cohesive sediment, however, the results on the intertidal area were not better. Including another type of sediment has an influence on the computational time and since the effect on a short run was not visible, only simulations with sand were performed. Between MLW- and MHW-line, net sedimentation/erosion can be observed on a much smaller scale. Once the sediment has settled onto this area, the forcing of the waves are able to (re)suspend the sediment and transport it further onto the intertidal area. With this part of the forcing missing, this process does not happen. However, conclusions regarding sediment transport towards the intertidal areas can be drawn considering the sedimentation/erosion patterns near the MLW-line.

Overall, the results of morphological simulations can be used as a tool to recognize sedimentation/erosion patterns in the channels, keeping in mind that the magnitude of these changes overshoots the reality by a factor 4. Regarding the intertidal area, the simulation shows no changes as a result of a lack of forcing. Changes near the MLW-line can be used as indicators for transport towards the intertidal areas.

4

Hydrodynamic study of a channel nourishment

The method that will be followed to answer the research question was introduced in Section 1.6. Steps 3 and 4 of the method will be carried out in this chapter. Step 3, the channel selection, in Section 4.1 and step 4, the effect of nourishments on the hydrodynamics in Section 4.2. The results from these two steps provide the information necessary to answer the second sub-question. Finally, conclusions will be drawn and locations will be chosen to carry out the morphodynamic study in Chapter 5 and 6.

4.1. Channel selection

4.1.1. Methodology

For this study, the choice was made to only take into account very distinct and 'large scale' channels for the reason of simplicity. It is required that the channels are directly surrounded by intertidal areas. The impact of a channel nourishment is not relevant if the channel is not surrounded by intertidal areas. Other factors that are taken into consideration are the depth and the velocities. Ideally, the channels should differ in those characteristics so that different situations can be investigated/studied. Considering the economical value of the navigational channels in the Eastern Scheldt and the aquaculture, these two factors are taken into consideration as well. The latter will be executed by means of a score-based assessment and substantiation. Considering the intertidal area around some of these channels has already been studied and even nourished, this study focuses on locations that have not been investigated or nourished before.

4.1.2. Selection

Applying the criteria discussed above results in 8 potential channels for the application of a tidal channel nourishment. The eight resulting channels are displayed in Table 4.1, together with the corresponding characteristics and scores. As can be observed, there is a great diversity between the channels when combining all the characteristics. There are deep slow channels as well as deep fast channels, and vice versa for shallow channels.

The scores that are given for the use for shipping and the aquaculture range from 1-5 where 1 stands for not used or rarely being used and 5 stands for a high rate of shipping passing through or a large area being occupied by aquaculture. These scores are given in a qualitative and relative way. As depicted in Section 2.4, the aquaculture is present in almost the entire basin. During the other pilot nourishments that have been carried out (see Section 1.2.3), the shellfish cultures have been taken into account but have never been a deciding factor. Since the Slaak is the only channel that scores well on aquaculture and shipping, this channel is considered further in this study. The other channels all score badly on the aquaculture, this will therefore not play a decisive role for the remaining channels. The usage of the channels regarding shipping is on the other hand diverse as is depicted in Figure 2.5a. The channels that are highly used as shipping routes are mostly channels with depths larger than 15 m. Nourishing a deep channel, therefore, does not directly imply negative effects on the shipping if minimal navigational

depth (≈5 m), is maintained.

Channel name	Averaged depth [m]	Velocities [m/s]	Used for shipping	Used for aqua culture
Oliegeul Hammen	25-30	0.6	1	5
Engelse vaarwater	15-45	0.8	4	4
Brabantsche vaarwater	15-20	0.85	5	5
Mastgat	20	0.45	5	5
Krabbenkreek	4-8	0.55	2	4
Slaak	7-9	0.2	2	1
Krammer	10-20	0.15	5	4
Marollegat	10-15	0.1	2	4

Table 4.1: Overview of large distinct channels that are surrounded by intertidal area. The range of velocities is representative for maximal velocities in the channel during flood. The scores regarding shipping and aqua culture range from 1-5.

Oligeul Hammen, Krabbenkreek, Slaak and Marollegat scored best on the usage for shipping. The Krabbenkreek, the Slaak and the Marollegat are surrounded by plenty of intertidal area on both sides of the channel and therefore fulfill the criteria. Oligeul Hammen on the other hand is only surrounded on one side by the Roggenplaat. There are other more interesting locations such as the Brabantsche Vaarwater which is surrounded on both sides by plenty of intertidal area and larger velocities. Although the Brabantsche Vaarwater scores badly on the effect on shipping and aquaculture, this channel is chosen as the 4th channel for further analysis. Considering the depth of the channel, its influence on shipping will be none if the size of the nourishment is small. The four chosen channels differ in depths ranging from ≈4-20 m and depth-averaged velocities ranging from ≈0.1-0.75 m/s. Furthermore, the channels differ in being open on both sides or being closed at the end. The four channels that have been chosen to undergo a hydrodynamical analysis are the following (Figure 4.1)

- Slaak which will further be referred to as channel 1
- Krabbenkreek which will further be referred to as channel 2
- Marollengat which will further be referred to as channel 3
- Brabantsche Vaarwater which will further be referred to as channel 4

Even though these four channels have been chosen to continue the analysis, the remaining channels in Table 4.1 should not be seen as bad options for further/other research.

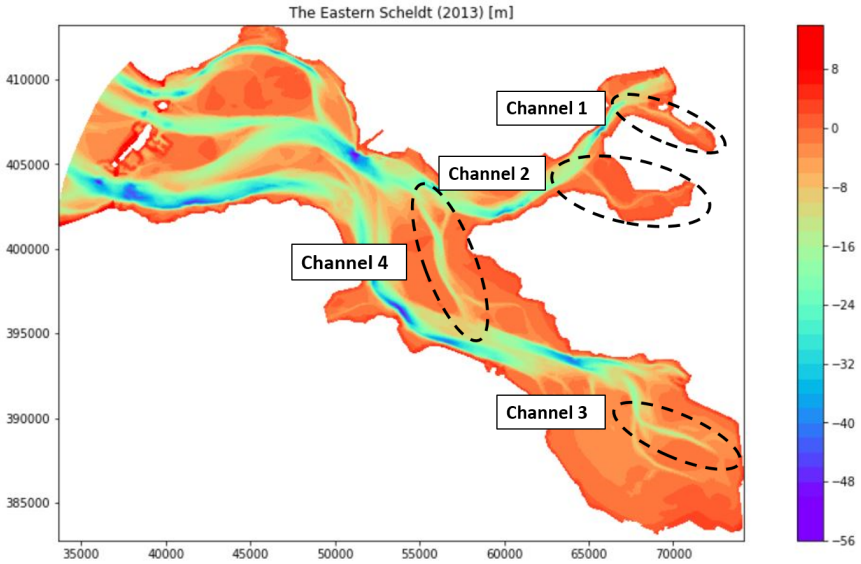

Figure 4.1: Overview of the chosen channels

4.2. The effects of channel nourishments on the flow

4.2.1. Methodology

By means of the ScalOost model, different tidal channel nourishments will be schematised as bathymetry changes. This is done through the QUICKIN module of Delft3D. The main purpose of the QUICKIN module is to create, manipulate and visualise the bathymetry for the Delft3D modules FLOW and WAVE (Delatres, 2020). Two ways can be identified, nourishing the bottom in a uniform way or nourishing the sides of the channel and in this way reducing the width of the channel as is schematized in the figure below. By drawing a certain polygon, the bathymetry can be modified in different ways. For instance, it can be multiplied, changed with a uniform value, smoothened, etc. Since the grid cell resolution differs in the model, some channels are only one grid cell wide which makes the narrowing in some cases complicated.

Figure 4.2: Schematic of different ways of supplying sediment, elevating the bed or narrowing the channel

The hypothesis is that by reducing the cross-sectional area, the velocities will increase in magnitude. The latter is the case assuming no significant redistribution of the discharge between the channels. The discharge is likely to diminish and deflect towards another channel if there is a significant increase in friction caused by a smaller cross-sectional area. By simulating both methods with comparable volumes, the impact of both methods can be compared and new insight can be gained.
The application of nourishments has as objective to increase the depth averaged velocities, preferably to such an extent that the critical velocity for sand (0.45 m/s, see A.3) is exceeded. Another objective is to influence the direction of the flow. To approach this in a systematic way, the following steps can be identified in order to approach every channel in the same way.

1. Run the default case. There has to be one case to which everything can be compared.
2. Define the default time. The output of the ScalOost model is a large time series of velocities over the whole domain, to be able to compare the different cases a specific moment in time has to be chosen. This is a moment during which the velocities are maximal during flood.
3. Apply bathymetry changes to the channel.
4. Analyse the differences in velocity magnitude and direction spatially.

Steps 3 and 4 are rather iterative and will be repeated for each case in each channel. The way the data is processed is explained next. The modified velocity magnitude is simply subtracted with the original velocity so that the difference in velocity is obtained. To visualise the difference in velocity direction, a series of calculations are needed. First, both the base and modified case are averaged around the flood peak. This is done by summing up the vectors of each time step one hour preceding the peak, and one hour following the peak. By dividing this vector by the number of time steps, the average vector per location is found. Finally, the angle of the averaged vectors is computed. To showcase which vectors differ significantly, only the vectors that have a larger angular difference than 10° are plotted.

In this section, there will be numerous types of plots which are shortly introduced next. All plots are either processed model results or processed measurement data. From Rijkswaterstaat data, the MHW- and MLW-line at Stavenisse have been derived to be +1.6 m NAP and -1.35 m NAP, these will be indicated by dashed contour lines on every plot. For more information on how these are computed, see A.1. Furthermore, there are three types of plots that can be identified: bathymetry plots, velocity plots and direction plots. Every velocity plot is a snapshot taken at a specific moment in time and is a simulation result of the ScalOost model. This is for every plot the same moment in time for which the flood velocities attain a certain maximum during flood peak. The bathymetry of the channel that

is run by the ScalOost model is plotted for every channel as well as all the modified bathymetries. The differences in bathymetry measurements between 2007 and 2019 are plotted for every channel to showcase the sediment transport patterns that have been occurring in the past 12 years. These are zoomed-in versions of the data that has been described and analysed in Section 2.5. Lastly, there are direction plots that showcase the difference in flow direction between the base case and the modified bathymetry case.

4.2.2. Channel 1 ”The Slaak”

Channel 1 also called ”de Slaak”, is located in the upper East corner of the Eastern Scheldt and its depth varies between 0 m NAP on the sides and up to 12 m NAP in a scour hole. It is surrounded by a significant amount of intertidal area which is covered with vegetation on the Southside. Some side channels have started to meander in this vegetation creating a very rich biotope better known as a salt marsh. The velocities in the channel decrease from 0.45 m/s at the entry of the channel down to 0.06 m/s at the end of the channel. The morphological evolution of the channel in the past 12 years showcases the characteristics of sediment starvation well. The channel is mostly accumulating sediment (red) while the intertidal areas show an eroding trend (blue). The quantities however are quite small indicating that the channel is less morphologically active than the rest of the basin. This is due to the velocities being smaller than the critical velocity for the majority of the time. The area between MLW- and MHW-line shows no significant changes, which can indicate that this area is near its equilibrium.

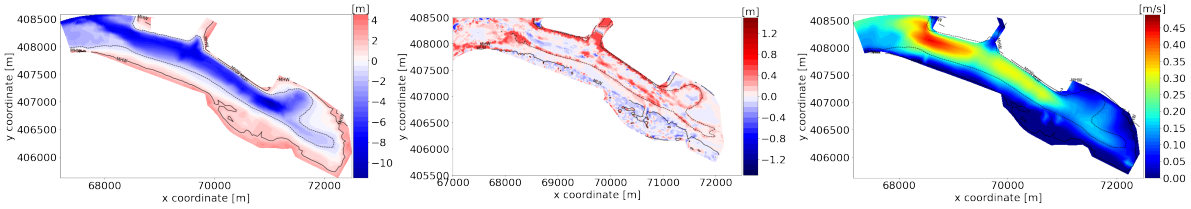

(a) Bathymetry (b) Morphological evolution 2019-2007 (c) Depth averaged velocity

Figure 4.3: Overview of Channel 1

Uniform way In order to create a more uniform bathymetry and reducing the cross-sectional area, the scour hole at the end of the channel is elevated as a test. In Figure 4.4c, a significant increase in velocity is observed on the nourished area. The discharge at the entry of the channel hasn’t changed significantly. Consequently, the outcome can be explained by the fact that the same amount of water comes in and out of the channel, only the cross-sectional area has decreased leading to an increase in velocity (0.24 m/s). Next to the increase in velocity, the direction of the flow gets influenced significantly by this measure. The flow is directed more towards the shoals around the channel. It is hypothesized that the latter is due to a larger overflow caused by the nourishment. Although the velocities double, the increase in velocity is in most cases not enough to attain the critical velocity for sand transport. The critical velocity for finer sediment, however, can be exceeded meaning there will be transport of the latter which could potentially feed the intertidal areas. For this to happen, the nourishment would have to consist out of finer sediment. The volume of sediment that would be necessary to realise this bathymetric change is approximately $740 * 10^3$ m^3.

Narrowing the channel Applying nourishment on the side of the channel under a certain slope is harder than just simply dumping sediment into a scour hole. However, this technique has been applied in the Western Scheldt and has been proven to be successful. Modelling this slope is complex considered the rather large computational cells and as a result, a ”blocky” bathymetry is created. In Figure 4.4b, the changes to the bathymetry are pictured in red. The sides of the channel have been set to -1.5m NAP with an acceptable accuracy, which transformed the channel to a narrower channel. This is done so that the cross-sectional area is reduced with the expectation that the velocities increase significantly. As can be seen in Figure 4.4d, the flow is concentrating in the now narrower channel which causes the flow to accelerate (by 0.12 m/s). Considering the increase in velocity is not large enough to initiate sand transport, this measure will not enhance the accretion of the surrounding intertidal areas. No clear pattern regarding the direction change can be identified nor explained. The volume necessary to

realise this bathymetric change is approximately $350 * 10^3$ m^3 which corresponds to half the volume for the uniform change. The increase in velocity is also half of the uniform change case. This leads to the hypothesis that the nourished volume is directly proportional to the increased velocity. The concept of narrowing down a channel has been proven to work here.

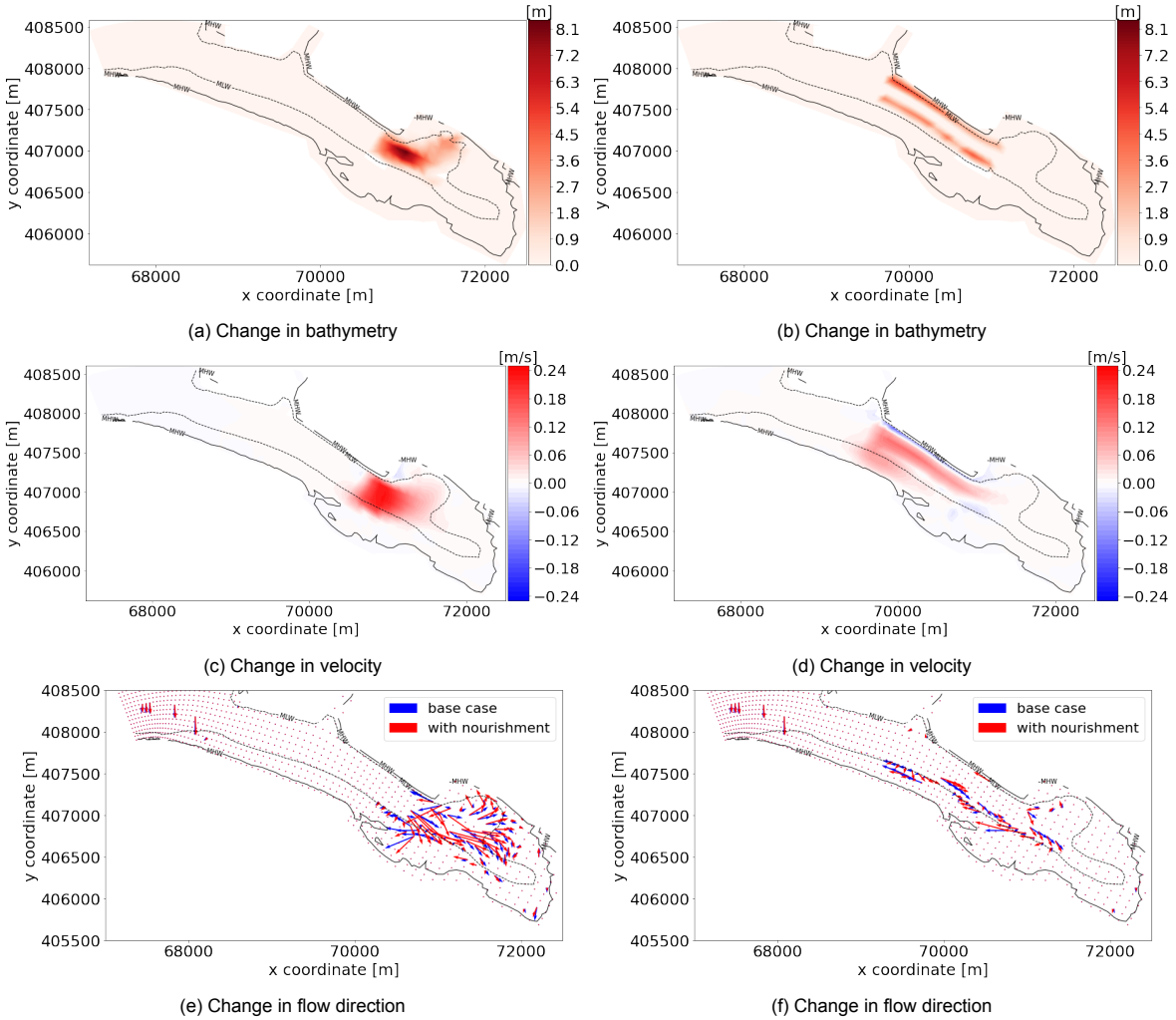

Figure 4.4: The left column represents the effect of a uniform nourishment on the velocities and on the flow direction. The right column represents the effect of a channel narrowing

As said in this section, the hypotheses were confirmed for both the uniform and the narrowing case. Relatively to the base velocity, some substantial increases have been observed. The direction change indicates that more flow on the intertidal area occurs, potentially leading to more sediment transport towards the intertidal area. However, the velocity increases are too small to initiate sand transport. If considering finer sediment, this could be a suitable location. However, in the scope of this thesis, this option is not further investigated.

4.2.3. Channel 2 ”The Krabbenkreek”

This channel has similarities with channel 1 as well as clear differences. The characteristic that they have got in common is that they are both closed at the end and surrounded by intertidal areas and on the south side the area is covered by salt marshes. The intertidal area on the north side is called the Anna Jacobapolder and on the south side Sint Annaland. Channel 3 is a meandering type of channel where the flow reaches velocities of 0.9 m/s at the entry and diminishes down to 0.2 m/s at the closed end. The channel has a depth of 10 m which decreases along the channel down to 3-4 m. There are two harbours in this channel, the first one is a yacht harbour for which a depth of -5 m NAP has to be

guaranteed and a work harbour at the end of the channel for which -3 m NAP has to be guaranteed (van Maldegem, 2007). From the historic data analysis, multiple things can be noted/concluded. The first one is that the first half of the channel is slightly eroding whereas the second half is accumulating sediment. This indicates that the first half of the channel does not experience sediment starvation while the second half does experience it. This could be due to the velocity decelerating along the x-axis, bringing sediment from the first half of the channel towards the second half of the channel. Next to that, the erosion in the bend is a clear sign of the formation of an ebb and flood channel. A flood channel is characterised by transporting the flood current and exhibiting a sill at the end, vice versa for an ebb channel (van Veen et al., 2005). Where these channels meet a sill is created which is clearly visible in Figure 4.5b. It is difficult to predict how this sill will affect the sediment transport of the channel. Because of the sand eddies created near the sill, particles can be transported towards the intertidal area or in another direction (van Veen et al., 2005).

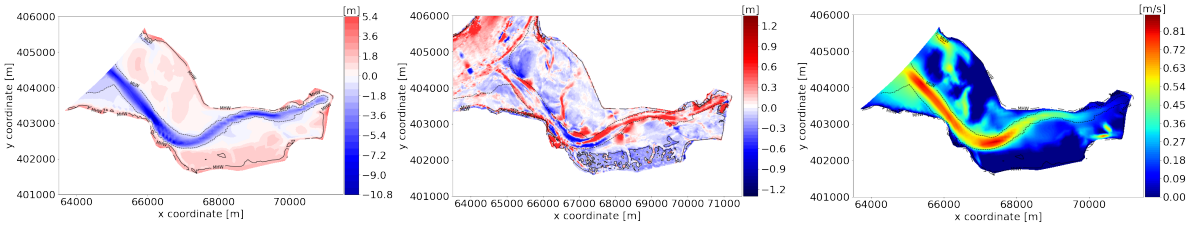

(a) Bathymetry (b) Morphological evolution 2019-2007 (c) Depth averaged velocity

Figure 4.5: Overview of Channel 2

Uniform way As for the previous channel, first, a uniform bathymetry was created. As can be seen in Figure 4.6a, the bottom of the channel has been raised to an equal depth of ≈ -3 m NAP. Some parts have been lifted by almost 6 m, whereas other parts were already at the desired level, hence needed no change. The results are significant increases in the tidal velocities along the nourished area. The larger changes occurred where the change in bathymetry was the largest which is as can be expected and again indicates a direct proportionality between nourished sediment and velocity change. The increase in velocities is significant (max 0.2 m/s), as the original velocity is larger than the critical velocity in the first part of the channel and is now accelerated in the second part of the channel. This means that the critical velocity for sand is guaranteed further along the x-axis. The observed velocity decreases upstream of the nourishment, which is not a significant downside considering the velocities will still be larger than the critical velocity. This deceleration is a sign that the flow experiences more friction when the cross-sectional area ahead is reduced. Figure 4.6e depicts a direction change of the flow in the channel which is more directed towards the end of the channel. Because this is averaged during a flood peak and the velocities increase significantly, this outcome is as expected. The volume of sediment that would be necessary to realise this bathymetric change is approximately $970 * 10^3$ m^3.

Narrowing the channel A different approach was used here than in all the other channels, the cross-sectional area was not changed but the path of the channel was. The channel is meandering and has a large bend which causes extra friction on the flow than if it were a straight line. The approach consisted of modifying the bathymetry in such a way that a straighter pathway would be created for the flow to follow. In order to create a straighter pathway, the inner bend was deepened while the outer bend was filled up as is visualised in Figure 4.6b. The effect of this measure is local and does not influence the flow up- or downstream from the changes. There is some acceleration but the anticipated effect has not been reached with this measure. Since the applied change is small, and that the direct proportionality between nourished sediment and velocity increase has been proven to be true in previous cases, it is argued that a larger change can result in better results. This situation also schematizes the situation where one would dredge the sill between the flood and ebb channel and recreate one larger main channel. When looking at the flow direction this measure has almost no effect. If the sediment that is retrieved from the dredging works can be used to fill up the outer bend, approximately $140 * 10^3$ m^3 of additional sediment would be needed to reach this bathymetry.

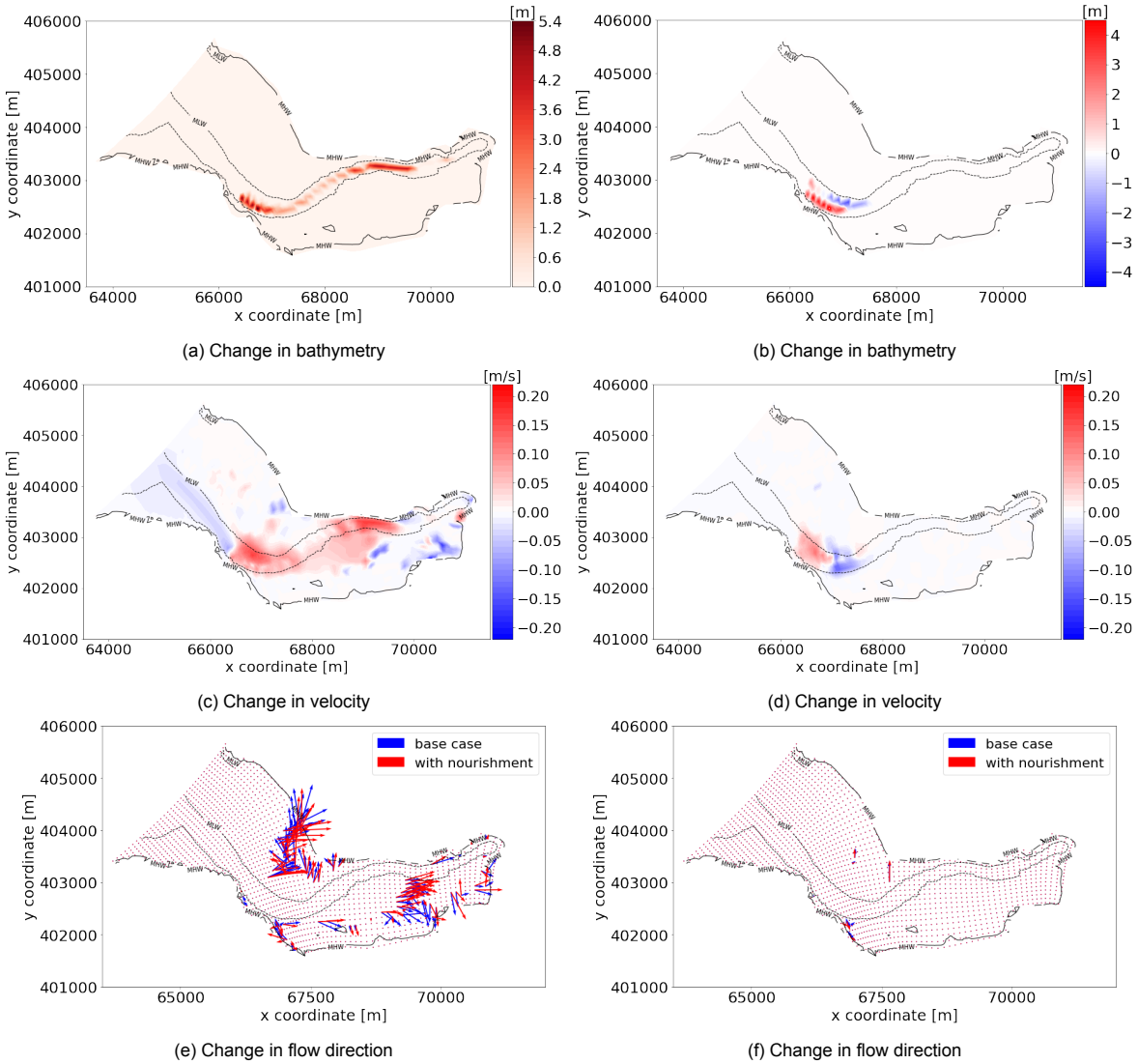

Figure 4.6: The left column represents the effect of a uniform nourishment on the velocities and on the flow direction. The right column represents the effect of a channel narrowing

The straight pathway idea turned out to not have a significant impact on the flow whereas the more standard uniform change in bathymetry caused a significant increase in the tidal velocity magnitude regarding the critical velocity. This measure shows great potential since the critical velocity for sand is reached much further into the channel. A sensitivity analysis can be applied to this channel in order to find out whether the direct proportionality between nourished sediment and velocity change is true and up to which point.

4.2.4. Channel 3 ”The Hooge Kraaier”

Channel 3 is situated in the southeast corner of the basin. This part of the basin consists of many channels, however, this one is the deepest and largest one in the area. Channel 3 is a deep channel reaching depths of almost 20 m and has velocities ranging from 0.8 m/s at the entry of the channel to 0.4 m/s at the end. From Figure 4.7b, sediment starvation is clearly visible. The deep channels are accumulating sediment (red) whereas almost all the shallower areas are eroding (blue). A harbour and a sluice are located in the upper east corner of Figure 4.7b. Since the construction of the barrier, most of the intertidal area has become permanently submerged which makes this area different from the two previous locations. Some of the larger intertidal areas still emerge during most of a tidal cycle and are called: ”Hooge Kraaier, Verdronken land van Zuid Beveland and Speelmansplaten”. In this part of the basin, the building forces (tidal velocities) are too small compared to the wave action that takes place,

especially in shallow environments. Once an intertidal area gets submerged for most of the tidal cycle or even permanently, building back the intertidal area without a nourishment is not likely to happen. The combination of small water depths and wind causes wind waves. These waves exert bed shear stresses on the intertidal areas which is the cause for their erosion. In 2013, there has been a pilot nourishment at the Oesterdam which consisted of saving a small part of the intertidal area by creating a sand bar in front of it to reduce wave action. Next to this, four artificial oyster reefs were placed to protect this intertidal area by reducing wave action.

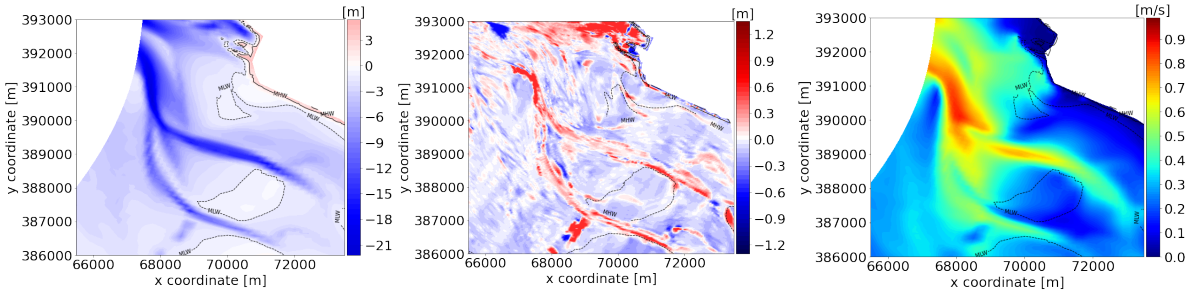

(a) Bathymetry (b) Morphological evolution 2019-2007 (c) Depth averaged velocity

Figure 4.7: Overview of Channel 3

Uniform way The same approach as with the other channels is applied here. Because the ultimate goal is that the sediment from the nourishment will end up on the intertidal area the bathymetry changes were applied near the intertidal area that is left. To this end, two scour holes were leveled with the rest of the bathymetry. These changes were relatively small, in the order of 3 m as is depicted in Figure 4.8a. The grid cells are much larger in this part of the basin resulting in approximate bed level changes. The critical velocity for transport is reached along almost the whole channel during this particular flood peak. In such a situation, the aim of a nourishment is to increase the velocity even more and increase the period in which this critical velocity is reached. As can be observed in Figure 4.8c, small local velocity differences (0.025 m/s) with the base case can be observed. The same conclusion can be drawn regarding the direction of the flow, no significant change can be observed. The small velocity changes confirm the direct proportionality between the size of the nourishment and the effect on the velocities as this nourishment would only require $170 * 10^3$ m^3. The hypothesis is thus that a larger nourishment would have a greater impact on the velocities.

Narrowing the channel For this measure, the decision was made to apply a larger change in terms of volume and have a larger impact on the flow than the uniform change had. The volume of sediment that would be necessary to realise this bathymetric change is approximately $2400 * 10^3$ m^3, 14 times more than the uniform change. Because of the large grid cell size in this part of the basin, the channel covers only two grid cells which makes it complex to apply a narrowing of the channel. Mostly the northern side of the channel has been reduced in width by reducing its depth by approximately 9 m on the whole length of the channel. The south side of the channel has only partly been modified. The effect of this measure is depicted in Figure 4.8d. Compared to the uniform case, the effect of this measure is observed on the whole area. The impact of the nourishment on the velocity magnitude in the narrowed channel is a deceleration of the flow. The nourishment has however positive impact on surrounding locations that were not the target of this measure. The change in flow direction depicted in Figure 4.8f shows that the flow is directed more towards the south, probably towards another channel. It can be the case that the change in bathymetry is large enough to cause significant resistance such that the discharge redistributes towards a channel with less resistance. Considering part of the volume that originally flows through channel 3 now flows through another channel, flow in channel 3 experiences a decrease in velocity. This measure gives new insight into the direct proportionality between the nourished sediment and the change in velocities. There seems to be a limit, after which the flow experiences too much resistance and redirects towards another channel.

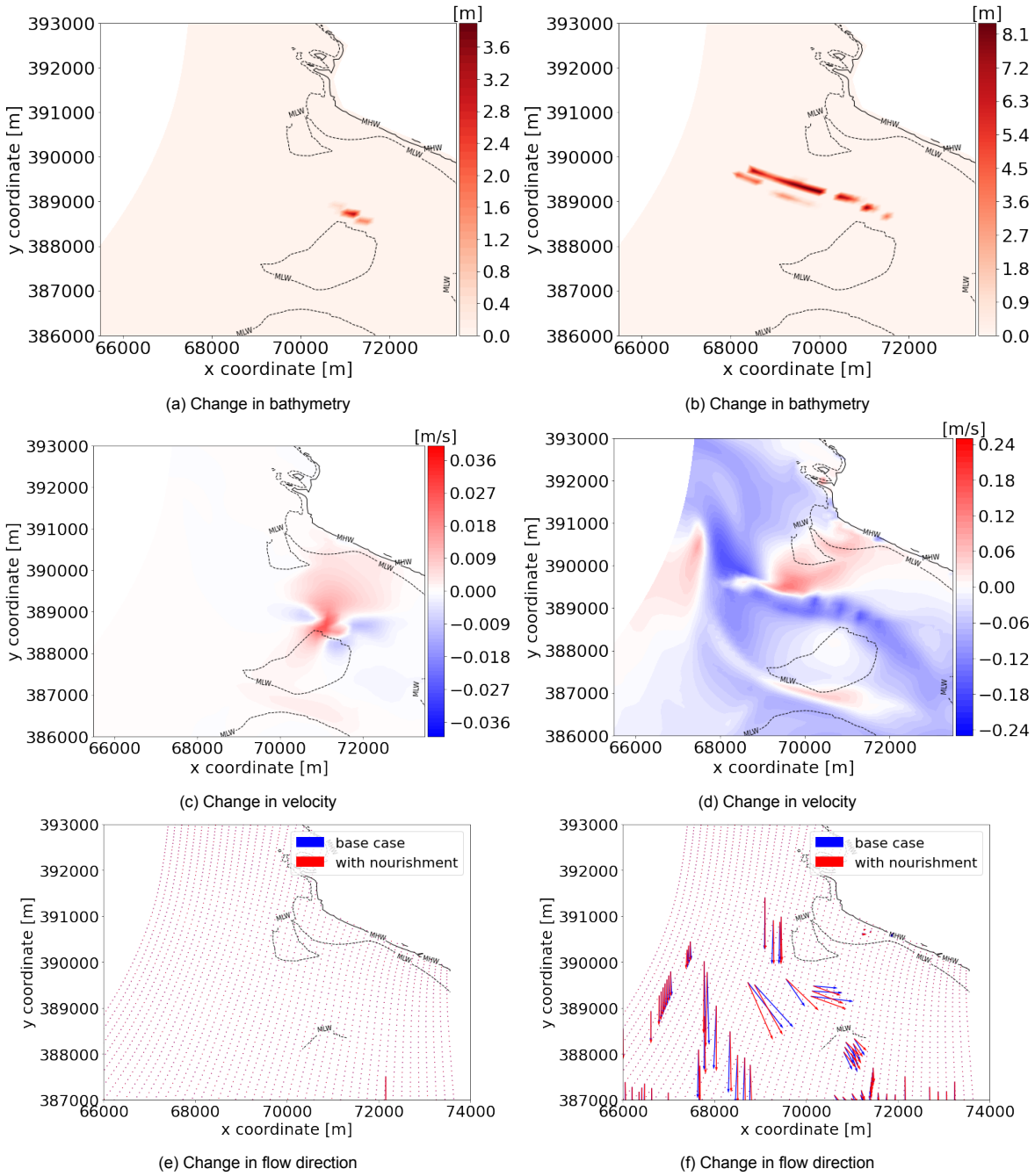

Figure 4.8: The left column represents the effect of a uniform nourishment on the velocities and on the flow direction. The right column represents the effect of a channel narrowing

Although channel 3 has been cited in multiple previous studies as an interesting location for a local nourishment, this preliminary study did not prove that by locally nourishing the channels significantly higher velocities could be obtained. In this channel analysis, the nourished volume seems to play a large role in whether a measure is successful or not. The direct proportionality between the nourished sediment and velocity change is not self-evident in every case and should be looked at carefully. Nevertheless, there are other channels in this part of the basin and thus many other possibilities to further elaborate on this part of the basin.

4.2.5. Channel 4 ”The Brabantsche Vaarwater”

Channel 4 is the channel with the highest velocities that will be considered in this study with velocities along the whole channel in the order of 0.8 m/s. The channel has one main entry and exit which makes

it different from channels 1 and 2 which had a closed end. Besides the main entrance and exit, there are some side channels disturbing the in and outflow. The channel is used as a navigational channel, vessels with a maximal draft of 5 m area allowed to sail in the Eastern Scheldt (2.4). This information has to be kept in mind when designing a nourishment regarding the depth. The channel is surrounded by intertidal areas which consist mostly out of sand such as the ”Galgenplaat” or the ”Slikken van den Dortsman”, see Figure 2.2a. Because of the large velocities, it can be assumed that there is already significant transport from the channels towards the intertidal areas. The fact that these intertidal areas still have a net eroding trend means that the supply from the channels is not enough compared to the eroding meteorological factors such as wind and waves. Measures will be investigated that could lead to more transport from the channel towards the intertidal areas. From Figure 4.9b it can be noted that apart from the large red circle on the Galgenplaat, most of the intertidal area surrounding the channel is though at a small rate, eroding. The red circle is the result of a pilot nourishment carried out in 2008 of approximately 130.000 m^3 of sand. The channel is mostly accumulating sediment with some exceptions on the shallower parts of the channel.

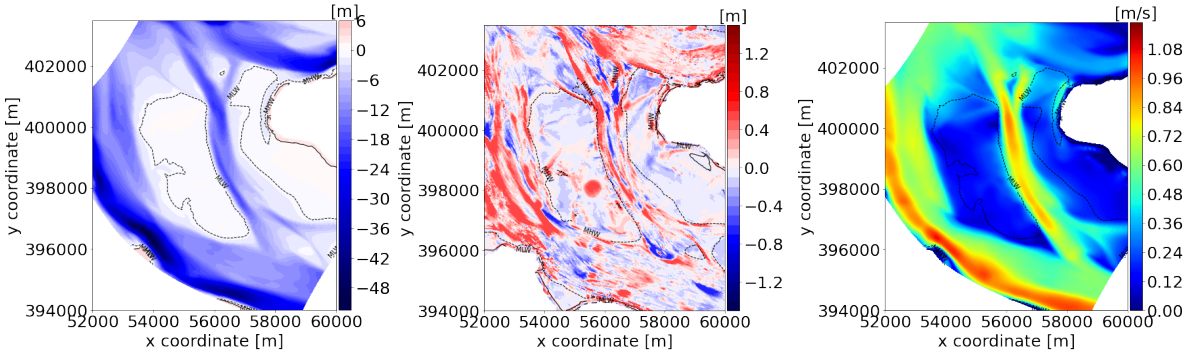

(a) Bathymetry (b) Morphological evolution 2019-2007 (c) Depth averaged velocity

Figure 4.9: Overview of Channel 4

Uniform way As can be observed in Figure 4.10a, the deepest part of the channel has been modified to a depth of approximately 14 m. By reducing the cross-sectional area, a local increase in velocity is observed while on the up- and downstream areas, the opposite is observed. By reducing the cross-sectional area of the channel, more friction is created leading to a minor decrease in discharge which consequently leads to a deceleration of the flow on the non-nourished areas. The results confirm the predictions in a qualitative way. The increase in velocities (max 0.2 m/s) is small considering the sediment volume that would be required to apply such a nourishment approximately $1670 * 10^3$ m^3. However, this increase in velocity on an original velocity ranging between 0.8-1 m/s and can have a significant effect on the sediment transport. The deceleration of the flow is smaller than the acceleration (max 0.15 m/s), the resulting velocity will thus still be larger than the critical velocity, hence transport will prevail. As previously discussed, applying a nourishment can lead to a redistribution of discharges between different channels. If the flow experiences more friction than before, part of the flow will go through another channel, reducing the local tidal prism. Also, if the cross-sectional area of a channel decreases overflow on the intertidal area is likely to increase. This effect is visible in Figure 4.10e where the red arrows point more towards the intertidal area than the blue ones.

Narrowing the channel The sides of the first half of the channel have been raised by approximately 7 m. The effect of the narrowing is small which could mean that the change in bathymetry wasn't large enough. As with the uniform change in bathymetry, the though local positive effect has both up- and downstream negative effects on the velocity (decrease). The desired effect of the flow being funneled down the now narrowed channel has not been accomplished. On the contrary, an increase is observed in the nourishment area. It is hypothesised that this is due to the narrowing did not take place over the whole depth. Consequently, the flow accelerates on the now shallower sides of the channel instead of accelerating in the middle. The sediment volume that would be necessary to realise this bathymetric change is approximately $1820 * 10^3$ m^3.

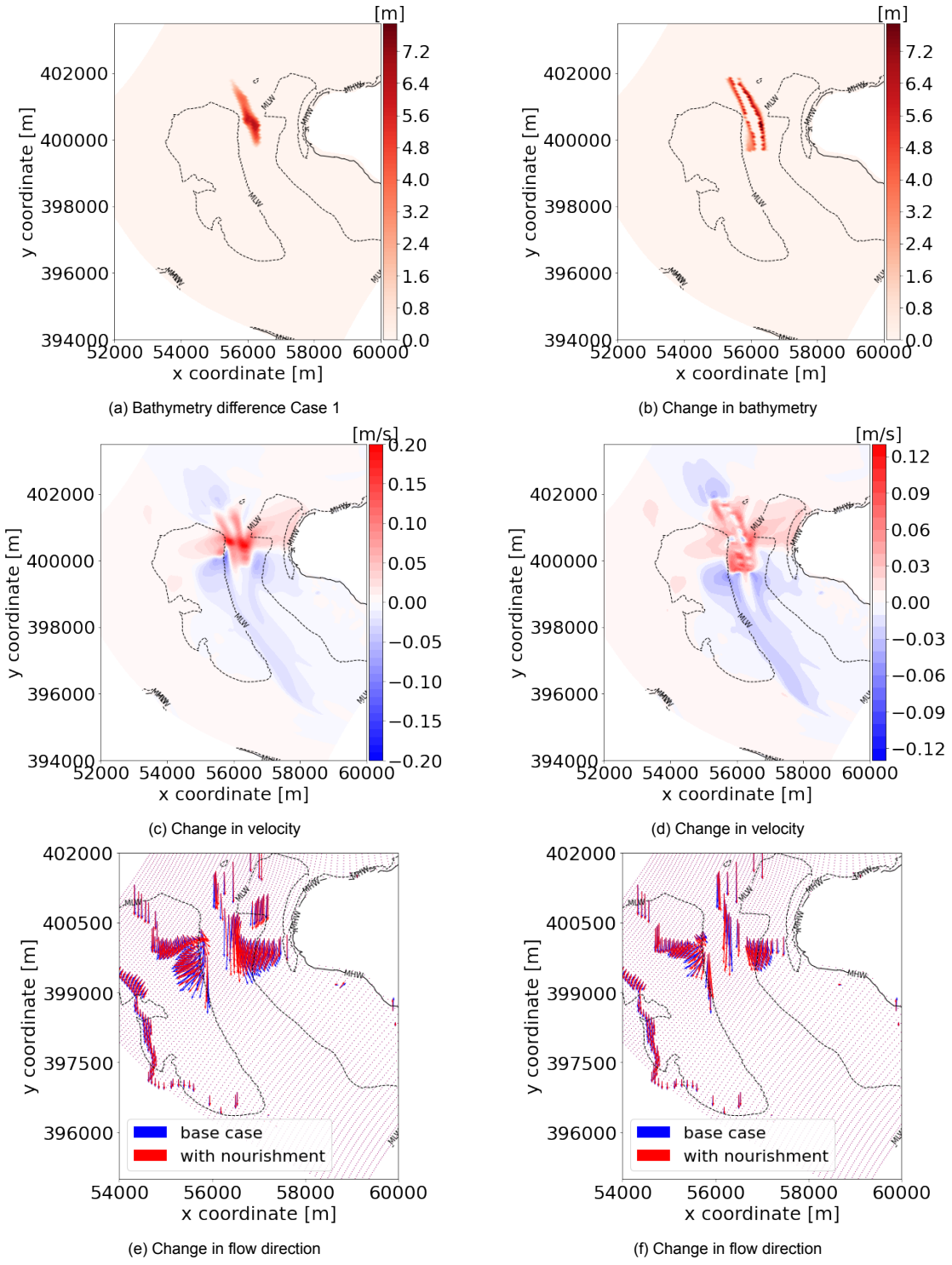

(a) Bathymetry difference Case 1

(b) Change in bathymetry

(c) Change in velocity

(d) Change in velocity

(e) Change in flow direction

(f) Change in flow direction

Figure 4.10: The left column represents the effect of a uniform nourishment on the velocities and on the flow direction. The right column represents the effect of a channel narrowing

Because the tidal velocities were already large enough to enhance sediment transport, the magnitude of the increases is relatively small but significant for enhancement of transport. The nourished sediment would erode faster in this channel than in channel 2 for example, thus indicating a smaller lifetime. The emphasis for this channel should be put on influencing the direction of the flow and creating additional flow on the intertidal areas, which potentially carries sediment. Making use of both bends and the secondary flow patterns could be a good solution here. Nevertheless, the previous simulations have

proved that an increase in velocities is obtained by applying both methods.

4.3. Discussion & Conclusion

Four different channels have been analysed in this chapter. Their morphodynamic history, their current hydrodynamics as well as how these channels react to bathymetric changes were investigated. The goal was that by reducing the cross-sectional areas of the channels (by elevating or narrowing the channel), the flow would locally accelerate. By increasing the velocities in certain areas, sediment transport from the channel towards the surrounding intertidal areas is enhanced. Next to an increase in velocity, the direction of the flow has been considered. Its potential effect on sediment transport, however, was found to be hard to analyse. The spatial influence of the nourishments on the velocity varied from being local to far up- or/and downstream. The local velocity changes (on the nourishment area), were in every case positive (increase in velocity), while the changes up or/and downstream were observed to be mostly negative (decrease in velocity). This confirms the main hypothesis: when the cross-sectional area of a channel is reduced, results show that the flow accelerates locally. The decrease in flow velocities on the non-nourished areas is due to a redistribution of the discharge between channels as a result of an increase in friction caused by the nourishments. If less discharge is flowing through a non-nourished part of the channel, the velocities will decrease.

Channel 1 shows substantial local accelerations for both methods, compared to the original velocity without any negative influence up or downstream. This acceleration, however, does not result in velocities able to stimulate sand transport (0.45 m/s). Both nourishment methods present positive results of the same order of magnitude. Results indicate that the sediment volume used for the nourishments is directly proportional to the velocity difference ($750 * 10^3$ m^3 and 0.25 m/s ; $350 * 10^3$ m^3 and 0.12 m/s). An increase in velocity is observed on the intertidal area when narrowing the channel. A sand nourishment in this channel could although be interesting to apply in view of reaching an equilibrium situation in the channel and stimulate the transport of finer sediment. In this hypothetical local equilibrium situation, the erosive trend of the surrounding intertidal area could turn into an accretive trend. Without any increased sediment supply, these areas will eventually disappear below the MLW as a result of the meteorological conditions and sea-level rise.

The velocity increase obtained with the uniform nourishment in channel 2 is significant. This increase in velocity has as result that the critical velocity for sand is exceeded approximately 1 km further into the channel when the velocities are maximal during flood. The negative influence on the velocity occurs locally on the intertidal area or upstream of the nourishment in the channel. The decrease in velocity upstream of the nourishment is minor and will therefore have a minor impact on the sediment transport as the critical velocity is still reached for most of the tidal cycle. A channel nourishment in this channel has the potential to increase the velocities and (partly) satisfy the sediment starvation in the channel. Most importantly, it can enhance sediment transport from the nourishment towards the intertidal area. In line with the results of disposing sediment in a channel in the Western Scheldt (see Section 2.6), the eroding salt marsh could benefit from this nourishment after a few years, when the accreting front has reached this area.

The two simulated nourishments in channel 3 did not result in desirable outcomes. Narrowing the channel influenced the surrounding area significantly in a negative way (velocity decreases). Simulation results indicate that it can be due to a deflection of the flow (observed in the direction change), induced by the nourishment. The nourishment was large enough to deflect the flow towards another channel which leads to a smaller discharge in channel 3. The uniform change in bathymetry showed as for all the other cases, a local velocity increase on the nourished area. Although there is an increase, this increase is in the order of 2 cm/s which can be neglected compared to the original velocity of 0.5 m/s. The direct proportionality between nourished sediment and velocity change should be investigated here, a larger uniform change might result in a larger increase.

Channel 4 is an example of a nourishment that has a large spatial influence on the velocities, approximately 4 km downstream. On the nourishment area, the changes are positive (velocity increase) while the changes elsewhere are either negative (velocity decrease) or none. The extra overflow caused by the nourishment can be beneficial to disperse the accreted sediment on the edges of the intertidal area. The uniform change in bathymetry performs better for this channel compared to a narrowing. For ap-

proximately the same sediment volume, the velocity increase is two times larger for a uniform change in bathymetry. The original velocities in channel 1 exceed the critical velocity for sand transport during flood and ebb peak. However, historic data shows that the surrounding intertidal areas are eroding. This indicates that although there is sediment supply from the tidal channel, the building forces are not large enough. This supply can be increased by influencing the direction of the flow combined with an increase in the velocities. Since the channel has two large bends, these can be used to influence the flow direction.

The hydrodynamic behaviour of channels 2 and 4 as a result of bathymetric changes, proved to have significant potential regarding a channel nourishment. These channels will therefore undergo a more detailed hydrodynamic and morphodynamic study in the form of two case studies. In the channel 2 case study, different bathymetry changes will be applied to the original bathymetry. Here the direct proportionality between the velocity changes and sediment volume will be studied as well as the location of the nourishment. The emphasis of the channel 4 case study will be on influencing the direction of the flow, thus the sediment transport. By first studying the hydrodynamic effect of the bends present in this channel, locations for a nourishment can be determined. Ultimately the effect on sediment transport for both cases will be studied regarding shape, volume and lifetime of a possible nourishment. Channel 2 and 4 will be further elaborated in Chapter 5 and Chapter 6 respectively.

5

Case Study: ”De Krabbenkreek”

In this chapter, we will elaborate on step 5 of the main research approach (see Section 1.6). In the first place, we will study the effect of different nourishments in the Krabbenkreek on the hydrodynamics in Section 5.2. Hereafter, the effect on sediment transport of one case will be analysed in Section 5.3.

5.1. Methodology

The Krabbenkreek channel, which was referred to as channel 2 in the previous chapter showed promising results regarding velocity increases. Considering the results presented in Chapter 4 and the grid size resolution in this channel, the uniform way of applying a nourishment is preferred. Firstly, in Section 5.2 different nourishments are simulated hydrodynamically. These nourishments differ in way of nourishing and in volume. Two ’new’ ways of nourishing are introduced in Figure 5.1. A channel can be nourished up to a certain depth (method 1) or a certain height can be added to its original depth (method 2). The downside of method 1 is that shallow regions are likely to get elevated above MSL. The downside of method 2 is that some locations are above the desired depth and need to be dredged which could be more time consuming. The cases will be analysed on efficiency (relation between the volume of sediment and the velocity magnitude change) and compared with each other. The case with the most potential will undergo a morphodynamic study in Section 5.3. In the first place, the sediment transport of the base case will be discussed as well as the model’s parameters. The effect of the nourishment on the sediment transport will thereafter be analysed in two different ways. Firstly, the effect of the nourishment on the surrounding sediment transport will be analysed. Secondly, solely the sediment transport induced by the nourishment will be studied. Finally, conclusions will be drawn regarding this channel and the feasibility of a tidal channel nourishment in the Krabbenkreek.

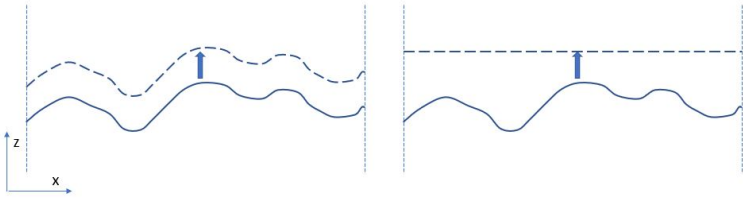

Figure 5.1: Schematic of a fictious longitudinal cross-section of a channel with on the left method 1 and on the right side method 2

5.2. Hydrodynamic study

The Krabbenkreek has been introduced in Chapter 4 and its main boundary condition regarding the depth is that there are two harbours present. In Figure 5.2a, a schematic version of the Krabbenkreek is depicted, showcasing the large surrounding intertidal area and its variation in the form of sand flats, fringing flats, and well-established salt marshes with an abundance of meandering channels. Next to that, the navigation channel is indicated in a dashed line, the colors indicate which depth has to

be guaranteed regarding the draft of the ships navigating through this channel, -5 & -3 m NAP(van Maldegem, 2007). Next to this schematic overview, the detailed bathymetry is depicted in Figure 5.2b, where the flood and ebb channels are indicated in red and black respectively. Here, the diversity in bed level can be observed.

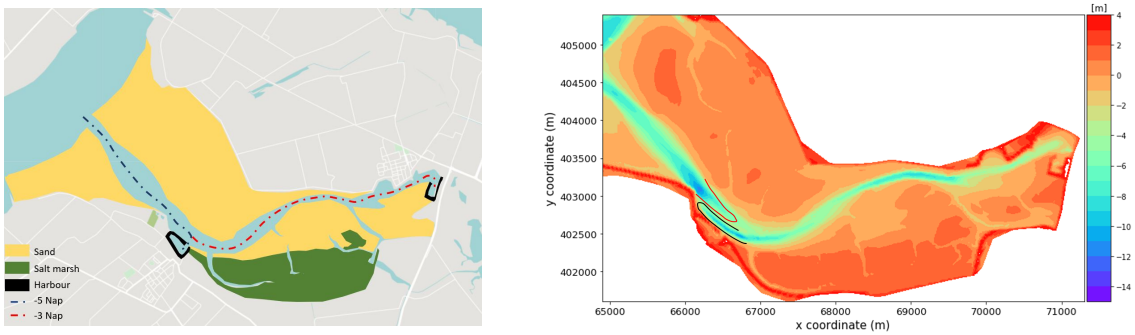

(a) Schematic overview of the Krabbenkreek study area

(b) Detailed bathymetry of the Krabbenkreek study area

Figure 5.2: Overview of the Krabbenkreek study area

In Chapter 4, we suggested that there is a direct proportionality between the nourished sediment volume and the local velocity increase. The bathymetry of the Krabbenkreek is therefore modified four times, applying each method twice with increasing volumes. The area over which the bathymetry has been modified is situated along the red dotted line which is indicated in Figure 5.2a, guaranteeing the minimum depth of -3 m NAP. By means of a polygon and the QUICKIN module of Delft3D, the bathymetry is modified to create the following four cases (see, Figure 5.3):

- **Case 1**: Method 1: Bathymetry raised by 1.5m, estimated volume = $1.9 * 10^6$ m^3
- **Case 2**: Method 1: Bathymetry raised by 2m , estimated volume = $2.5 * 10^6$ m^3
- **Case 3**: Method 2: Uniform depth of -3.5m , estimated volume = $2 * 10^6$ m^3
- **Case 4**: Method 2: Uniform depth of -3m , estimated volume = $5 * 10^6$ m^3

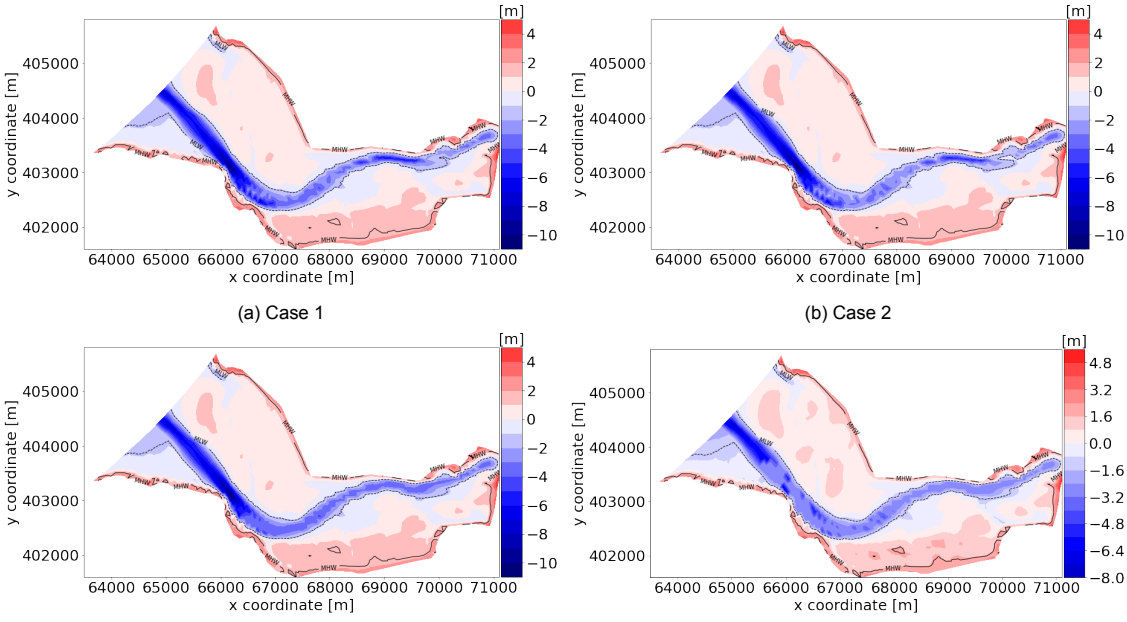

(a) Case 1

(b) Case 2

(c) Case 3

(d) Case 4

Figure 5.3: Overview of the new bathymetry for each case. The depths are relative to NAP.

The goal of these bathymetry modifications is to increase the velocities in the channel such that the velocities exceed the threshold of motion for sand as has been computed in Section A.3 to be 0.45 m/s. The change in bathymetry and its impact on the tidal velocities for all cases are depicted in Figure 5.4. See Section 4.2 for an explanation of the plots.

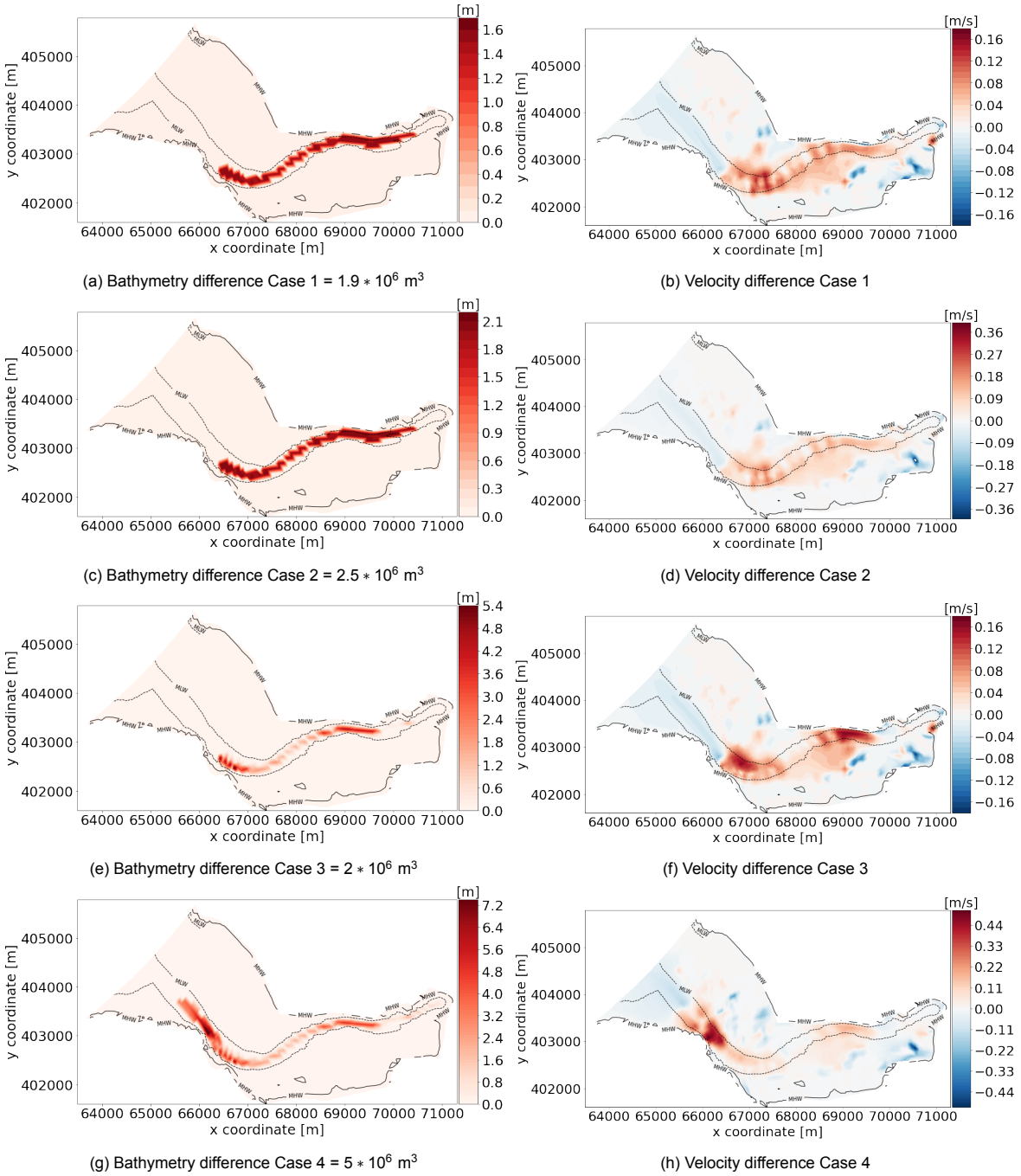

(a) Bathymetry difference Case 1 = $1.9 * 10^6$ m^3

(b) Velocity difference Case 1

(c) Bathymetry difference Case 2 = $2.5 * 10^6$ m^3

(d) Velocity difference Case 2

(e) Bathymetry difference Case 3 = $2 * 10^6$ m^3

(f) Velocity difference Case 3

(g) Bathymetry difference Case 4 = $5 * 10^6$ m^3

(h) Velocity difference Case 4

Figure 5.4: On the left column, changes in bathymetry representing a possible nourishment are depicted. On the right column, the resulting change in velocity representative for when the velocities are maximal during flood, this moment is indicated on Figure 5.7 as a blue vertical dotted line.

On the left column, the two methods are clearly recognizable, the first two cases undergo the same bed change over the whole polygon while the second two cases undergo different bed changes along the polygon. A similar pattern is visible in the velocity difference plots, the velocity difference pattern is approximately in line with the bed level differences. One difference that does stand out between both

methods is the shape of the increase in velocity. When comparing cases 1 and 3, the difference in case 3 has a more diffusive look whereas the difference in case 1 has a more step-wise look. This is due to the fact that the shape of the original bathymetry is conserved with method 1 and thus for case 1. On the contrary, with method 2, the bathymetry has been flattened out which leads to this more diffusive look in the velocity. The aim of reducing the cross-sectional area is to increase the velocities. What can be observed in every case, is that the change in bathymetry has an increasing impact on the velocity of the nourished areas. There are however some locations where the flow decelerates compared to the base case. One is a minor deceleration zone in the first, deeper part of the channel where no bottom changes are applied. These decelerations can be the consequence of a minor discharge redistribution between the channels. As the nourishments induce extra friction on the flow, the discharge reduced by 1-8 % (see Appendix B.2.1). Consequently, the flow velocities on the areas without a reduction in cross-sectional area reduce. Considering the velocities in the Krabbenkreek channel as a result of the nourishment increased by 0.1-0.2 m/s, the reduction in discharge can be neglected. However, this indicates that the system is adapting to the extra friction caused by the nourishment and that part of the discharge is deflected towards one or more channels. Furthermore, in general in the intertidal area, some single locations experience larger decelerations.
The order of magnitude of the positive velocity change is the same for cases 1 and 3 (0.15-0.2 m/s) for approximately the same nourished volume. This shows that the way of supplying sediment (different method but exact same area) doesn't impact the outcome significantly in this specific situation. Furthermore, the difference in velocity increase between cases 1 & 2 and between cases 3 & 4 is clearly visible. This confirms the hypothesis that with larger nourishment, larger increases can be obtained, hence the nourished volume is directly proportional to the change in velocity.
Although the largest changes can be observed below MLW-line, there are some positive velocity changes occurring between MLW- and MHW-line which could be beneficial for sediment transport towards the intertidal area as was discussed in Section 2.6.
From the previous simulation results, it is hard to draw conclusions regarding which case has the most potential. To be able to analyse these cases effectively a step back towards the aim of this case study is taken. With the reduced tidal prism and the waves eroding the intertidal area at the same rate as before the construction of the barrier, the aim of this case study is to increase the velocities and thus increase the building forces of the intertidal area. To this end, in the following plots, the cases are compared with each other regarding the critical velocity for sand. In Figure 5.5, the velocity of the base case is plotted in a masked way, only velocities larger than 0.45 m/s are plotted, velocities smaller are plotted in blue. This figure visualises that the critical velocity is reached until half of the channel (x coordinate 69 km). This means that when velocities are near maximum in the channel, no sand transport as a result of the tidal propagation is enhanced in the second half of the channel. All 4 modified cases will be compared to the base case and judged based on how far the critical velocity is guaranteed, these results are depicted in Figure 5.6.

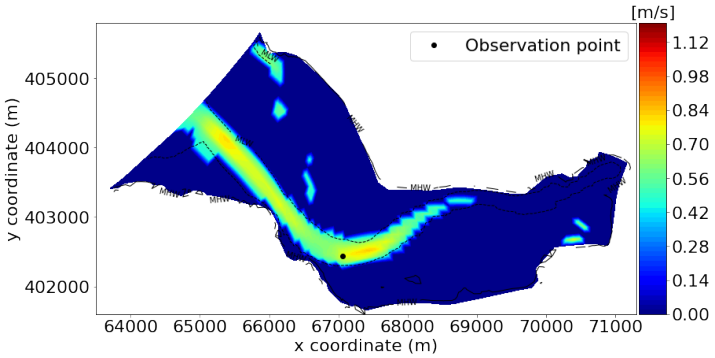

Figure 5.5: The depth averaged velocities larger than 0.45 m/s are plotted according to the color bar, values smaller than that are plotted in dark blue. This plot represents a specific time step during a flood peak, when the velocities are expected to be maximal, this time step is the same for every plot. The observation point is used to measure the simulated velocities that are plotted in Figure 5.7

To be able to compare the four cases efficiently, the depth averaged velocities are plotted schematically. Four conditions can be identified and are given in Figure 5.6e. Firstly, it can be observed that for cases

2, 3, and 4, the critical velocity for sand transport reaches approximately the same location, 750 m further than the base case. Case 4 is the only case to present a significant decrease in velocities at the entry of the channel. Elsewhere and for other cases, the nourishment has no negative impact on the critical velocity. Considering the relation between nourished volume and the effect on the velocities, it can be concluded that for method 1 no difference is observed while for method 2, case 4 presents the same positive impacts while also presenting a large deceleration. Furthermore, it is clear that method 2 performs better than method 1 when comparing the results of cases 1 and 3. With approximately the same nourished volume, the effect on the velocities is significantly larger for case 3. In addition, case 3 has the same impact as case 4 with less than half the amount of sediment regarding how far the velocity is guaranteed.

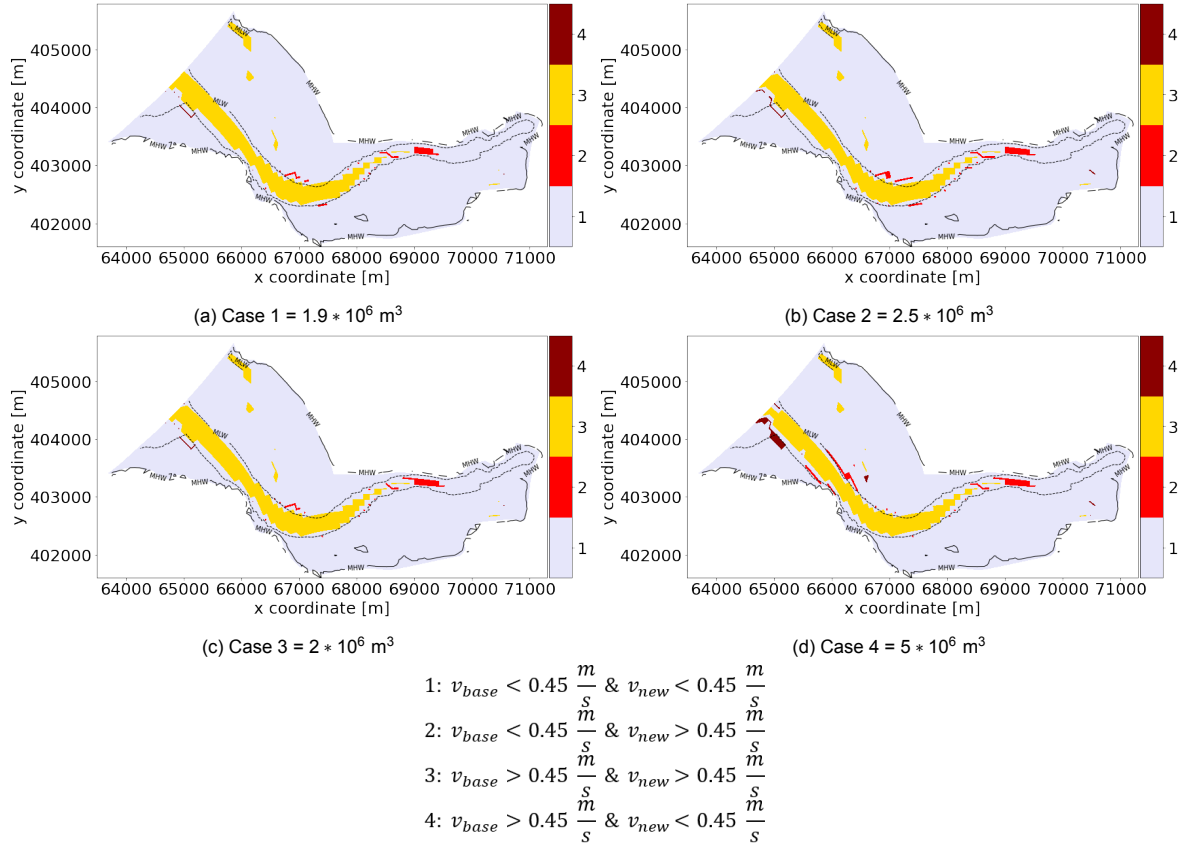

(a) Case 1 = $1.9 * 10^6$ m^3

(b) Case 2 = $2.5 * 10^6$ m^3

(c) Case 3 = $2 * 10^6$ m^3

(d) Case 4 = $5 * 10^6$ m^3

1: $v_{base} < 0.45 \frac{m}{s}$ & $v_{new} < 0.45 \frac{m}{s}$

2: $v_{base} < 0.45 \frac{m}{s}$ & $v_{new} > 0.45 \frac{m}{s}$

3: $v_{base} > 0.45 \frac{m}{s}$ & $v_{new} > 0.45 \frac{m}{s}$

4: $v_{base} > 0.45 \frac{m}{s}$ & $v_{new} < 0.45 \frac{m}{s}$

(e) Scale explanation

Figure 5.6: These plots represent the depth averaged velocities at a specific time step when the velocities are maximal during flood, this time step is the same for every plot (indicated in Figure 5.7). The scale on the plots is numbered 1-4, Figure 5.6e illustrates what the scale stands for.

All the previous results are representing a specific moment in time during flood when the velocities are maximal. The emphasis is in this way on the maximal velocity at a specific moment in time and not on the period over which this velocity is reached. Increasing the period over which this critical velocity is reached is valuable considering sediment transport. If the period during which sediment transport takes place is able to expand, it is hypothesised that the sediment transport rates will expand accordingly. In Figure 5.7, a time series of the velocity for the base case and the nourished cases is plotted for the observation point indicated in Figure 5.2b. These model results show that next to an increase in maximal velocities both during flood and ebb, the period along which the critical velocity is reached has extended for all cases. In some cases, this period increases significantly, especially during ebb. In Case 2 for example, an increase of approximately one hour is observed on the original 3 hours which is roughly a 33% increase. The applied bed changes led to a decrease in the flood period and an increase in the ebb period. Furthermore, it can be observed that the ebb velocities are at their maximum during a

longer period than the flood velocities although the maximal flood velocities are larger. This can be due to bathymetry-induced residual currents that occur in channels with a deep central part and shallower sides. In the deeper central part, there is a net ebb current and a net flood current on the shallower parts (Bosboom and Stive, 2015). Since this observation point is in the middle of the channel and thus in the deeper part, this theory can be applied here as an explanation for the observations. Although method 1 presents better results regarding the extension of the critical velocity period, it will be disregarded from this point on as it is not likely to be executed regarding constructability. The increase in period for case 4 is larger than for case 3 even though the differences are small. Considering the difference in volume needed to complete these nourishments and the small differences presented in Figure 5.6, case 3 has more potential and will be further analysed in Section 5.3.

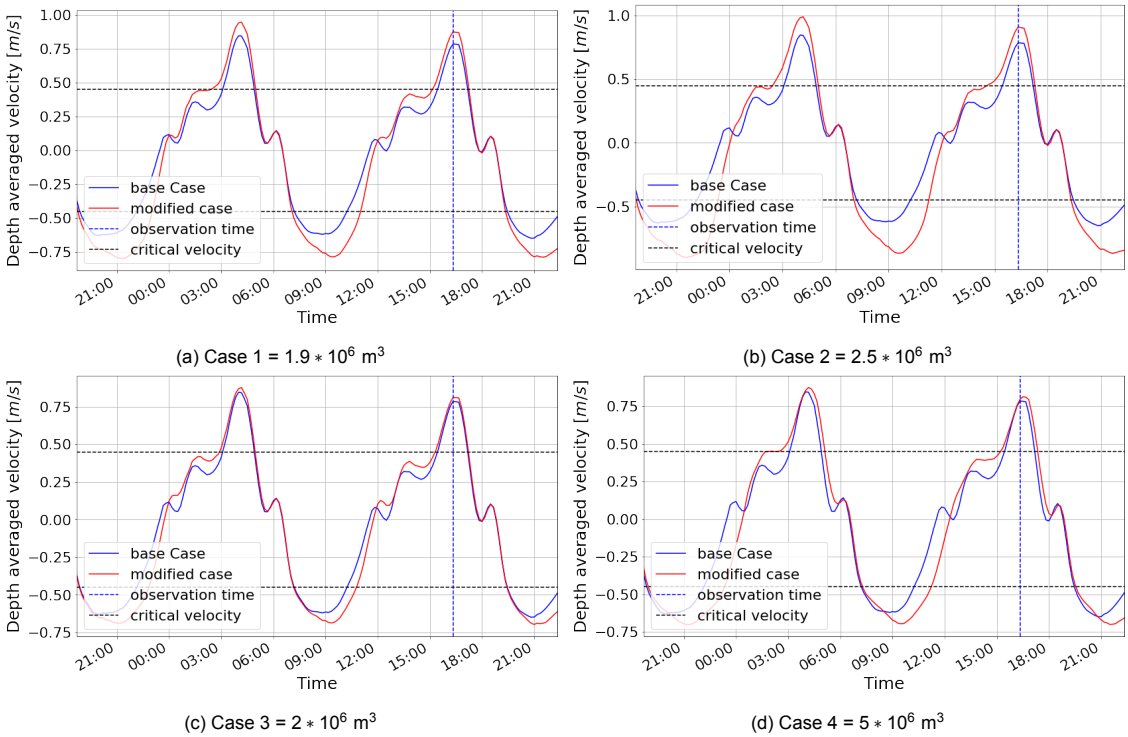

(a) Case 1 = $1.9 * 10^6$ m^3

(b) Case 2 = $2.5 * 10^6$ m^3

(c) Case 3 = $2 * 10^6$ m^3

(d) Case 4 = $5 * 10^6$ m^3

Figure 5.7: Depth averaged velocity time series from the ScalOost model for all 4 cases. The positive velocities are representing flood and negative velocities ebb. The base case is plotted in blue and the same for all 4 plots while the red plot is the modified case and different for each case.

5.3. Morphodynamic study

5.3.1. The base case

In Section 3.3.2, the performance of the model regarding simulating sediment transport is discussed. Mostly, large patterns are treated in that section whereas here a more location-specific validation is performed by looking at smaller scale patterns. This is done with the aim of better understanding the results of the simulations and ultimately knowing to what extent the results can be used in conclusions. In Figure 5.8, both the measured data and the simulation results are depicted. In Figure 5.8b, it can be observed that the center part of the channel is eroding and depositing on the sides near the MLW-line. There are two side channels that also seem to follow the trend of deepening and narrowing. The lozenge shape of the bed level changes is caused by a combination of the grid cell dimensions being large compared to the channel width (+- 2 cells) and by the orientation of the cells compared to the channel. This results in a bathymetry around the bend consisting out of many small lozenges the one after the other. Simulations with larger morphological scale factors or longer simulation periods all result in the same lozenges pattern and consequently do not indicate any numerical instability. The data in Figure 5.8a, show erosion/sedimentation in the first half of the channel with clear erosion in the large bend and clear sedimentation in the second half of the channel. The combination of the intertidal

area mostly eroding, and the channel accreting (second half of the channel) are indicators for sediment starvation. The large differences between the data and the simulation results are a consequence of a lack of forcing. Considering the forcing only consists out of the tide and wind-induced stresses, locations where the critical velocity is not reached, no other forcing is present to initiate sediment transport. As discussed in Section 3.3.2, this is due to three things: not taking waves into account, only taking one sediment type into account, and finally, the wind climate that is not representative for storms. Where the velocities are relatively high, in the first part of the channel, the simulated patterns and measured patterns are comparable. For locations where the velocities are lower than the critical velocity, the effect of other processes that are not taken into account by the model increase, leading to totally different patterns. The sediment transport results of the ScalOost model for this part of the basin must be analysed with care. It is assumed that the obtained simulation results coincide with the transport as a consequence of the tidal propagation only. However, no direct conclusions can be drawn regarding total sediment transport, the result can only indicate the effect of the velocities on the sediment transport.

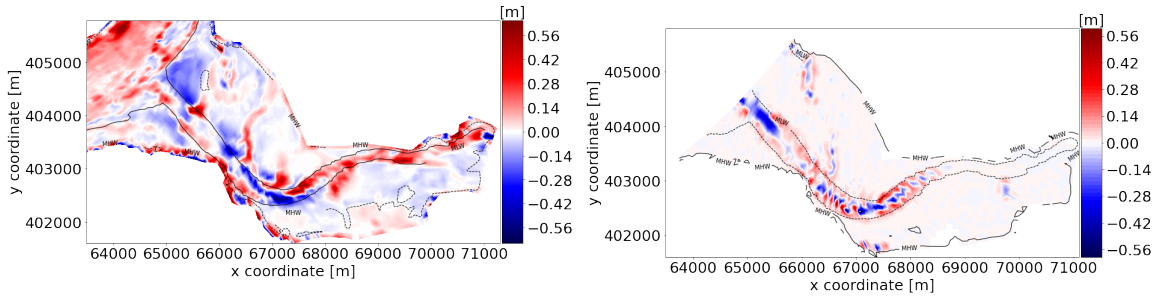

(a) Data (LiDAR) of the sedimentation/erosion in the period 2013-2019

(b) Simulation results of net sedimentation/erosion in 2013-2014

Figure 5.8: Comparison between data and model predictions of the Krabbenkreek. Both have the same scale, values that are larger than 0.6 or smaller than -0.6 are assigned as 0.6 and -0.6 respectively for comparing purposes

5.3.2. Nourishment

Considering the positive impacts of the case 3 tidal channel nourishment on the hydrodynamics, case 3 was chosen to have the most potential. Here the effect of the nourishment on the existing sediment transport and the evolution of the nourishment solely is analysed in two ways as stated in the methodology. The first one being that the whole bottom is erodible and the effects on the surroundings are taken into account. The second one being that only the nourishment is made erodible and in this way, the behavior of strictly the nourishment can be analysed. The results are presented in Figure 5.9. It can be observed that in both figures, changes are limited to the channel and up to the MLW-line. Considering that multiple factors are not taken into account such as waves, storms, and different grain sizes and that the critical velocity for transport is not exceeded elsewhere, this result was expected. Waves do not only erode the intertidal area but are also part of the building process by (re)suspending sediment and spatially distributing it onto the intertidal area (Malvarez et al., 2001). Consequently, sediment particles that are accumulating near the MLW-line (on the edges of the intertidal area), are likely to be brought in suspension and deposit further on the intertidal area. Sedimentation around the MLW-line is therefore seen as a positive result.

The results depicted in Figure 5.9a, represent the whole Eastern Scheldt basin being erodible. This result has lozenge patterns in the centre of the channel that alternate between erosion and sedimentation. The cause for these patterns is discussed in Section 5.3.1. Even though the nourishment has created a flat bathymetry, the results presented are the differences between the base case (where these lozenges are still present) and the nourished case. Besides the lozenge pattern in the central part of the channel, the edges of the intertidal area are accumulating more sediment than in the base case. This result indicates that the nourished sediment in the central part of the channel is eroding and settling on the sides of the channel which could be beneficial.

The result presented in Figure 5.9b represents the nourishment only. Comparing both results shows how much the surrounding sediment transport can influence the behavior of a nourishment. In this case, the results are comparable with a mostly eroding central part of the channel and accumulating sides of the channel, near the MLW-line. Furthermore, no significant difference in magnitude is ob-

served between both methods. As previously introduced, the result is regarded as positive if there is an accumulation of sediment around the MLW-line. On these spatial plots it is hard to observe and quantify the accumulation of sediment near the MLW-line. To this end, cross-sections are introduced in Figure 5.9b to illustrate the smaller scale changes above the MLW (-1.35 m NAP). The location of these cross-sections is arbitrary and is at approximately the same interval.

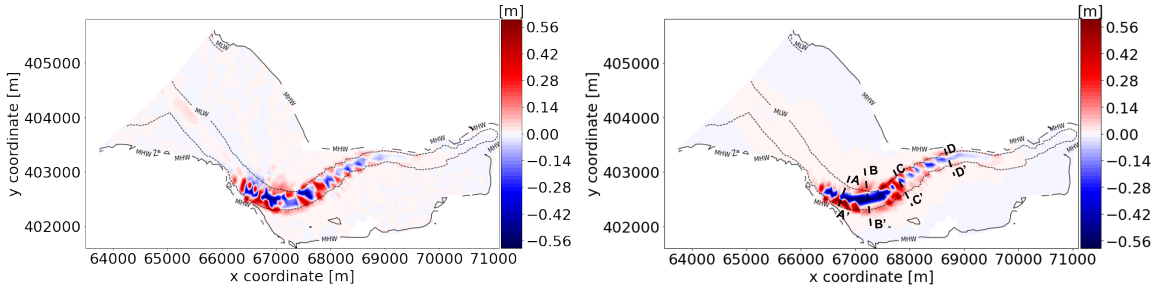

(a) The whole bathymetry is erodible

(b) Only the nourishment is erodible

Figure 5.9: On Figure 5.9a, the difference between the sedimentation/erosion of the base case model result depicted in Figure 5.8b and the model result of the case 3 nourishment depicted in Figure 5.4e is plotted. In Figure 5.9b, the model result of the sedimentation/erosion is plotted where only the nourishment consists out of an erodible layer of 5 m of sand.

Figure 5.10 depicts the evolution of the nourishment on the various cross-sections. As was previously observed on the 2D plots, the various cross-sections are deepening and narrowing after the application of the nourishments. The consequence of the grid cell resolution and orientation can be observed in the accuracy of the execution of the nourishment. The depth should be reduced to a depth of -3.5 m on all cross-sections whereas on cross-sections B-B’ and D-D’, the depth has been reduced to -3 m. On the right column of Figure 5.10, the cumulative sedimentation/erosion is depicted for locations that are above the MLW-line on the cross-section, where sedimentation is indicated as positive and erosion as negative. This is done to better illustrate the changes in the area of interest. The results are bed changes in the order of 5 cm and are mostly positive. Cross-section B-B’ illustrates an example where both sides of the channel are accumulating sediment which could thus be positive for the intertidal area to the north and to the south of the channel. Only cross-section C-C’ presents a negative result in the form o erosion above the MLW-line. Furthermore, it can be observed that the changes occur near the MLW-line and not much higher, due to the forcing.

In order to quantify the results in the form of a volume fraction of the nourished volume that eventually reaches the intertidal area, the following calculation is introduced. All bed changes above the MLW-line have been summed up and multiplied with the average grid cell dimensions which are estimated to be 80 m x 95 m. The sediment volume that originates from the nourishment and settles above the MLW-line following this calculation is estimated to be 40.000 m^3 which accounts for 2% of the original nourishment. Considering 2.5% of the nourishment erodes, the percentage of the eroded sediment that settles onto the intertidal area is 80%. This is for the simulation with only the nourishment as erodible sediment. For the simulation with the whole bottom being erodible, this volume is estimated to be 53.000 m^3. The volume that originally settles above the MLW-line in the base case is estimated to be 26.000 m^3. Subtracting both simulations with the whole bottom as erodible gives a volume difference of 27.000 m^3, which is an increase of 100% compared to the base case.

As stated in Section 5.3.1, the simulated changes on the intertidal area are not comparable to the data and can not be used to draw any conclusions. However, these numbers give an indication that the nourishment could have the potential to counter the sediment starvation in this part of the basin. Furthermore, it was argued that the changes near the MLW are hypothesised as having an acceptable accuracy. The simulation with only the nourishment as an erodible layer resulted in bed changes no much higher than the MLW-line and can therefore, be seen as results with acceptable accuracy. These results present an increase of approximately 100 % compared to the base case which can be valuable. Considering the simulation period being one year, long-term evolution has to be approached by means of a hypothesis based on the results of the simulation. The nourished sediment is not migrating towards the entry of the channel but is rather dispersing towards the sides by eroding the centre part and settling on the sides. When comparing the bed level changes at the start of the simulation with the end of the

simulation, the changes are comparable in size. This indicates that the nourishment could continue to supply the intertidal area with the trend of 2% per year. This trend is however expected to slow down due to the negative feedback system between the velocity and the cross-sectional area of the channel.

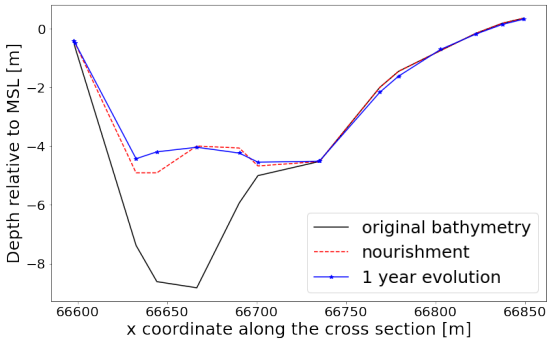

(a) 1 year evolution nourishment cross-section A-A'

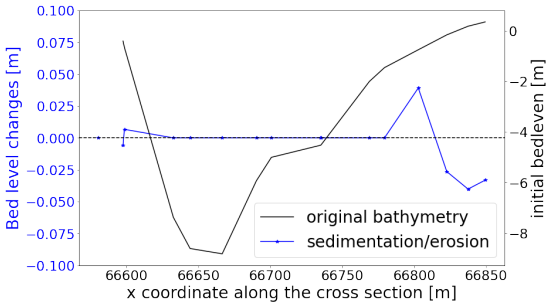

(b) Cumulative sedimentation/erosion above MLW after 1 year

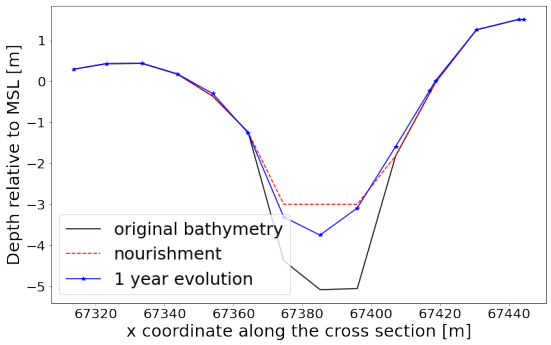

(c) 1 year evolution nourishment cross-section B-B'

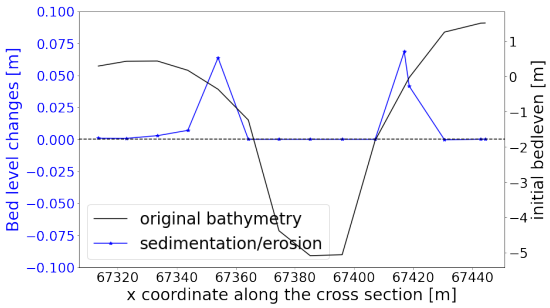

(d) Cumulative sedimentation/erosion above MLW after 1 year

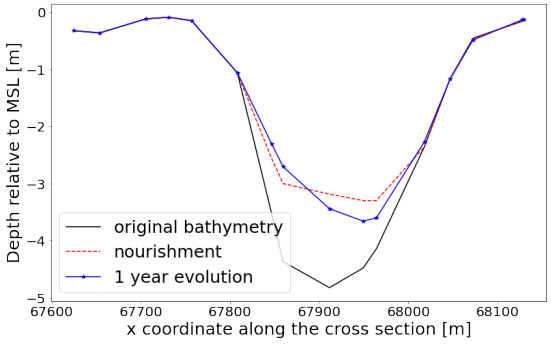

(e) 1 year evolution nourishment cross-section C-C'

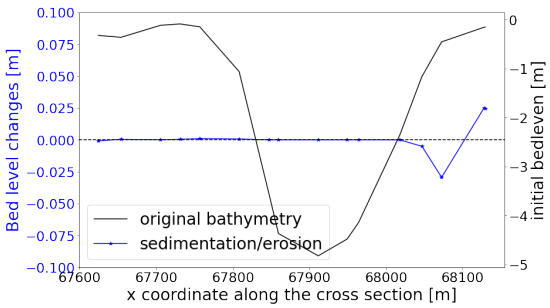

(f) Cumulative sedimentation/erosion above MLW after 1 year

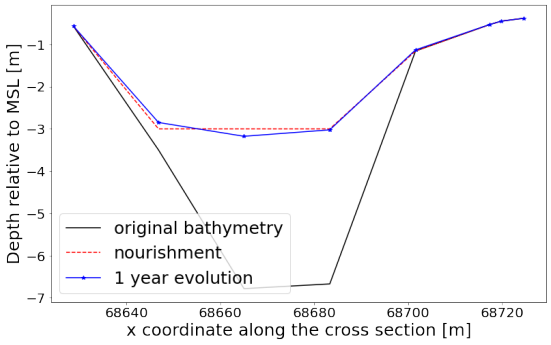

(g) 1 year evolution nourishment cross-section D-D'

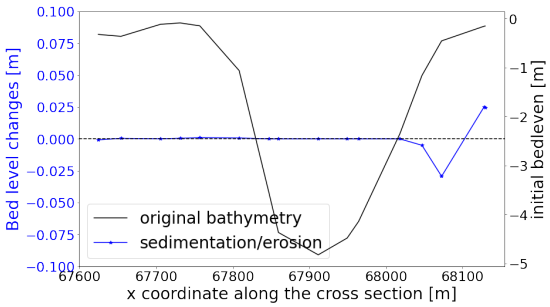

(h) Cumulative sedimentation/erosion above MLW after 1 year

Figure 5.10: On the left plots, the evolution of the cross-sections is illustrated. The original bathymetry is indicated in black, the resulting bathymetry after a nourishment is indicated in a dashed orange line and finally the 1 year evolution of the nourishment is indicated in blue with stars. On the right plots, next to the original bathymetry, the sedimentation (positive) /erosion (negative) above the MLW line is illustrated together with a new axis.

5.4. Discussion & Conclusion

The Krabbenkreek showed promising results regarding the hydrodynamics in Chapter 4 and confirmed its expectations in this chapter. Reducing the cross-sectional area of the Krabbenkreek channel in various ways increases both the ebb and flood velocities on the area where the bed changes are applied. Accelerations in the order of 0.15 m/s were obtained such that the critical velocity for sand transport (0.45 m/s) was reached approximately 750 metres further into the channel. Besides an absolute velocity increase, the period along which the critical velocity is reached has increased in the order of 15 minutes up to 1 hour. Elsewhere, minor decelerations were observed as a consequence of the increase in friction due to the nourishment. Evening the bed up to a certain depth (method 2) has been chosen as the way of nourishing in view of constructability. The direct proportionality between nourished volume and velocity increases has been observed in the results. However, this should be applied with care as simulation results show a decrease in discharge as a result of the nourishments.

The objective of the Krabbenkreek nourishment has been described as increasing the velocities in the channel above the critical velocity, such that sediment transport from the channel towards the intertidal area is enhanced. Considering the aim of the nourishment, the ratio of nourished volume / effect on the velocities and the channel to be a navigation channel with a minimum depth, a uniform nourishment of 2 million m^3 was chosen to be the case with the most potential. The nourishment shallows the second half of the channel up to a depth of -3.5 m NAP, leaving a margin of 0.5 m for navigational purposes.

Considering the limited accuracy of the model regarding sediment transport in this area of the Eastern Scheldt basin, direct conclusions can not be drawn. The latter is the consequence of a simplification. More specifically, waves are not taken into account in view of keeping computational times relatively low, although waves play a major role in sediment transport on the intertidal areas. Furthermore, the sediment type and diameter are not representative for the whole basin as sand with a diameter of 190 μm is only representative for the channel.

There are however multiple results that give indications that a tidal channel nourishment in the Krabbenkreek channel has the potential to feed the surrounding intertidal areas, thus relieve the sediment starvation locally. It is found that a nourishment of 2 million m^3 of sand could lead to an increase in sedimentation on the intertidal area of 100% per year, with regards to the actual situation. The sediment that settles onto the intertidal area after one year represents 2% of the initial nourishment. It is hypothesised that the local system changed from a sediment starvation regime towards a sediment excess regime. This together with a significant velocity increase and extra sediment settling on the intertidal area, is a positive result in view of maintaining the present levels of the surrounding intertidal areas. Furthermore, it is hypothesised that the rate at which the nourishment is feeding the intertidal areas will be constant and eventually decreases due to the negative feedback mechanism between the velocity and the cross-sectional area. Simulated erosion rates indicate that the lifetime of the nourishment is in the order of decades. Besides the uncertainties that lead to limited accuracy of the simulation results, the concept of nourishing a tidal channel as a mitigation measure against sediment starvation has been proven to have potential. This way of nourishing counters the sediment starvation at its core, the imbalance between the tidal prism and the cross-sectional area of the channels.

6

Case Study: Secondary flow in The Brabantsche Vaarwater

In this chapter, we will elaborate on step 5 of the methodology introduced in Section 1.6. Here we will study the effects on the hydrodynamics, especially the secondary flow of different nourishments in the Brabantsche Vaarwater. Hereafter, this effect will be related to sediment transport and analysed.

6.1. Methodology

Considering the tidal velocities already exceed the critical velocity for sand for half a day, the emphasis will be on influencing and using the direction of the flow in order to increase the sediment transport from the channel towards the intertidal areas. The hydrodynamic study, will in a first-place start with a theoretical approach to estimate the impact of bends on the flow in Section 6.2.1. Here, the physical properties and mechanisms that play a major role are introduced. This theory is then applied in the form of theoretical analysis to the two major bends depicted in Figure 6.1. In Section 6.2.2, numerical computations are executed, such that the secondary flow in bends is computed and can be compared with the results of the theoretical approach. The next steps are similar to the steps in the previous chapter. The first one will be to modify the bed level in both bends and simulate the hydrodynamics influenced by a nourishment in Section 6.2.3. The results of these simulations will then be analysed based on flow direction, secondary flow intensities, and transverse water level differences. After the model has been validated for this specific area regarding sediment transport, the bed level changes as a consequence of the secondary flow solely are estimated by means of numerical calculations. Hereafter, the effects of the nourishment on sediment transport will be analysed in two different ways as was done in the previous chapter. Firstly, the effect of sediment transport of the nourishment and the entire basin is determined by making the whole Eastern Scheldt basin erodible. Secondly, solely the sediment transport induced by the nourishment will be studied by making only the nourishment erodible. In order to visualise the effect of secondary flow on the nourishment, various cross-sections are introduced in Figure 6.1a. Finally, in Section 6.4, conclusions will be drawn regarding this channel and the potential outcome of a channel nourishment.

(a) Schematic overview of the Brabentsche Vaarwater study area along with cross-sections used in Section 6.3.3

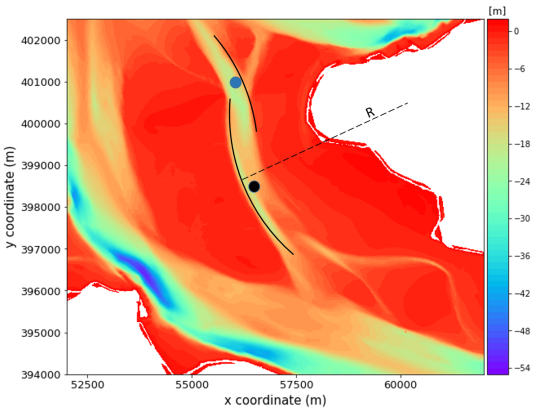

(b) Detailed bathymetry of the Brabentsche Vaarwater study area. The dashed line indicates the radius of the first bend. The blue dot represents observation point 1 and the black dot represents observation point 2.

Figure 6.1: Overview of the Brabentsche Vaarwater study area

6.2. Hydrodynamic study

6.2.1. Coriolis vs Centrifugal effect

Transverse water level differences are the origin of transverse flow and can be caused by 4 mechanisms that can be split up into primary, and secondary mechanisms. The primary mechanism being the tidal wave propagation is hypothesized as being dominant (Swinkels et al., 2009). The secondary flow consists out of the Coriolis and centrifugal effect in the case of bends being present in the channel. The latter two are fictitious forces and are therefore referred to as effects rather than forces. The loss of momentum is not considered here because it being an order of magnitude smaller than the secondary mechanisms (Swinkels et al., 2009). For both the Coriolis and centrifugal effect, the definitions will be discussed together with calculations in order to compare their relative magnitude in this particular situation. The calculations are carried out with the characteristics of the bend corresponding to cross-section A-A', although both bends approximately have the same characteristics.

The Coriolis force acts on every moving particle in the rotating reference frame, to the right in the Northern hemisphere and to the left in the Southern hemisphere (Bosboom and Stive, 2015). The Coriolis effect, therefore, causes water currents to deflect to the right in the Eastern Scheldt basin. The latter means that the effect changes direction when the flow changes from ebb to flood and vice versa. The transverse water level difference caused by the Coriolis effect can be approximated by the following formula (Van Rijn, 1990):

$$\Delta h_{cor} = \frac{f\bar{u}}{g} B \tag{6.1}$$

Where:

- $f = 2\omega \sin(\phi)$
- ω is the radian frequency in [rad/s]
- ϕ is the latitude [degrees]
- $\bar{u}$ is the depth averaged velocity [m/s]
- g is the gravitational force [m/s^2]
- B is the width of the channel which is estimated to be 650 m

When a water particle moves through a bend it does not only experience the Coriolis effect, but also the centrifugal effect. The relative importance of the centrifugal effect is highly dependent on the radius of curvature of the bend. In contrast to the Coriolis effect, the centrifugal effect acts on the same side

of the bend, the outer bend, for both ebb and flood flow. For fully developed flow in the middle part of a wide rectangular bend, the transverse water level difference can be approximated by (Van Rijn, 1990):

$$\Delta h_{cf} = (1 + 3\alpha^2 - 2\alpha^3)\frac{\bar{u}^2}{gR}B \tag{6.2}$$

Where:

- $\alpha = \frac{\sqrt{g}}{\kappa^* C}$
- κ is the Von Karman's constant which is 0.4
- C is the Chezy coefficient and is computed to be ≈80$m^{0.5}/s$
- $\bar{u}$ is the depth averaged velocity [m/s]
- g is the gravitational force [m/s^2]
- R is the radius of curvature which is estimated to be 3800 m for both bends
- B is the width of the channel which is estimated to be 650 m

Now that both forces are formulated and can be computed, the relative effect between both components can be computed for both bends. If stratification is neglected, the transversal pressure gradient is due to the water level slope which counteracts the centrifugal and Coriolis effect (Bosboom and Stive, 2015). In order to compute and compare both forces, a depth averaged velocity of 1 m/s is taken for both cases considering the aim here is to analyze the relative importance.

In Figure 6.2, a schematic overview of both bends in the Brabantsche Vaarwater is given together with the effect of the two components respectively. It can be concluded that although the difference in water level is small, it is present and that the centrifugal effect seems to have a dominant role in the secondary flow. The resulting secondary flow patterns, in cross-section A-A' and B-B', are given in Figure 6.3. On the water surface, the flow is directed towards the outer bend while near the bed, the flow is directed towards the inner bend resulting in the circular pattern. This phenomenon leads the outer bend to erode and the inner bend to accrete, which is visible in the present bathymetry. The latter one can be used to design a channel nourishment where this circular flow is used as means to transport the nourishment towards the intertidal area. An example is sketched in Figure 6.3 and will be further studied by means of the ScalOost model. Next, the simulation results of the base case are discussed and compared with these obtained in the theoretical analysis.

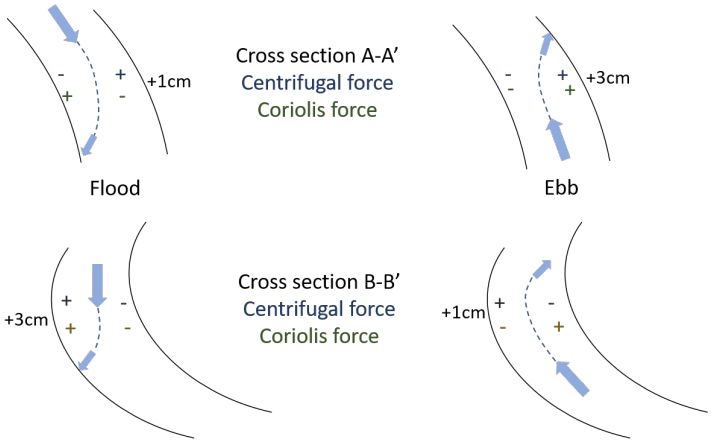

Figure 6.2: A schematic overview of the centrifugal effect compared to the Coriolis effect for both cross sections A-A' and B-B'

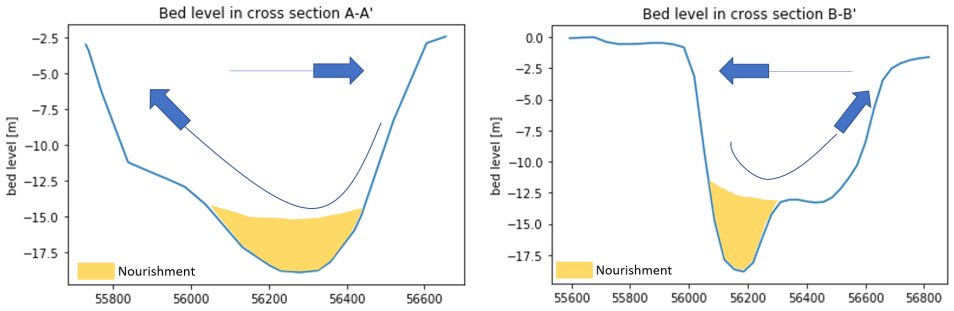

Figure 6.3: Bed level in cross section A-A' and B-B' and the corresponding secondary flow patterns. In yellow, a possible nourishment is schematised.

6.2.2. Secondary flow in the ScalOost model

The ScalOost model is able to take secondary flow into account as is discussed in Section 3.2. The secondary flow intensity is defined here as the velocity component normal to the depth averaged main flow (Delatres). The two plots in Figure 6.4, display the hydrodynamic model results in both bends of the Brabantsche Vaarwater. Two y-axes can be identified. The first one, indicated in blue, represents the depth averaged velocity at an observation point in the bend (see Figure 6.1b). The second one, indicated in red, represents the secondary flow intensity at the same observation point in the bend.

The first plot shows that the secondary flow is in phase with the depth averaged velocity. It can be observed that when the ebb velocities are maximal, the secondary flow (on the bottom) is directed towards the inner bend and is maximal (0.006 m/s). During flood, the magnitude reduces until the direction of the secondary flow changes and is directed towards the outer bend for 3-4 hours (0.002 m/s). These results indicate that although the Coriolis effect is weakly dominant over the centrifugal effect, the net secondary flow averaged over a tidal cycle, is directed towards the inner bend. Due to the curvature of the second bend being in opposite direction than the first bend, the opposite is observed for the second bend. When the flood velocities reach their maximum, the secondary flow is maximal (0.004 m/s), directed towards the inner bend. During ebb, the secondary flow decreases to be close to zero. Since no change in direction is observed, these simulation results indicate that the centrifugal effect is dominant over the Coriolis effect for the second bend. Hence, simulation results show for both bends, near-bottom, the net secondary flow is directed towards the inner bend.

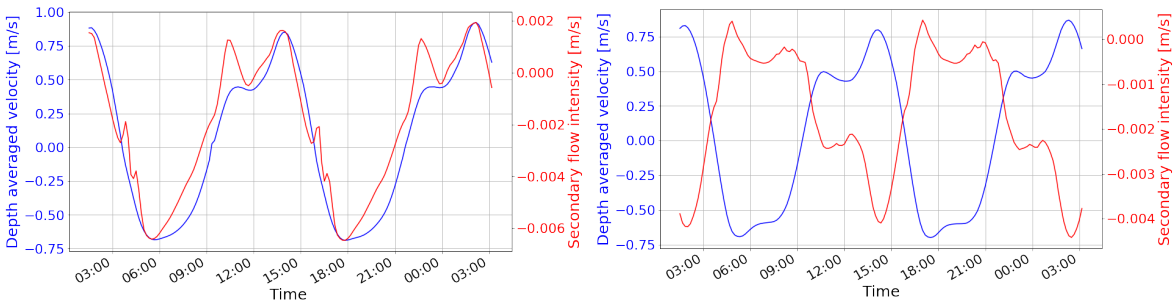

(a) Water level in cross section A-A' during flood

(b) Water level in cross section A-A' during ebb

Figure 6.4: Secondary flow intensity for the base case [m/s] for observation point 1 and 2 depicted on Figure 6.1

The theoretical analysis performed in Section 6.2.1, is compared with the base case simulation results for two cross-sections A-A' and B-B'. The transverse water levels for flood and ebb are depicted in Figure 6.5. The transversal water slope for A-A', changes direction from the inner bend towards the outer bend for flood and vice versa for ebb. During ebb, the Coriolis and centrifugal effect strengthen each other while during flood the Coriolis effect is larger and opposite than the centrifugal effect, thus counteract each other. This indicates that the Coriolis effect is dominant in this bend as was observed in Figure 6.4a. On cross-section B-B', it can be observed that both during flood and ebb, there is a transversal water slope from the outer bend towards the inner bend. Furthermore, the model predicts

that during ebb, the water level difference is smaller (5 mm) between the outer and inner bend compared to flood (15 mm). The latter is the result of the Coriolis effect strengthening the centrifugal effect during flood and weakening during ebb. This result coincides with the theoretical analysis as well as the secondary flow intensity depicted in Figure 6.4b. Considering the main bend characteristics (width and radius), are comparable for both bends, it is hypothesised that the secondary flow in A-A', is influenced by the in and out flow of a side channel to the north of the Brabantsche Vaarwater. Overall, the simulation results indicate that the model can predict the Coriolis and centrifugal effects. The results in cross-section A-A' however, indicate that the desired effect of the secondary flow from the outer bend towards the inner bend is not self-evident during an entire tidal cycle.

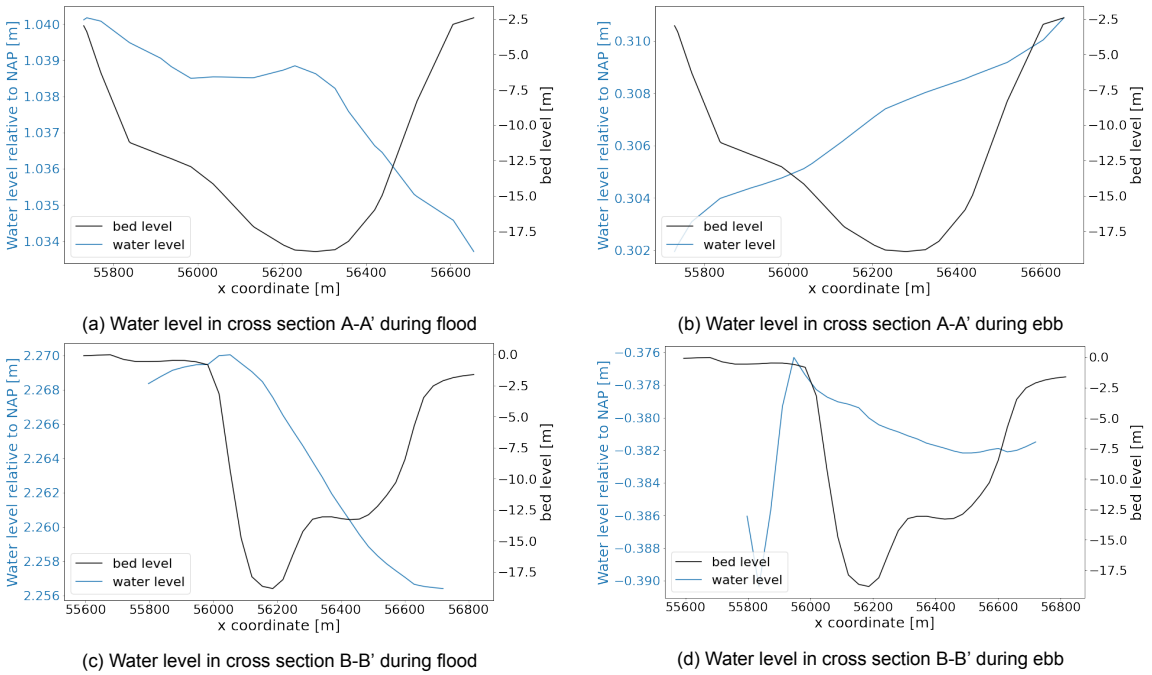

(a) Water level in cross section A-A' during flood

(b) Water level in cross section A-A' during ebb

(c) Water level in cross section B-B' during flood

(d) Water level in cross section B-B' during ebb

Figure 6.5: The transversal waterlevel (blue) and the bed level (black) of cross sections A-A' and B-B'. These plots are representations of specific time periods.

6.2.3. Effect of bathymetry changes on the flow

In Figure 6.3, possible ways of nourishing both bends were introduced (nourishing the deeper, outer bends). By changing the bathymetry in this way, the hypothesis is that the secondary flow will suffer a minor reduction due to a smaller centrifugal effect as a result of a reduction in depth. Next to that, it is hypothesised that the flow will locally accelerate and overflow due to a reduction in cross-sectional area, under the assumption that the flow is not deflected towards another channel. This assumption is confirmed in Appendix B.2.1, where simulation results show that the effect of both nourishment on the discharge is negligible as the discharge reduces by 1-3 %. The effect of such a change in bathymetry is simulated and studied next. In Figure 6.6, the simulated nourishment is depicted for both cases as well as its effect on the depth averaged velocities and the direction of the flow. In Figure 6.6e and 6.6f, only changes larger than 10°are depicted. See section 4.2 for an explanation of the plots. Both cases have the following characteristics:

- **Case 1**, the maximal depth has been set to a depth of 17 m requiring a sediment volume of $750 * 10^3$ m^3
- **Case 2**, the maximal depth has been set to a depth of 13 m requiring a sediment volume of $920 * 10^3$ m^3

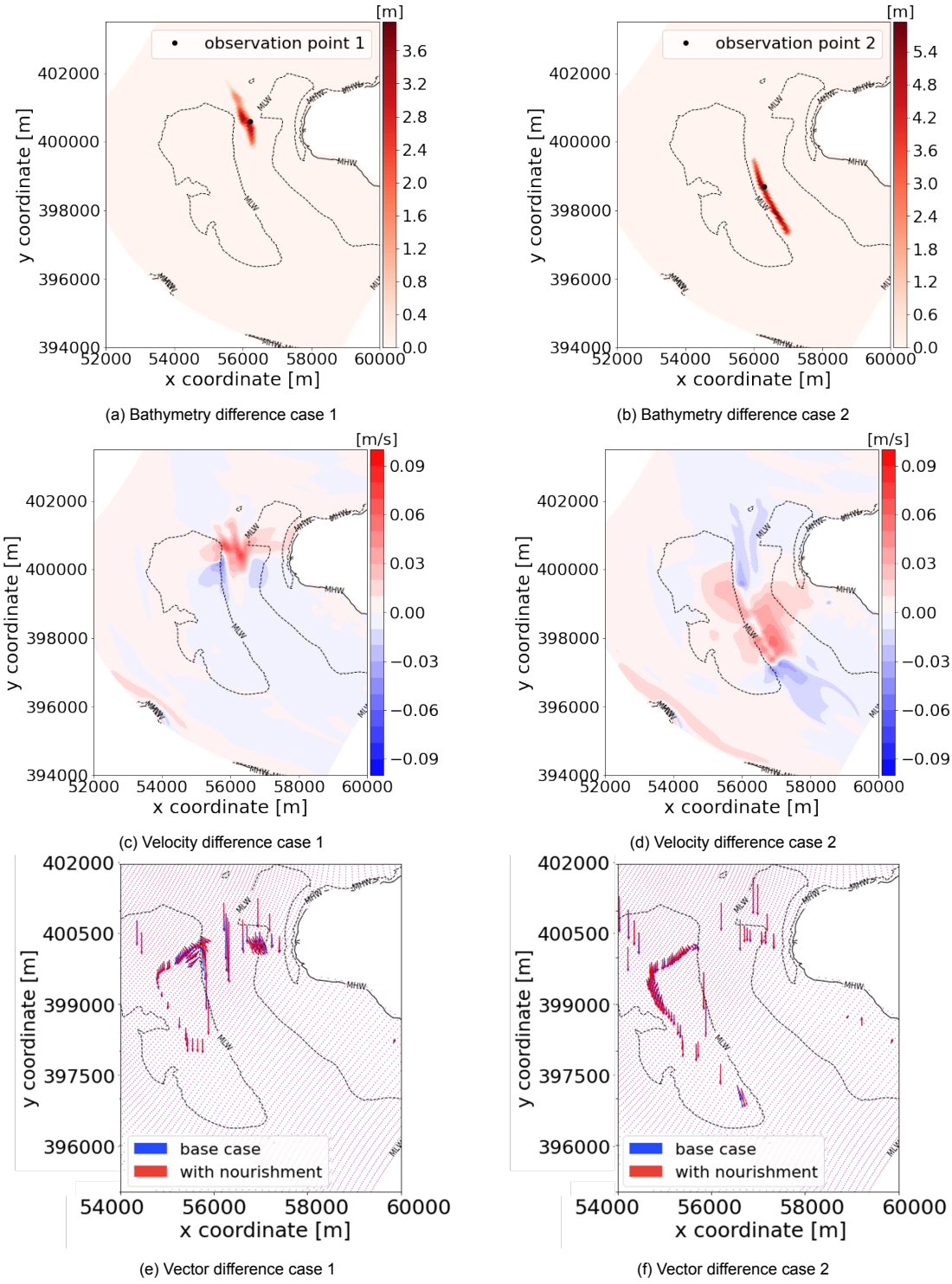

(a) Bathymetry difference case 1

(b) Bathymetry difference case 2

(c) Velocity difference case 1

(d) Velocity difference case 2

(e) Vector difference case 1

(f) Vector difference case 2

Figure 6.6: On the first row, changes in bathymetry representing a possible nourishment are depicted as well as observation points used to measure the simulated velocities in Figure 6.7. On the second row, the resulting change in velocity representative of a moment when the velocities are maximal during flood. This time period is indicated in Figure 6.7 as a vertical blue dashed line. Lastly, the change in vectors is computed following the same method as described in section 4.2.

It can be observed that for case 1, the velocity has increased on the nourishment area as well as on the border of the intertidal areas. Since no significant changes are observed in the channel to the south, it is concluded that no discharge redistribution has taken place between the surrounding channels. Considering approximately the same volume needs to flow through a smaller cross-section, the velocity increases as well and the additional flow on the intertidal areas are confirming the hypothesis. Little

changes in direction occur on the acceleration area, the most changes occur on the Galgenplaat. In Appendix B.1, larger versions of these vector plots are depicted in order to better visualise the direction changes. The direction changes on the Galgenplaat coincide with the assumption that the excess water, flows over a part of the Galgenplaat and then back into the channel. Considering the effect of a nourishment on the transverse water level is negligible (estimated to be 5 mm), the changes in the primary direction cause by a change in secondary flow are hardly visible.

The effect of the second nourishment, is visible on a larger area, although the required volume is similar. Almost no change in velocity occurs on the precise nourished area. On the contrary, significant accelerations (0.09 m/s), are observed on the inner bend as well as on the edge of the outer bend. This indicates that there has been a redistribution of the discharge in a cross-channel direction as more discharge goes through the inner bend than initially. Accelerations on relatively large areas on both the Galgenplaat and the Slikken of Viane are observed. This indicates that more sediment transport towards the intertidal areas may take place. This observation is in line with the observations as a result of sediment disposals in the Western Scheldt (Section 2.6) and the results presented in Chapter 5. Considering the accelerations are located in the originally slower area of the channel, the velocity along the cross-section is distributed more evenly. Both up- and downstream of the nourishment, the flow decelerates. This could be explained by the small decrease in discharge as a consequence of the increase in friction due to the reduction in the cross-sectional area of the channel. As less discharge flows through the same cross-section, the flow will flow slower, thus decelerations are observed. On the nourished areas, the excess water is flowing over both intertidal areas and back into the channel. The primary direction of the flow seems to change and point more towards the Galgenplaat. Furthermore, the same direction pattern as with case 1 is observed on the Galgenplaat.

As discussed in Chapter 5, the period along which the critical velocity is exceeded is a valuable indicator regarding sediment transport. To this end, a time series of the depth averaged velocity for the base case is compared with the nourished cases which are depicted in Figure 6.7. In Figure 6.6c & 6.6d, the location of the observation points is depicted. The velocity magnitude coincides with the spatial velocity plots (Figure 6.6c & 6.6d) and gives therefore a good indication of how the velocities are influenced over time by the nourishments. The period along which the critical velocity is simulated increases slightly, in the order of 10-20 minutes in observation point 1. On the second nourishment, it can be observed that this period could potentially be extended for a total of 3 hours. During flood, two peaks are observed, the physics behind this observation is that during the first peak, the channel overflows onto the intertidal area which causes a temporal decrease in velocity, after which it increases again until its maximal value.

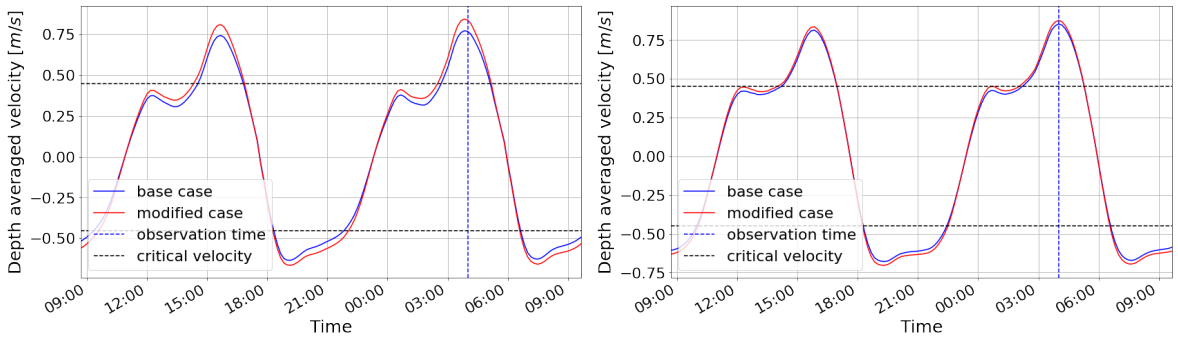

(a) Observation point 1, nourishment = $750 * 10^3$ m^3

(b) Observation point 2, nourishment = $920 * 10^3$ m^3

Figure 6.7: Depth averaged velocity simulation results for the two bends. The positive velocities are representing flood and negative velocities ebb. The base case is plotted in blue and the same for both plots while the red plot is the modified case and different for each case. The vertical blue line indicates the observation time.

Although the changes in velocity magnitude are small, it is a desirable result regarding sediment transport as these would still enhance the latter. The additional flow on the intertidal area is favorable for transport towards the intertidal area considering this flow carries suspended sediment which could potentially settle onto the intertidal area. This is the case unless the velocities on the intertidal area are large enough to (re)suspend sediment and thus cause erosion of the intertidal area. Furthermore, the

period along which the critical velocity is reached increases. The simulation results show that the secondary flow in the second nourishment is likely to cause more sedimentation on the inner bend than on the outer bend. The difference between sedimentation on the inner and outer bend for the first bend is expected to be less. All these factors lead to the conclusion that from a hydrodynamic point of view, both measures may enhance sediment transport towards the intertidal areas. Considering both measures roughly need the same sediment volume and that the effects are comparable in magnitude, the effect on the sediment transport for both measures is investigated next.

6.3. Morphodynamic study

6.3.1. Base Case

In Section 3.3.2, the performance of the model in terms of simulating sediment transport is discussed regarding large patterns. As for the Krabbenkreek case study, smaller patterns are analysed in this section and compared to the data. The result of the base case simulation as well as the data are depicted in Figure 6.8. The intertidal area does not experience any net sedimentation/erosion in the one year base simulation. This is due to a lack of forcing (waves and wind) and the bed only consisting out of one type of sediment (sand with D_{50} of 190 μm). The area below the MLW-line however, does experience bed level changes during the one year base simulation. The sedimentation/erosion patterns below the MLW-line for both the data and the simulation results are comparable. In Figure 6.8b, 4 zones are introduced and are numbered from 1 to 4. To what extent these patterns match with the data is discussed next. Zone 1 is similar to the data. Zone 1 illustrates that there are two major bends in this channel. In the top half of the channel, sedimentation occurs on the inner bend. In the lower half of the channel, zone 1 moves towards the inner bend of the second bend. The presence of bends is also illustrated with zones 2 and 4 which are eroding zones and are located on the outer bends. The latter two are similar to the data, in particular zone 2. Zone 3 is a full sedimentation zone and matches the data. This zone is characterized by being shallower, with smaller velocities where sediment can settle. Regarding the magnitude of bed level changes, there is a significant overshoot by a factor of 5-6, as is discussed in Section 3.3.2. It can be concluded that the model predicts the general erosion/sedimentation patterns below the MLW-line well and that model results can be used to draw conclusions regarding sediment transport patterns.

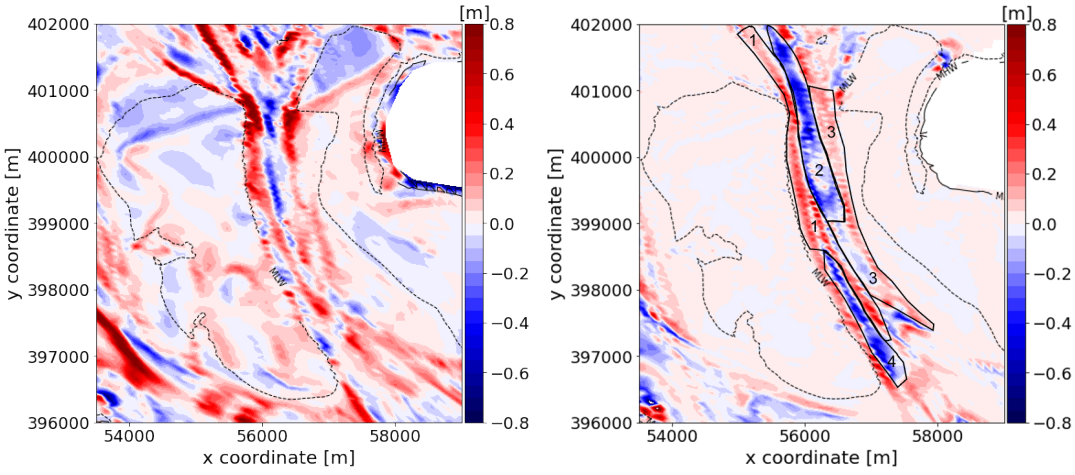

(a) Simulation results of the sedimentation/erosion in the period 2013-2019

(b) Model result of sedimentation/erosion in 2013-2014

Figure 6.8: Comparison between data and numerical simulation results of the Brabantsche Vaarwater. Both have the same scale, values that are larger than 0.8 m or smaller than -0.8 m are assigned as 0.8 m and -0.8 m respectively for plotting purposes

6.3.2. The effect of secondary flow on sediment transport

As discussed in Section 6.2.2, there is a possibility of taking secondary flow into account in Delft 3D. Its effect on the hydrodynamics has been discussed and shown to be comparable to estimations based on theoretical analysis. In this section, the effect of the secondary flow on the sediment transport is

analysed. To this end, simulations of the base case with and without taking the secondary flow into account have been performed. By subtracting the simulated cumulative erosion/sedimentation values from each other, the net effect of secondary flow on sediment transport is obtained as depicted in Figure 6.9. The effect of the secondary flow is in the order of a few centimeters per year. As the base case results overshoot by a factor 5-6, the same overshoot can be expected for the secondary flow. Figure 6.9, shows the same patterns as the base case depicted in Figure 6.8b, indicating that the secondary flow enhances the base case patterns. Here the typical erosion/sedimentation patterns of bends are visible which indicates that the ScalOost model is able to simulate the effect of secondary flow on the sediment transport. The result depicted in Figure 6.9 coincides well with the secondary flow theory dominated by the centrifugal effect as the outer bends erode and inner bends accrete.

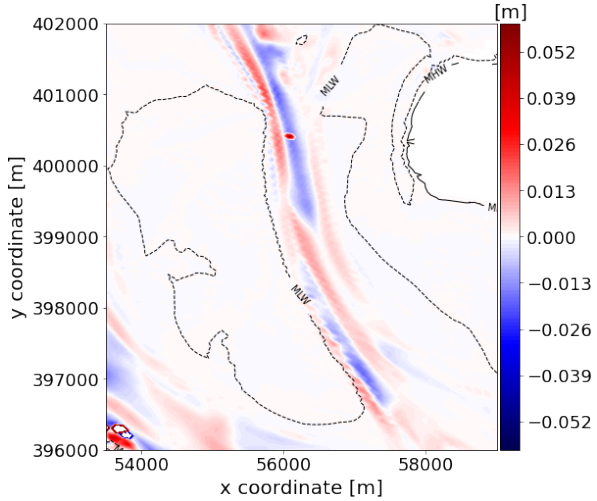

Figure 6.9: Magnitude of bed level changes as a result of the secondary flow

6.3.3. Case 1: Nourishing the first bend

In this section, the behaviour of the case 1 nourishment is analysed by means of two numerical simulations. In a first simulation, the whole bottom of the Eastern Scheldt consists of an erodible layer of 5 m of sand. In the second simulation, only the nourishment is made of an erodible layer of 5 m of sand. The results of both simulations are depicted in Figure 6.10.

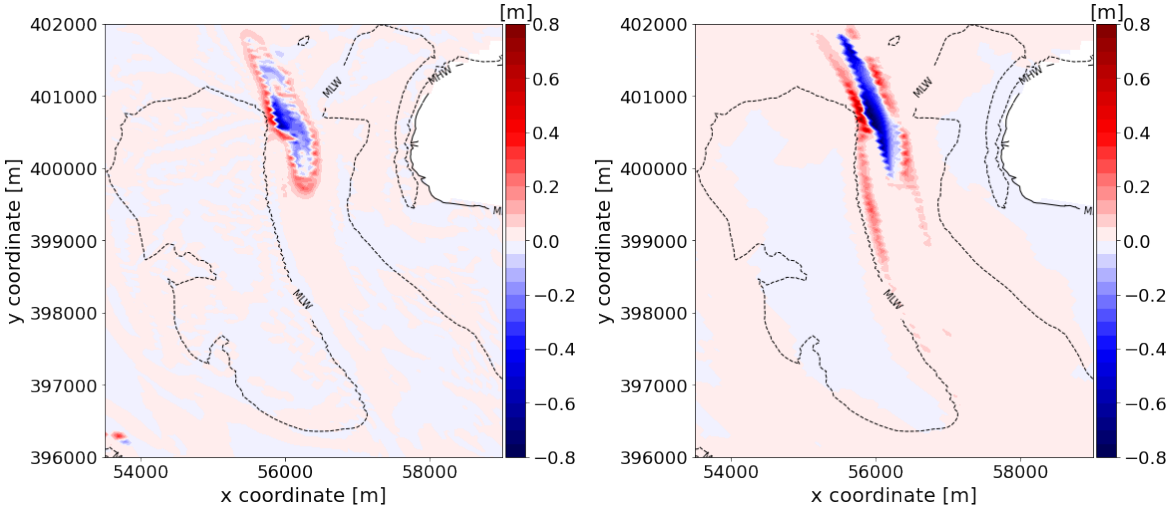

(a) The whole bathymetry is erodible

(b) Only the nourishment is erodible

Figure 6.10: Figure 6.10a depicts the difference between the bed changes of the base case model result depicted in Figure 6.8b and the sedimentation/erosion of the nourishment in the first bend. In Figure 6.10b, the model results of the bed changes are plotted for the case with only the nourishment being an erodible layer of 5 m of sand.

The differences in cumulative erosion/sedimentation between both simulations are significant. In Figure 6.10a, when the whole Eastern Scheldt basin is erodible, the eroded sediment is settling evenly around the nourished area. In Figure 6.10b, the eroded sediment is settling along the sides of the channel, where the tidal velocities are smaller than the critical velocity for sand. During flood, the sediment is transported towards the south and during ebb towards the north. Furthermore, it can be observed in Figure 6.10b that the whole nourished area is eroding while Figure 6.10a also shows some accretion or no changes at all on this area. The latter is also observed on the historic data where either erosion or no changes at all occur in this particular area. For the second simulation, the nourishment is the only sediment available in the entire basin and the velocities exceed the critical velocity for sand transport (see Figure 6.7a). As a consequence, erosion of the entire nourishment area is as expected and observed. These results suggest that the effect of the nourishment on the sediment transport of the entire basin is local as the hydrodynamic changes suggested (see Figure 6.6c). The difference between both simulation results (whole basin vs only nourishment erodible) indicates that the surrounding sediment transport has a strong influence on the evolution of the nourishment. This can be explained by the large velocities and relatively large morphological activity in the surrounding area.

As with the base case, no visible sedimentation/erosion occurs on the intertidal area as a consequence of lack of forcing. Only 0.6% of the nourished sediment (whole basin erodible) reaches the MLW-line or higher in the first year. This volume is representative of 3.5% of the eroded sediment. The remaining eroded sediment is settling in deeper parts of the channel. In Section 6.2.3, it is argued that the velocity magnitude changes together with the direction changes indicate additional flow on the intertidal area compared to the base case. From the results depicted in Figure 6.10, it is hypothesised that the additional flow does not carry suspended sediment due to the relatively small velocity magnitude. The impact of secondary flow on the sediment transport, discussed in Section 6.3.2, is hardly visible in both simulations. A difference in sedimentation between the outer and inner bend of 5 cm is expected (see Section 6.3.2). In order to visualise the evolution near the MLW-line, cross-sections are introduced and elaborated on next.

The longitudinal evolution of the nourishment is depicted in Figure 6.11. It shows that the nourishment has been applied at a constant depth of -17 m NAP and that less than 1 m of the nourishment has been eroded. Calculations show that approximately 16 % of the initial nourishment has eroded in the first year. Furthermore, the sedimentation on both the upstream and downstream parts of the nourishment can be explained by a longitudinal slope adjustment. It should be noticed that the way the nourishment erodes, seems to follow the shape of the original bathymetry.

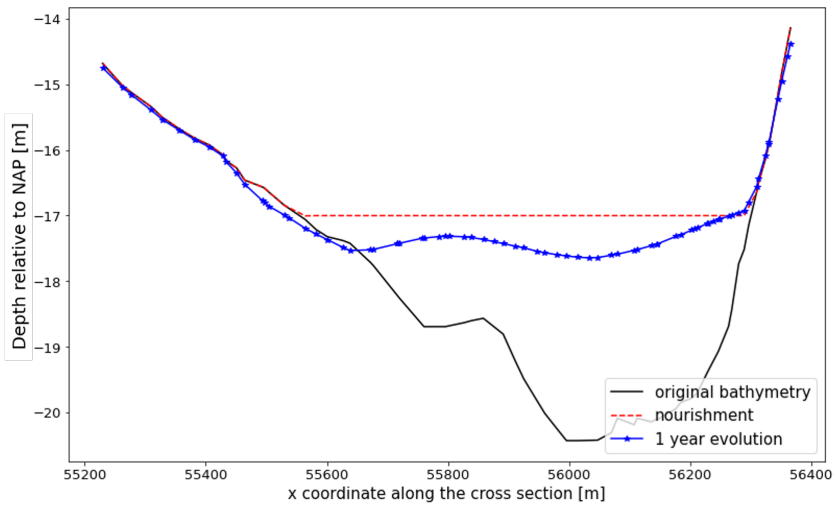

Figure 6.11: 1 year longitudinal evolution of nourishing the first bend (whole bathymetry erodible). The original bathymetry of 2013 is indicated in black, the resulting bathymetry after a nourishment is indicated in a dashed orange line and finally the 1 year evolution of the nourishment is indicated in blue stars

In Figure 6.12, the one year morphological evolution of the nourishment on cross-section A-A' an C-C' is depicted together with the nourishment and the original bed level. Due to the nourished area

being 4-5 grid cells wide, the applied nourishment is accurate, resulting in a uniform nourishment at the required depth of -17 m NAP. Cross-section A-A' presents a typical bend cross-section profile with a shallower inner bend and a deeper outer bend. Cross-section C-C' on the other hand, which is further to the south, has a parabolic shape which indicates that this cross-section is less influenced by the secondary flow than cross-section A-A'.

The nourishment on cross-section A-A', does not erode over its whole width, minor sedimentation occurs towards the outer bend which also happens in the base case. The aim of nourishing the outer bend is to use the secondary flow in order to transport sediment towards the inner bend and eventually, onto the intertidal area. A desirable result of applying this method is therefore defined as sedimentation on the inner bend in the first place and eventually sedimentation on the intertidal area. Considering the inner bend reaching depths of -12.5 m NAP, the changes in bed level above -12.5 m NAP are depicted in Figure 6.12b. Positive bed changes in the order of 10 cm are observed on both sides of the channel. The total bed level changes on the inner bend as well as the one on the outer bend are mostly the result of the increase in velocity magnitudes as is depicted in Figure 6.6c. On the inner bend, extra bed level changes in the order of 5 cm due to the secondary flow were expected which are not visible on this cross-section. In the hydrodynamic study (Section 6.2.2), the Coriolis effect was shown to be weakly dominant with respect to the centrifugal effect. This can be an explanation for no clear difference in sedimentation is found between the inner or outer bend.

As stated earlier, the bathymetry of cross-section C-C' does not show signs of being influenced by the secondary flow. The supposedly inner bend shows most signs of erosion. Although the desired result is not reached here, sedimentation on the edges of the intertidal area occurs as is depicted in Figure 6.15d.

80% of the eroded sediment reaches depths of -12.5 m NAP or higher in the first year. Due to the sediment accreting on both sides of the channel, this percentage is not representative for the inner bend only but for the whole channel. Simulations with larger morphological scale factors showed that the nourishment erodes at a rate of approximately 16% per year, for 5-10 years.

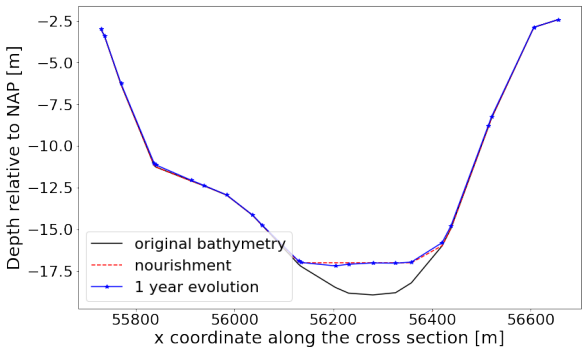

(a) 1 year evolution nourishment cross section A-A'

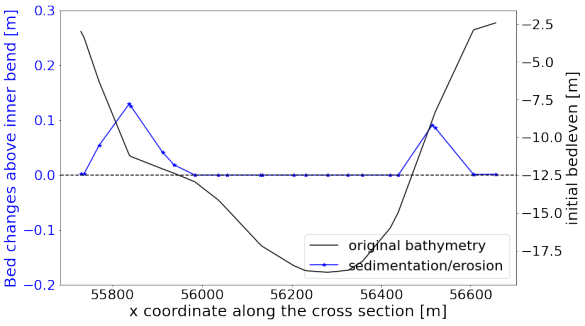

(b) Cumulative sedimentation/erosion above -12.5 m MSL after 1 year

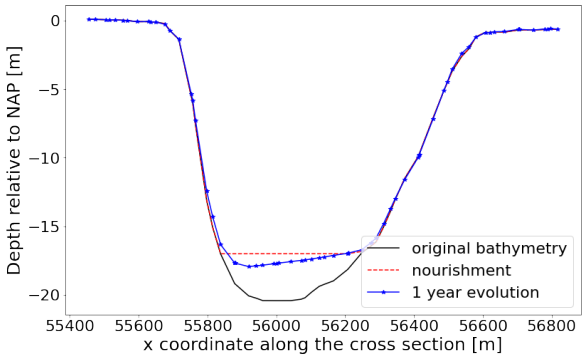

(c) 1 year evolution nourishment cross section C-C'

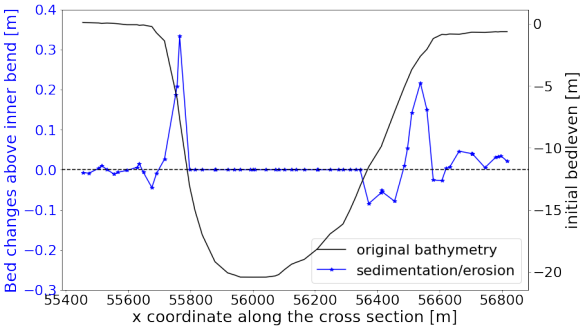

(d) Cumulative sedimentation/erosion above -12.5 m MSL after 1 year

Figure 6.12: Overview of the 1 year morphological evolution of cross section A-A' and C-C' in bend 1

6.3.4. Case 2: Nourishing the second bend

Here the behaviour of the case 2 nourishment is analysed by means of two simulations applying the same methodology as case 1. In a first simulation, the whole bottom of the Eastern Scheldt consists of an erodible layer of 5 m of sand. Hereafter, only the nourishment is made of an erodible layer of 5 m of sand. The results of both these simulations are depicted in Figure 6.13.

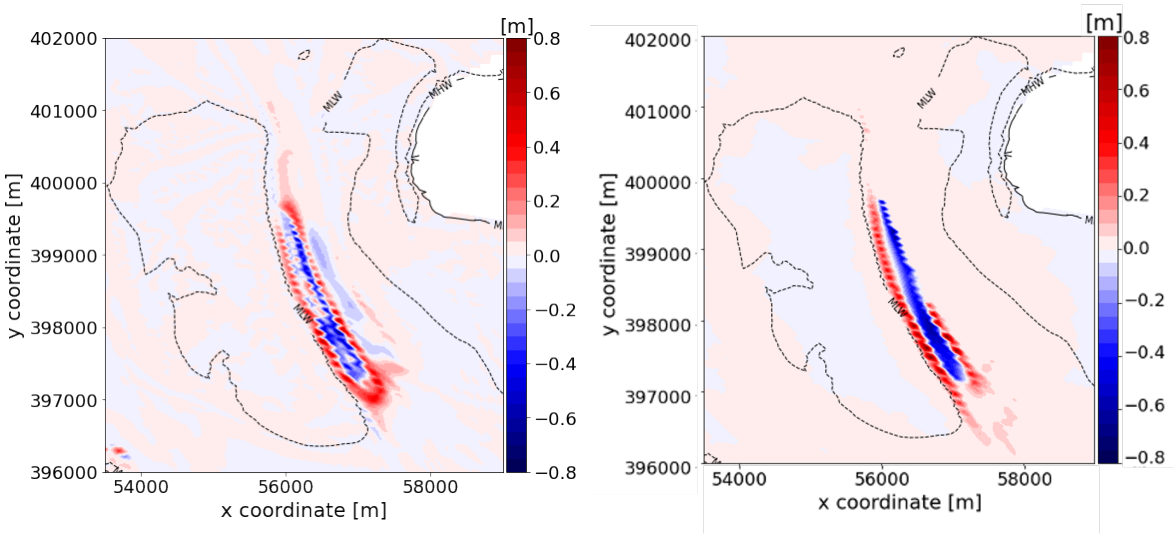

(a) The whole bathymetry is erodible

(b) Only the nourishment is erodible

Figure 6.13: Figure 6.13a depicts the difference between the bed changes of the base case model result depicted in Figure 6.8b and the sedimentation/erosion of the nourishment in the first bend. In Figure 6.13b, the model result of the bed changes is plotted for the case with only the nourishment being an erodible layer of 5 m of sand.

The effect of the surrounding sediment transport in the basin is clearly visible as both morphological simulation results present differences. The results present bed level changes on approximately the same area, whereas case 1 showed bed level changes on different areas. This difference between both cases suggests that the bed level changes in the second bend are less dependent on the surrounding transport in the basin than the first one. The main difference that can be observed between both morphological simulation results (Figure 6.13a & 6.13b), is the area over which the nourishment erodes. When the whole Eastern Scheldt basin is erodible, the cumulative erosion/sedimentation patterns show that part of the nourishment erodes while part of it accretes. This observation is due to the entire system adapting to this new input of sediment. As can be observed on the historic data (Figure 6.8a), this part of the channel has been accumulating sediment over the last 7 years. It is suggested that the nourished area that shows significant sedimentation, needs a further reduction in cross-section in order to relieve the sediment starvation locally. Yet when only the nourishment is erodible, the entire nourishment area erodes. The latter can be explained by the following: as there is no sediment supply from up- or downstream, while the velocity magnitude exceeds the critical velocity magnitude during a significant part of the tidal cycle period as is indicated in Figure 6.7b, erosion on the whole nourished area can be observed. Furthermore, sedimentation occurs along the entire inner bend in Figure 6.13a while it only occurs on the bottom half in Figure 6.13b. The latter indicates that the sediment settling on the inner bend is not originating from the nourishment but from up- or downstream.

There are however many similarities between both results. One of the similarities is the magnitude of cumulative erosion/sedimentation for both cases. In addition, the nourishment does not result in any bed changes higher than the MLW-line, although the hydrodynamic results suggested an additional flow on the flats and a velocity increases on the edges of the intertidal areas. As stated earlier, this is due to a lack of forcing (waves, wind) as well as taking only 1 type of sediment into account (sand) which requires a velocity of 0.45 m/s in order to initiate transport. In Figure 6.14, the longitudinal evolution of the nourishment is depicted along with the original bed level. Firstly, it can be observed that 12% of the nourishment has eroded during the first year. Secondly, it can be observed that the middle part of the nourishment erodes the most and settles on both the up- and downstream parts of the nourishment.

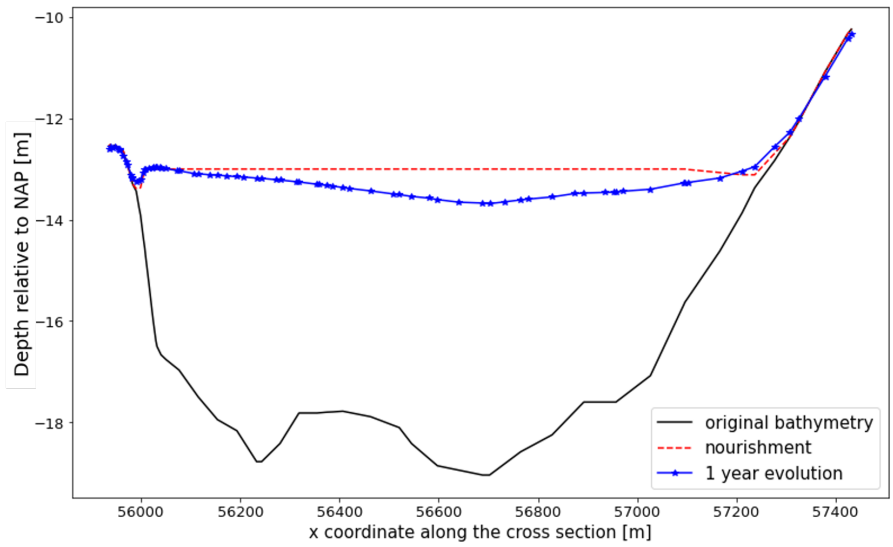

Figure 6.14: 1 year longitudinal evolution of nourishing the second bend. The original bathymetry of 2013 is indicated in black, the resulting bathymetry after a nourishment is indicated in a dashed orange line and finally the 1 year evolution of the nourishment is indicated in blue stars

Following the results depicted in Figure 6.9, sedimentation on the inner bend is expected to be larger while the results (Figure 6.13a, 6.13b) show comparable sedimentation in both the inner and outer bend. In order to visualise the evolution of the nourishment in more detail, the evolution of cross-sections B-B' and D-D' are depicted in Figure 6.15, together with the original bed level. The shape of both cross-sections is considerably different. The outer bend reaches the same depths for both cross-sections (-17.5 m NAP) while the inner bend elevation differs considerably, -13 m NAP for B-B' and -5 m NAP for D-D'. Furthermore, it can be observed that the nourishment has been applied accurately at a depth of -13 m NAP at both cross-sections.

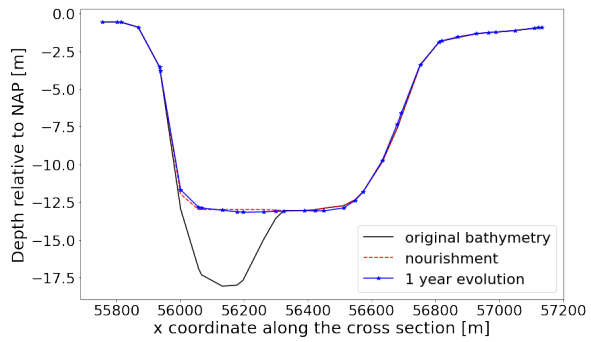

(a) 1 year evolution nourishment cross section B-B'

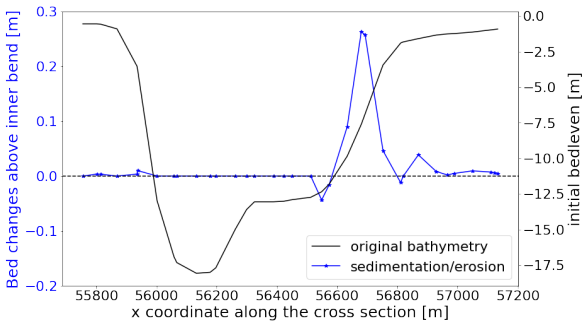

(b) Cumulative sedimentation/erosion above MLW after 1 year

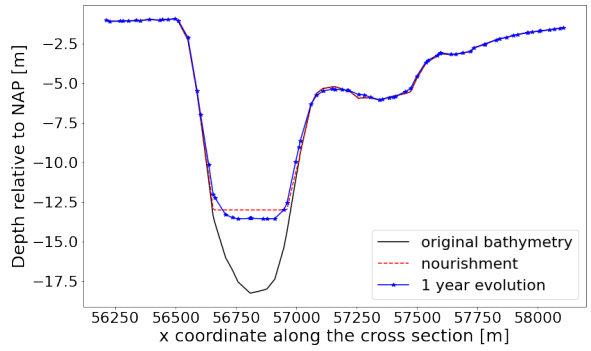

(c) 1 year evolution nourishment cross section D-D'

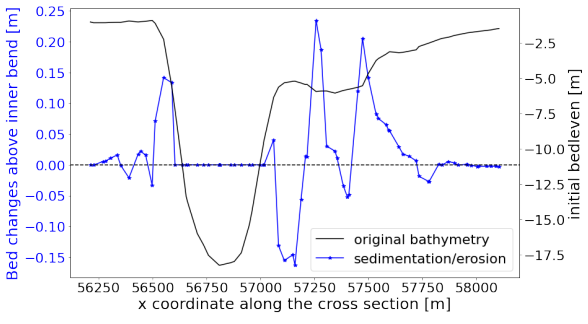

(d) Cumulative sedimentation/erosion above MLW after 1 year

Figure 6.15: Overview of the 1 year morphological evolution of cross section B-B' and D-D' in bend 2

On cross-section B-B', the nourishment has changed the shape of the channel from the typical cross-section of a bend to a typical cross-section of a straight wide channel. During the one year numerical simulation, the morphological activity does not show clear signs of evolving back towards the original shape of the channel. There is some erosion observed in the once deeper part of the channel, in the order of 0.3 m which is not significant compared to the depth of the nourishment. As with case 1, sedimentation on the inner bend accompanied by sedimentation on the intertidal area is desirable. In Figure 6.15b, the 1 year bed changes above -13 m NAP are depicted. Here it can be observed that most of the eroded sediment is either settling on the slope of the inner bend as well as a minor part just below the MLW-line.

The simulation results of the 1 year evolution of the nourishment on cross-section D-D' show that the outer bend erodes approximately 0.5 m. Considering the central part of the outer bend erodes first, a slope adjustment takes place such that the sedimentation is observed on the edges of the outer bend. In addition, the results show that the edge of the inner bend is eroding. Figure 6.15d, visualises all bed level changes higher than -13 m NAP. The previously discussed sedimentation of the outer edge of the outer bend is visualised as well as some major sedimentation on the higher elevations of the inner bend. The results suggest that part of the eroded nourishment settles onto the inner bend.

6.4. Discussion & Conclusion

In Chapter 4, the Brabantsche Vaarwater showed significant accelerations as a result of a channel nourishment, although the magnitude of the velocity was already exceeding the critical velocity. The patterns observed on the historic data indicated that there was a relatively strong secondary flow in the two bends of the Brabantsche Vaarwater, dominated by the centrifugal effect. In this chapter, theoretical analysis confirmed the dominance of the centrifugal effect in form of transverse water level gradients in the order of 1-3 cm. The secondary flow intensity results show that in both bends the net secondary flow (over a tidal cycle) is directed towards the inner bend with maximal magnitudes in the order of 0.006-0.004 m/s, yet this effect is more pronounced in the second bend. By nourishing the deep, outer bend of both bends, the aim is to use the secondary flow, dominated by the centrifugal effect, as means to transport the nourished sediment from the outer bend towards the inner bend and eventually onto the intertidal area. Depth averaged velocity simulation results show that by nourishing the outer bend, the inner bend as well as the edge of the outer bend accelerate, order 0.1 m/s, while the velocity in the nourished area is not influenced significantly. The nourishments thus cause a redistribution of the discharge in the cross direction. In addition, no significant changes in direction are observed in the channel. There are however changes in velocity direction on both the Galgenplaat and the Slikken van Viane, combined with velocity magnitude increases in the order of 0.05 m/s, the results indicate additional flow on both intertidal areas.

Below the MLW-line, sedimentation is observed on both the inner and outer bend. Numerical simulation results show that approximately 16 & 13% of the initial nourishments erode for bend 1 & 2 respectively during the first year. Bearing in mind that the model overshoots the bed changes by a factor 5-6, the erosion of the nourishments is estimated to be 3%. Approximately 0.6% of the nourishment settles above the MLW-line during the first year. Hence, the influence of the secondary flow, as well as the increase in velocity, have not been proven to be large enough in order to generate significant sedimentation above the MLW-line. This conclusion, however, must be drawn taking into account the numerous limitations/simplifications of the ScalOost model.

The largest limitations/simplifications which are most likely the cause for no morphological activity on the intertidal areas lie within the model's forcing. Firstly, no waves have been taken into account for the simulations, which are responsible for a large amount of morphological activity on the intertidal areas, both positive and negative. Secondly, a mild wind climate has been applied. The largest morphological activity on the intertidal areas occurs during storms, hence periods with high wind velocities. Lastly, the Eastern Scheldt basin consists out of a large variety of grain sizes, which lie within 150-200 μm for the channels and decrease down to 50 μm on the intertidal areas. By considering only one sediment type with grain size: 190 μm, the model approximates the transport in the channel well while it undershoots the sediment transport on the intertidal areas significantly. In the channel, the ScalOost model is able to reproduce the bed level changes as a result of secondary flow. Considering the model's capabilities and limitations, sedimentation on the inner bend is used as an indication in order to judge the importance

of secondary flow in sediment transport.

Considering two bends have been analysed in the form of case studies, these will be treated separately in this section. The hydrodynamic results in form of transverse water level gradients show that the centrifugal effect is not as dominant in the first bend, compared to the Coriolis effect, although the first bend has approximately the same width and radius as the second bend. It is suggested that this is due to the bend being connected to two channels, hence the flow having two routes. Consequently, the secondary flow is disturbed by the in and outflow in the bend. However, secondary flow intensity results show that over a whole tidal cycle, the centrifugal effect is dominant. Significant sedimentation on the edges of the intertidal area is observed, which is mostly due to the velocities exceeding the critical velocity for sand transport. Results show that the nourishment volume settling higher than the initial nourishment is approximately 13% in the first year, representing 80% of the eroded nourishment. Considering both sides of the channel showing the same amount of sedimentation, no direct link between secondary flow and the sedimentation can be established.

The bathymetry of the second bend has a pronounced shape characterised by a deep outer bend and a shallow inner bend confirming the effect and presence of the secondary flow dominated by the centrifugal effect. The morphological results show that the nourished eroded sediment settles on the edge of the outer bend as well as on the entire inner bend. There is no sign of sediment migration on the inner bend towards the Slikken van Viane after the first year. Monitoring of sediment disposals in the Western Scheldt showed that sedimentation fronts decrease in celerity as they reach higher elevations, suggesting that migration can not be excluded. Furthermore, the model's limitations at higher elevations are likely to be the cause of no sedimentation. Taking into account the model's capabilities, a direct link between secondary flow and the hydrodynamics has been established. However, this does not translate into morphological results linking the secondary flow to bed level changes.

Although the link between the secondary flow and sediment transport has not been established through simulation results, bathymetric data shows that it is present. Nourishing the channel, thus reducing the cross-sectional area, proved to cause accelerations of the flow as well as sedimentation of the edges of the intertidal area.

7

Conclusions and recommendations

7.1. Conclusions

The research objective of this thesis is summarized through the following research question:

"Is a tidal channel nourishment in the Eastern Scheldt, a feasible way of supplying the channel's surrounding intertidal areas?"

In this chapter, the key findings related to each sub-question are summarized. Subsequently, the main research question is addressed.

1. **What are the current problems for the intertidal areas in the Eastern Scheldt and why is a human interference necessary?**

The Storm Surge Barrier (SSB) in the Eastern Scheldt, has been constructed as part of the Delta Works and was completed in 1986. This event lead to a decrease in tidal range from 3.7 to 3.25 m and the average tidal velocity to decrease from 1.2 to 0.8 m/s which subsequently led to a decrease in tidal prism of 0.4 million m^3. As the cross-sectional areas of the tidal channels became too large for the reduced tidal prism, the tidal channels suffered a large sediment deficit estimated at approximately 500 million m^3. Furthermore, the sediment exchange between the basin and the outer delta became hindered by the barrier, due to its position and the reduced inlet area. This combination of factors led to the severe erosion of the intertidal areas, because these are the only available sources of sediment to reduce the cross-sectional areas of the tidal channels. The intertidal areas form the habitats for the benthic community, foraging ground for wader birds, and rest area for aquatic animals. In addition to their ecological value, the intertidal areas are valuable wave dampers and therefore important for flood protection of the hinterland. Nourishments can locally provide solutions, thus possibly guarantee the existence of the intertidal areas.

2. **How does a tidal channel nourishment affect the sediment transport between the channel and the surrounding intertidal flat?**

The building forces of the intertidal areas are highly dependent on the tidal velocities, because these are responsible for the initiation of motion and (re)suspension of sediment in the tidal channels. Meteorological conditions (wind-induced flow and waves) are identified as the largest erosive factors for the intertidal areas, because these bring previously settled sediment on the intertidal areas back into suspension. Considering the equilibrium level of an intertidal area can be described as a stochastic process with variables, the equilibrium level changes when the variables change. The level of an intertidal area is therefore dependent on the supply of sediment which can be seen as constant (over a tidal cycle) and dependent on the meteorological conditions, which alternate between calm weather and high wind periods. As the tidal velocities are reduced (as a result of the SSB), the constant sediment supply was lowered. The accretion during the calm weather periods reduced while the erosion during the high wind periods remained leading to a net erosion. Simulation results show that a tidal channel nourishment can increase the velocities locally. Hence, a tidal channel nourishment can increase the

sediment supply, which can ultimately result in net accretion of the intertidal area as the simulation results show.

3. **What are the benefits and downsides of nourishing a tidal channel?**

Nourishing a tidal channel has both benefits and downsides compared to directly nourishing the intertidal areas, depending on different perspectives. From an efficiency perspective, nourishing the intertidal area directly has an immediate positive effect on the elevation of the intertidal area as 100% of the nourishment is applied on the intertidal area. The simulation results of a channel nourishment in the Krabbenkreek, indicate that 2% of the initial nourishment can be expected to supply the intertidal area on a yearly basis. Bearing in mind the model's uncertainties, this trend is expected to continue for a period of time in the order of a decade. Hence, there is a significant efficiency difference between both methods, 100% at once or 2% on a yearly basis.

From an ecological perspective, nourishing the intertidal area directly, has a negative impact as the nourishment buries the benthic species. Data showed that although it only takes 3-5 years for benthic life to recolonise the nourished area, the number of species permanently reduced. In addition, these types of nourishments are more work intensive and dependent on the tide, hence relatively costly. On the contrary, nourishing a tidal channel can have a positive impact on the ecology, considering that the supply of nourished sediment from the channel towards the intertidal area is gradual and benthic species present on the flat are not buried by the nourishment. Monitoring of sediment disposals in tidal channels in the Western Scheldt shows that a gradual increase in bed elevations result in an increase in abundance of the benthic species. In addition, the targeted intertidal area stays available as foraging grounds for birds, and rest areas for aquatic animals, during and after the application of the nourishment.

Ultimately, the choice is a trade-off between the efficiency, the ecology, and the costs.

4. **What are the effects of nourishing two specific tidal channels: The Krabbenkreek and the Brabantsche Vaarwater on the hydrodynamics and morphodynamics?**

This question is answered by means of two case studies. The aim of the first case study, in the Krabbenkreek channel, was to increase the tidal velocities by reducing the cross-sectional area of the tidal channel. In the second case study, in the Brabanstsche Vaarwater channel, the aim was to determine the relative importance of secondary flow patterns in bends and how these affect the sediment transport between the channel and the intertidal area.

A nourishment of 2 million m^3 in the Krabbenkreek led to an increase of both the flood and ebb velocities as well as the period along which the velocity exceeds the critical velocity for sand (190 μm), 0.45 m/s. The velocity increases were in the order of 0.15 m/s, such that the critical velocity was reached approximately 750 m further into the channel. Locations with the largest bathymetry changes showed the largest velocity increases, confirming the hypothesis that a reduction in cross-sectional area in the Krabbenkreek, leads to local velocity increases. Combined with a prolongation of the period along which the velocities exceed the critical velocity, between 15 to 60 minutes, the exchange between the water fluxes of the tidal channel and intertidal area is enhanced. The simulation results show an erosion of 2.5% of the initial nourishment during the first year, of which 80% settles above the MLW-line. This represents an increase in accretion of the intertidal area of 100% compared to the base case simulation. Although the percentage reaching the intertidal area is limited, previous studies show that the propagation of an accretion front is slow (0.5 km/year) and that waves are necessary to further distribute these accretion fronts over the intertidal area. Considering simulations are representative for longer time scales, substantially more sand from the nourishment may reach the flats in the long term.

Two bends are identified in the Brabantsche Vaarwater. From the bed level changes observed between 2013 and 2019 and results from the theoretical analysis it can be assumed that; the morphology of the bends is influenced by the secondary flow, which is dominated by the centrifugal force. The secondary flow intensity (order 0.004-0.006 m/s), confirms the dominance of the Coriolis effect in both bends, yet weaker in the first bend. The results show that the net secondary flow (near-bed) is directed towards the inner bend for bend 1 and 2. Based on this assumption, two outer bend nourishments are simulated with corresponding sand volumes of $750 * 10^3 m^3$ in the first bend and $920 * 10^3 m^3$ in the second bend. The hydrodynamic simulation results show a redistribution of the discharge within the cross-section

as the non-nourished part of the cross-section accelerates in the order of 0.1m/s, while the nourished part hardly experiences velocity changes. A change in primary flow direction on the intertidal area, in combination with an increase in velocity magnitude indicate additional flow over the intertidal areas. The primary flow direction changes in the channel do not show any indication of the secondary flow.

The morphodynamic results show that 3% of the initial nourishments erode within the first year. Furthermore, it is estimated that 80% of the eroded sediment, reaches elevations of the inner bends. No difference in accretion between the outer or inner bend is observed for the first or second bend although a surplus was expected for both inner bends due to the secondary flow. Hence, no link can be established between secondary flow and additional accretion of the inner bend. It is argued that this is due to the model's limitations at higher elevations due to a lack of forcing and sediment type.

5. **Can general conclusions be drawn from the two case studies?**

Considering tidal basins are dynamic and diverse and that this study is based on numerical modelling results that come with uncertainties, general conclusions can not be drawn. Nevertheless, the results obtained in this study can give indications regarding the feasibility of tidal channel nourishments.

This research showed that for specific case studies, a tidal channel nourishment can result in local velocity increases, given that no significant redistribution of the discharge takes place between the surrounding channels. Tidal channel nourishments applied in closed channels (where the flow only has one path option) such as the Krabbenkreek, showed large increases in velocity magnitudes and can be expected to eventually lead to a gradual accretion of the surrounding intertidal areas. The evolution of tidal channel nourishment has not been proven to be influenced by secondary flow patterns. Nevertheless, considering the limitations of this study and the bathymetric data, secondary flow is not excluded as means of causing sedimentation of the intertidal area. Furthermore, simulation results indicate that tidal channel nourishments in the order of 1-3 million m^3 have a lifetime in the order of a decade.

7.2. Recommendations for future research

This section contains recommendations in view of a finalising the design of a nourishment. In addition, recommendations for future development of the ScalOost model in view of studying the proposed case studies in this research with higher accuracy are given.

7.2.1. General recommendations

In Chapter 4, choices were made to further investigate two channels out of four. The remaining two channels still have the potential for further investigation. Especially channel 1, better known as ”De Slaak”, showed significant velocity increases as a result of a reduction in cross-sectional area. Although the velocities doubled on the nourished area, these were not large enough to initiate sand transport. A nourishment of finer sediment and thus a smaller critical velocity, has a large potential of feeding the surrounding intertidal area. Channel 3, did not show the expected results. If this channel is to be further investigated, the direct proportionality between nourished sediment and velocity changes is recommended to be investigated as the results indicated a strong relation.

The studied nourishments were simulated as being completed in one go. In the Western Scheldt, constant sediment disposals (1/year) have been proven to be successful regarding sedimentation of the surrounding intertidal areas. Hence, it is recommended to study the effect of disposing sediment on a constant basis over a long period of time (order ≈5 years).

Considering the wide scope of this research, not much attention has been paid to the potential lifetime of the nourishment, whereas these nourishments may especially pay out in the long run. By means of simulations with larger morphological scale factors, the pace at which a nourishment is eroding has been estimated. This estimation however comes with some uncertainties that lie within the morphological scale factor. A way to reduce the uncertainty is to simulate larger periods, this, unfortunately, comes with longer computational time.

The only threat to the existence of the intertidal areas accounted for was sediment starvation. Another important threat is sea-level rise. It is thus recommended to investigate the effect of sea-level rise on the emergence of the intertidal areas and take it into account when discussing the efficiency of a tidal channel nourishment.

In view of gaining knowledge on how secondary flow affects sediment transport in tidal channels, a monitoring campaign could be set up to measure the latter. Information on how the suspended sediment concentration is distributed along the depth of a tidal channel bend combined with the cross channel velocity can be valuable in the future design of tidal channel nourishments. This could for example be set up in the second bend of the Brabantsche Vaarwater.

The last general recommendation is to investigate the feasibility of the nourishment regarding practical issues. The origin of the nourished sediment should be investigated in view of the scarcity of sand in the whole North Sea. Furthermore, the type of vessels transporting and applying the nourishment is recommended to investigate.

7.2.2. Model recommendations

As mentioned throughout the report, the lack of forcing prevented bed level changes in the intertidal areas. The largest uncertainty of this research lies within the behaviour of the sediment transport that reaches the edges of the intertidal areas. Adding wind-induced waves to the forcing can improve the model’s accuracy in areas where the tidal flow is not governing for sediment transport. Furthermore, it is recommended to simulate extreme events with high wind velocities and surges.

The Eastern Scheldt basin is composed of a variety of sediment types and grain sizes. In this study, simulations have been carried out with a non-cohesive sediment type a with a nominal grain size diameter of 190μm. This grain size is representative of the channels of the Eastern Scheldt only. In order to improve the model’s accuracy on these intertidal areas, it is recommended to apply a corresponding grain size in the order of 50 – 100μm. Furthermore, it is recommended to look into the presence of cohesive sediment types on the intertidal areas.

The grid size resolution varies over the model’s domain quite significantly, between approximately 100x100 m and 45x45 m. This has as consequence that some channels are only one or two grid cells

wide which make the accuracy of a nourishment questionable. In future research, it is therefore recommended to study a smaller area and perform a grid refinement. This can be done by either nesting or by online domain decomposition. Previous research in the Eastern Scheldt showed that a grid smaller than 30x30 m is not recommended since smaller grids can not reproduce small-scale effects better. Furthermore, the computational time dramatically increases when reducing the grid size.

References

Aarninkhof, S. G. J. and van Kessel, T. (1999). Data analyse Voordelta, Grootschalige morfologische veranderingen 1960 – 1996: Report WL | Delft Hydraulics Z2694. pages 1–33.

Arts, F., Hoekstein, M., Lilipaly, S., van Straalen, K., Sluijter, M., and Wolf, P. (2018). Watervogels en zeezoogdieren in de Zoute Delta in 2016/2017.

Binnenvaartkennis.nlToegestane afmetingen en diepgang vaarweggedeelten. https://www.binnenvaartkennis.nl/toegestane-afmetingen-en-diepgang-vaarweggedeelten/.

Boersema, M., van der Werf, J., Salvador de Paiva, J., van den Brink, A., Soissons, L., Walles, B., Bouma, T., de Vet, P. L. M., Ysebaert, T., Paree, E., Bijleveld, M., van Zanten, E., van Westenbrugge, K., Stronkhorst, J., and de Jong, D. (2018). Oesterdam sand nourishment. ecological and morphological development of a local sand nourishment. doi: 10.18174/448529.

Bosboom, J. (2019). Chapter 9 of Coastal Dynamics 1 lecture slides, Coastal inlets and tidal basins.

Bosboom, J. and Stive, M. J. F. (2015). Coastal Dynamics 1, lecture notes CIE4305.

Brand, N., Kothuis, B. L. M., and van Prooijen, B. C. (2016). The Eastern Scheldt Survey A concise overview of the estuary pre-and post barrier -Part 2: SURVEY. *Urban Integrity*.

Cox, J. R. (2018). Effects of dredging and dumping in laboratory scale experiments of estuaries.

De Ronde, J. G., Mulder, J. P. M., Van Duren, L. A., and Ysebaert, T. J. W. (2013). Eindadvies ANT Oosterschelde. *Deltares rapport 1207722-000-ZKS-0010*.

de Vet, P. L. M. (2019). Intertidal flats in engineerd estuaries.

de Vet, P. L. M., van Prooijen, B. C., and Wang, Z. B. (2017). The differences in morphological development between the intertidal flats of the Eastern and Western Scheldt. 281:31–42. ISSN 0169555X. doi: 10.1016/j.geomorph.2016.12.031.

de Vet, P. L. M., van Prooijen, B. C., Colosimo, I., Ysebaert, T., Herman, P. M. J., and Wang, Z. B. (2020). Sediment disposals in estuarine channels alter the eco-morphology of intertidal flats. *Journal of Geophysical Research: Earth Surface*, 125(2).

De Vriend, H. J., Dronkers, J., Stive, M. J. F., and Wang, J. H. (2002). Coastal inlets and tidal basins, CT5303.

de Vriend, H. J., van Koningsveld, M., Aarninkhof, S. G. J., de Vries, M. B., and Baptist, M. J. (2014). Sustainable hydraulic engineering through building with nature.

DelatresDelft3d-flow simulation of multi-dimensional hydrodynamic flows and transport phenomena, including sediments user manual.

Delatres (2020). Delft3d-quickin generation and manipulation of grid-related parameters such as bathymetry, initial conditions and roughness.

Deltares (2014). Het optimaliseren van duurzame aquacultuur.

Depreiter, D., Sas, M., Beirinckx, K., and Liek, G. J. (2011). understanding and steering environmental responses to dredging and disposal in the scheldt estuary.

Ecoshape (2012). Tidal flat nourishment – galgeplaat.

Eelkema, M. (2013). Eastern Scheldt Inlet Morphodynamics.

Eelkema, M., Wang, Z. B., and Stive, J. F. (2013). Coastal Dynamics 2013 Coastal Dynamics 2013. (1996):327–338.

Friedrichs, C. T. (2011). Tidal flat morphodynamics: A synthesis. *E. Wolanski, McLuskyDonald (Eds.), Treatise on estuarine and coastal science*.

Guijt, K. (2018). Impact of Tidal Energy Extraction in the Eastern Scheldt Storm Surge Barrier on Basin Hydrodynamics and Morphology.

Henkens, R. J. H. G., Wijsman, J. W. M., Goossen, C. M., and Jochem, R. (2012). Duurzaam ruimtegebruik Oosterschelde.

Huisman, B. J. A. and Luijendijk, A. P. (2009). Sand demand of the Eastern Scheldt, morphology around the barrier.

Jörissen, J. G. L. (2003). Herstructurering sluizencomplex Krammer. Rijkswaterstaat Bouwdienst Kater.

Kana, T. W., Hayter, E. J., and Work, P. A. (1999). "Mesoscale sediment transport at southeastern U.S. tidal inlets: Conceptual model applicable to mixed energy settings".

Kohsiek, L. H. M., Mulder, J. P. M., and Louters, T. (1987). De Oosterschelde naar een nieuw onderwaterlandschap. *Nota DGW. AO*, pages 1–49.

Kohsiek, L. H. M., Buist, H. J., Bloks, P., Misdorp, R., Van den Berg, J. H., and Visser, J. (1988). Sedimentary processes on a sandy shoal in a mesotidal estuary (oosterschelde, the netherlands). *Tide-influenced sedimentary environments and facies*.

Malvarez, G., Cooper, A., Jackson, D., and Navas, F. (2001). The role of wave action on sedimentation of tidal flats: Application of high spatial resolution numerical modelling in strangford lough, northern ireland. *Journal of Coastal Research*, page 172.

NatuurparkOosterschelde*Scheepvaart*. `https://www.np-oosterschelde.nl/nl/over-het-park/economie/scheepvaart.htm`.

Partheniades, E. (1965). "Erosion and Deposition of Cohesive Soils." Journal of the Hydraulics Division.

Pezij, M. (2013). ScalOost read me file.

Pezij, M. (2015). Understanding the morphological development of the Oesterdam nourishment.

Postma, H. (1961). Transport and accumulation of suspended matter in the dutch wadden sea). *Netherlands Journal of Sea Research 1: 148–190*.

Quyen, B. N. (2010). Morphology of the Eastern Scheldt Ebb Tidal Delta. (June):62.

Schelling, T., van der Steeg, L. J., and Leopold, M. F. (2014). Wageningen UR. *IMARES Wageningen UR*, 011(September):11–12.

SercMedia (2007). Shields diagram. URL `https://serc.carleton.edu/details/images/11032.html`.

Speer, P. E. and Aubrey, D. G. (1985). A study of non-linear tidal propagation in shallow inlet/estuarine systems, part II: theory. Estuarine, coastal and shelf science, 21, 207-224.

Svasek Hydraulics (2004). De Overschelde, baggeren voor de veiligheid.

Swinkels, C., Jeuken, C., Wang, Z. B., and Nicholls, R. (2009). Presence of connecting channels in the western scheldt estuary. *Journal of Coastal Research*, 25:627–640. doi: 10.2112/06-0719.1.

Ten Brinke, W. B. M. (1993). The impact of biological factors on the deposition of fine-grained sediment in the Oosterschelde (The Netherlands).

Ten Brinke, W. B. M., Dronkers, J., and Mulder, J. P. M. (1994). Fine sediments in the Oosterschelde tidal basin before and after partial closure.

van der Werf, J., Reinders, J., van Rooijen, A., Holzhauer, H., and Ysebaert, T. (2015). Evaluation of a tidal flat sediment nourishment as estuarine management measure. *Ocean and Coastal Management*, 114:77–87. ISSN 09645691. doi: 10.1016/j.ocecoaman.2015.06.006.

Van der Werf, J., Boersema, M., Bouma, T., Schrijvershof, R., Stronkhorst, J., De Vet, P. L. M., and Ysebaert, T. (2016). Definitief ontwerp roggenplaat suppletie. (November):99.

van der Werf, J. J., de Vet, P. L. M., Boersema, M. P., Bouma, T. J., Nolte, A. J., Schrijvershof, R. A., Soissons, L. M., Stronkhorst, J., van Zanten, E., and Ysebaert, T. (2019). An integral approach to design the Roggenplaat intertidal shoal nourishment. *Ocean and Coastal Management*, 172(January): 30–40. ISSN 09645691. doi: 10.1016/j.ocecoaman.2019.01.023.

van Ieperen, H. J. (1987). The fall velocity of grain particles.

Van Maldegem, D. (2004). Ontwikkeling morfologie oosterschelde in relatie tot de zandhongerproblematiek.

van Maldegem, D. (2007). Optimalisatie baggeren krabbenkreek oosterschelde t.b.v. scheepvaart.

van Maldegem, D. and de Jong, D. (2004). Opwassen of verdrinekn. Sedimentaanvoer naar schorren in de Oosterschelde, een zandhongerig gedempt getijdesysteem.

van Maldegem, D. C. and van Pagee, J. A. (2005). Zandhonger Oosterschelde een verkenning naar mogelijke maatregelen .

Van Rijn, L. (1990). Principles of fluid flow and surface waves in rivers, estuaries, seas and oceans.

Van Rijn, L. C. (2012). Simple general formulae for sand transport in rivers, esturaries and coastal waters.

van Veen, J., van der Spek, A. J. F., Stive, M. J. F., and Zitman, T. (2005). Ebb and Flood Channel Systems in the Netherlands Tidal Waters.

van Zanten, E. and Adriaanse, L. A. (2008). Verminderd getij.

Wang, Z. B., Elias, E. P. L., van der Spek, A. J. F., and Lodder, Q. J. (2018). Sediment budget and morphological development of the dutch wadden sea: impact of accelerated sea-level rise and subsidence until 2100. *Netherlands Journal of Geosciences*.

Ysebaert, T. (2016). Roggenplaat nourishment, ecological considerations.

Zijl, F. (2016). Hydrodynamic modeling on the Northwest European Shelf and North Sea: New opportunities with Delft3D Flexible Mesh.

Appendices

A

The Eastern Scheldt tidal basin

This appendix presents additional information for Chapter 2.

A.1. The intertidal area delimitation

The mean high water (MHW) and mean low water (MLW) are derived by means of water level data obtained at Stavenisse, a Rijkswaterstaat measuring station. On Figure A.1, the water level data is visualised together with typical tidal levels. From this data, the MHW and MLW have been derived to be +1.61 m NAP and -1.35 m NAP respectively. These values represent the avearge of all the high-low levels over a given period. It is assumed that these values are equal for every channel which is a valid assumption since the variation in tidal range is more or less 0.1m along the basin (de Vet et al., 2017). The values for all the tidal levels are summarized in Table A.1.

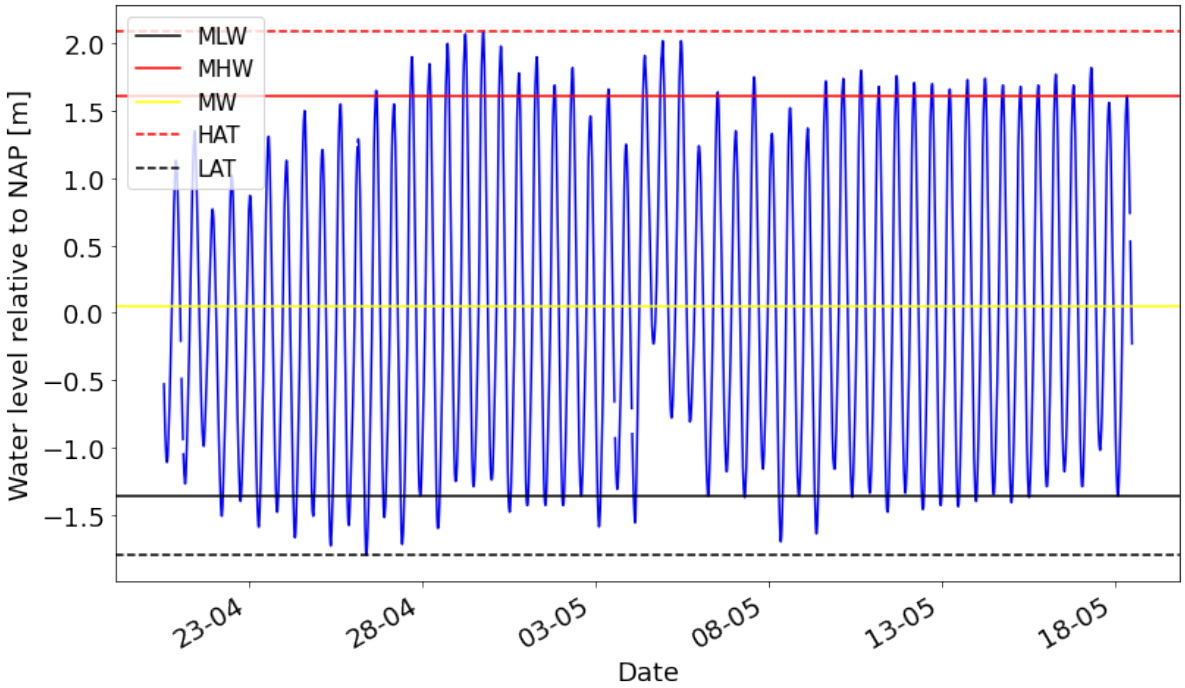

Figure A.1: Water level relative to NAP [m] at measuring station Stavenisse. The horizontal lines represent different typical tidal levels, their value is given in Table A.1. Period: 20/04/2021 - 18/05/2021 (Rijkswaterstaat)

	Abbreviation	Level with respect to NAP [m]
Mean high water	MHW	+ 1.61
Mean low water	MLW	- 1.35
Highest astronomical tide	HAT	+ 2.1
Lowest astronomical tide	LAT	- 1.8
Mean water level	MW	+ 0.045

Table A.1: Tidal levels

A.2. The Eastern Scheldt's basin characteristics

Here, the characteristics of all the intertidal areas are given in Table A.2. This information is meant as support for Section 2.2.

Intertidal Area	Type	Sediment type	Attached (y/n)
Roggenplaat	Shoal	Sand	N
Neeltje Jans	Shoal	Sand	Y
Vondelingsplaat/Galgenplaat	Shoal	Sand	N
Zandkreek	Fringing flat	Sand	Y
Oost Yerseke	Fringing flat	Sand	N
Verdronken land van Zuid Beveland	Salt marsh	Clay/Silt	Y
Hooge Kraaier	Silt permanently under water	Sand	N
Speelmansplaten	Beach	Sand	Y
Dortsman	Salt marsh / Silt	Clay/Sand	Y
Sint Annaland	Salt marsh	Clay/Silt	Y
Stavenisse	Fringing flat	Sand	Y
Anna Jacoba	Fringing flat	Sand	Y
Slaak	Salt marsh	Clay/Silt	Y
Plaat van oude Tonge	Fringing flat	Sand	Y
Slikken van Viane	Fringing flat	Sand	Y

Table A.2: Inventory of the intertidal area's characteristics

A.3. Sediment transport

The essence of the thesis is to stimulate sediment transport from the tidal channels towards the inter-tidal areas as it used to be before the construction of the storm surge barrier. In this section the basic principles of sediment transport will be discussed such as initiation of motion and fall velocity.

A.3.1. Initiation of motion

Whether a particle gets transported or not depends on the forces acting on a specific particle. Three forces can be identified:

1. Drag force: the horizontal force of the fluid exerting on the particle. It is a combination of the skin friction and pressure difference.(Bosboom and Stive, 2015)

2. Lift force: the vertical force of the fluid exerting on the particle. The pressure difference as a result of flow separation and contraction leads to a lift force.(Bosboom and Stive, 2015)

3. Gravitational force: the force that the mass of the particle is exerting in the vertical direction. (Bosboom and Stive, 2015)

Whether a particle will start moving is therefor the sum of the drag and lift force against the gravitational force. All of the above lead to the following relations:

$$(\rho_s - \rho)gD^3 \infty \rho u_{cr}^2 D^2 \tag{A.1}$$

$$\theta_{cr} = \frac{\tau_{b,cr}}{(\rho_s - \rho)gD} = C \tag{A.2}$$

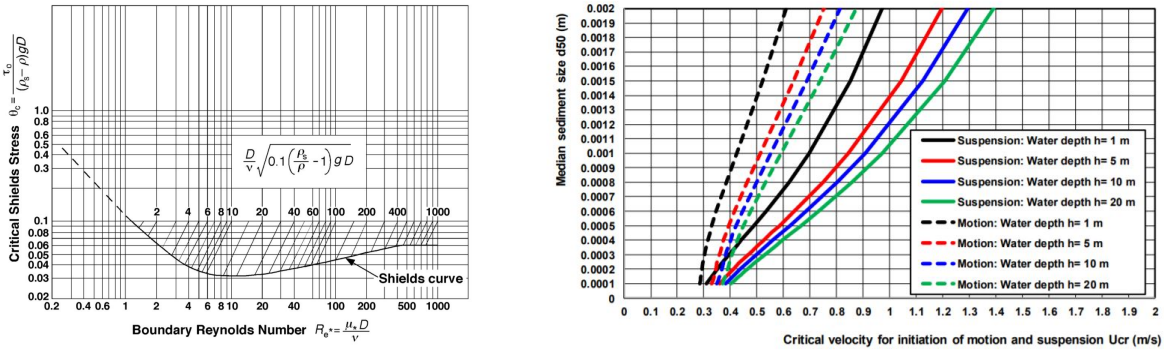

(a) Shields curve (SercMedia, 2007)

(b) Initiation of motion (Van Rijn, 2012)

Figure A.2: Sediment transport diagrams

In equation A.2, θ_{cr} is the critical Shields parameter and has to be determined experimentally which has been done for idealised conditions. The results of these experiments is plotted on the Shields curve which is depicted on Figure A.2a on which it can be noted that the curve attains a value of 0.05 for larger grain sizes and stays constant. On the x-axis the dimensionless diameter is given and on the y-axis Shields parameter is given. For sand with a diameter of 200μm such as the sand in the Eastern Scheldt, the critical bed shear stress equals roughly 0.16N/m^2 which corresponds to a critical velocity of around 0.45 m/s (Figure A.2b). The idealised situation has the following charateristics (Bosboom and Stive, 2015):

1. Uniform flow on a flat bed
2. The soil is non-cohesive
3. The soil is well graded

Cohesive sediment such as silt can floculate and bind together. The critical bed shear stress that will cause the soil to erode is therefor larger than the critical bed shear stress for sedimentation. When the bed shear stress is between the critical bed shear stress for erosion and bed shear stress for sedimentation there will be no exchange of sediment between the water column and the bed. Two types of sediment transport mechanisms can be identified: bed load transport and suspended load transport.

Bed load transport

When particles are transported by rolling, sliding and saltating(jumping) we can speak of bed load transport (Van Rijn, 2012). Between bed and suspended load there is sheet-flow transport that in many cases is seen as bed load transport. This is when particles are saltating (jumping) but just not high enough to be suspended load. Many people have come up with definitions of bed load transport in such as: instantaneous shear stress transport, time averaged bed shear stress transport and transport based on the energy approach (Bosboom and Stive, 2015). They all represent bed load transport as a function of the dimensionless Shields parameter θ_{cr}. Bed load transport is influenced by both the current and the waves, whereas suspended load is only influenced by the current. For particles that are smaller or equal to a few milimeters the quasi-steady approach may be applied (Bosboom and Stive, 2015). This approach assumes that inertia plays a minor role which allows the transport of sediment to be written as an instantaneous reaction to change in bed shear stresses due to waves and currents (Bosboom and Stive, 2015). This transport vector $S_b(t)$ can be written in a dimensionless form in the following way:

$$\phi_b(t) = \frac{S_b(t)}{\sqrt{(s-1)gD_{50}^3}} \tag{A.3}$$

Suspended load transport

For the condition that the bed shear velocity of a particle exceeds its fall velocity a particle is brought into suspension (Van Rijn, 2012). Here the particle trajectories are quite random due to the velocity variations as a result to turbulence. Suspended load transport is expressed as sediment concentration in the water column which is highest near the bed and decreases towards the water surface (Figure A.3). The transport capacity of the flow is not largest near the bed as can be seen on Figure A.3 but is the product of the velocity profile and the concentration profile (Van Rijn, 2012). The suspended load concentration in the water column has been described by Van Rijn using the diffusion approach:

$$cw_s + \varepsilon_s dc/dz = 0 \tag{A.4}$$

Where C is the sediment concentration, w_s is the fall velocity, dc/dz is the sand concentration gradient over the depth of the water column and ϵ_s is the diffusivity coefficient. This equation is only valid for steady uniform flow (Van Rijn, 2012). By using a parabolic sediment diffusivity coefficient the expression for sediment concentration becomes easier to apply. It can be expressed using the Rouse profile and looks like this:

$$\frac{C}{C_a} = \left(\frac{(h-z)}{z}\frac{a}{(h-a)}\right)^{\frac{w_s}{\kappa u^*}} \tag{A.5}$$

On the left hand side of equation A.5, the ratio between the actual concentration and the equilibrium concentration illustrates if there is a sediment 'demand' in the water column or a 'supply' of sediment. This will lead to sediment leaving or joining the bed load transport.

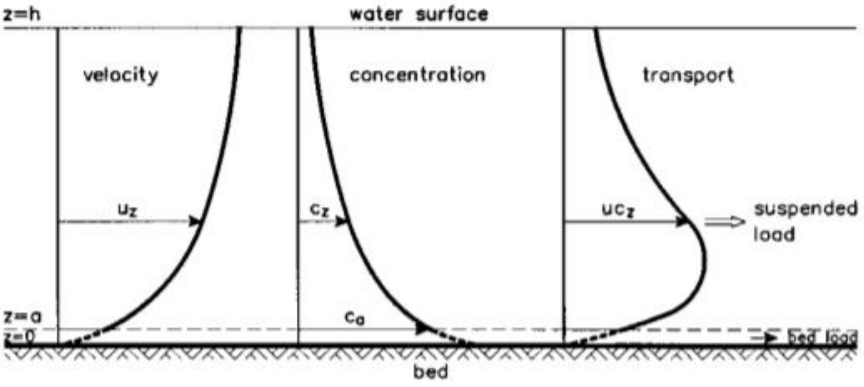

Figure A.3: Suspended load transport for a uniform flow on a flat bed (Van Rijn, 2012)

A.3.2. Fall velocity

In the previous section fall velocity has been mentioned a couple of times and is expressed as w_s. This velocity represents the mechanism behind sedimentation. It is a function of the particle size, shape and density, fluid characteristics and density of the particles (van Ieperen, 1987). A particle will start falling when its submerged weight equals the drag force. Combining the equations for drag force on a spherical particle and its submerged weight results in the following equation:

$$w_s^2 = \frac{4gD\Delta}{3C_D} \tag{A.6}$$

The drag coefficient C_D takes into account that particles are not perfect spheres, but mainly the grain Reynolds number (Bosboom and Stive, 2015). For laminar or Stokes-range ($Re < 0.1 - 0.5$) C_D can be approached by $\frac{24}{Re}$, for turbulent flow ($400 < Re < 2.10^5$) the drag coefficient becomes constant ≈ 0.5 (van Ieperen, 1987). When the drag coefficient is not a function of the grain Reynolds number, the fall velocity becomes a function of the grain diameter and shape only. In the example of sand, the fall velocity can be dependent to D^2 and $\sqrt{D}$ whereas small particles like silt are depended on D^2 only (Bosboom and Stive, 2015). In reality the water column can be quite busy with particles as we saw with the suspended sediment section. Settling can therefor be hindered by the presence of other particles, the effective fall velocity is therefor introduced:

$$w_e = (1 - C)^{\alpha} w_s \tag{A.7}$$

Because the Eastern Scheldt is a tide dominated system, see section 2.1, the transport will be tide generated. The latter one dominates in the inlet and channels and tends to occur in depths higher than the wave-breaking zone (Kana et al., 1999). The wave generated transport will mostly play a role on the shallow parts of the basin, the intertidal areas. The tide dominated transport is the building force of the intertidal area and the wave dominated transport is the erosive force that brings sediment from the intertidal area towards the channels.

B

Additional results

This appendix serves as additional information to Chapter 4, 5 and 6

B.1. Larger visualisation of plots indicating direction change

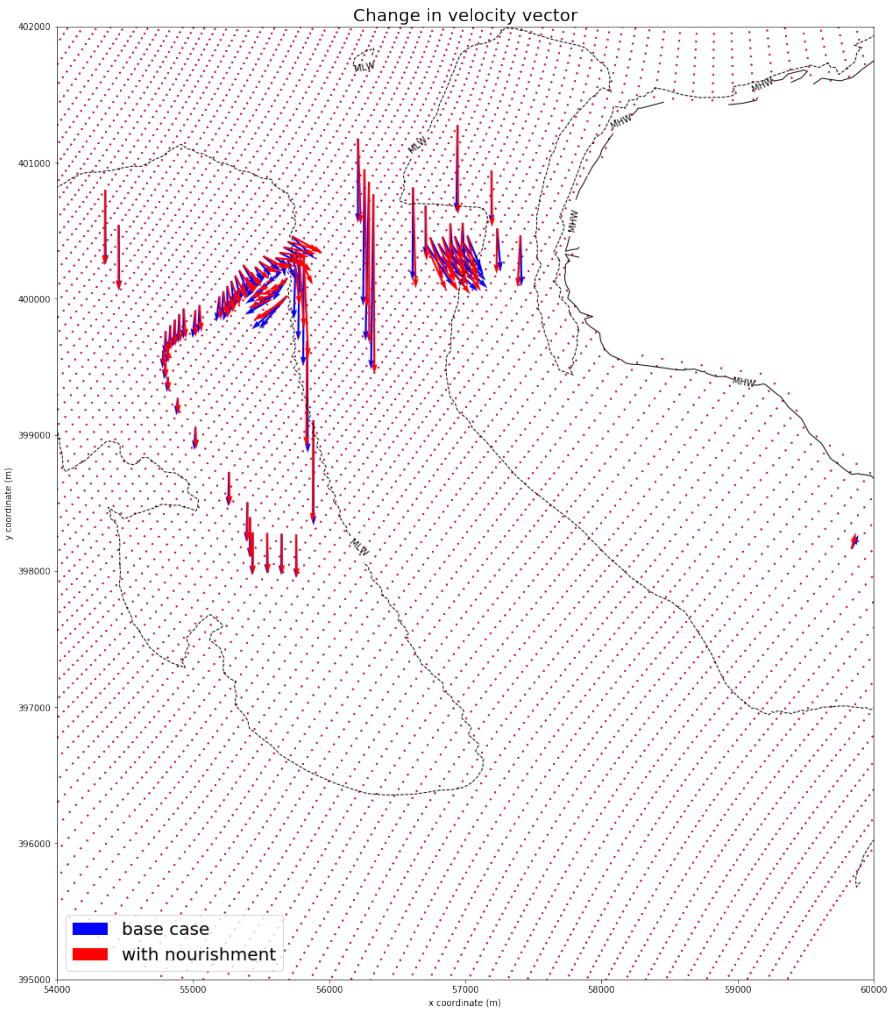

Figure B.1: The change in flow direction as a result of case 1 nourishment in the Brabantsche Vaarwater. The change in direction is computed following the same method as described in section 4.2.

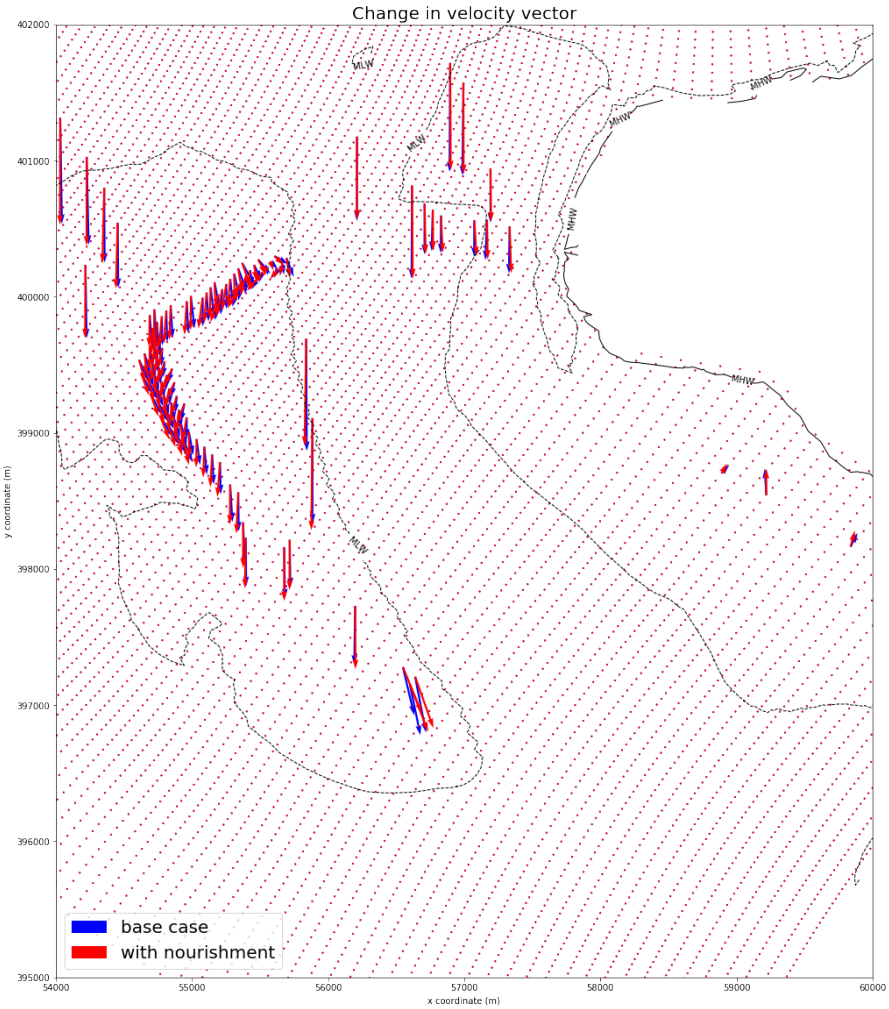

Figure B.2: The change in flow direction as a result of case 2 nourishment in the Brabantsche Vaarwater. The change in direction is computed following the same method as described in section 4.2.

B.2. Effect of a channel nourishment on the discharge

B.2.1. The Krabbenkreek

A channel nourishment can influence the discharge flowing through the channel. The objective of nourishing the Krabbenkreek channel is to locally increase the velocities. Following the law of continuity, if the cross-sectional area is reduced, and the same discharge has to flow through, the velocities will increase. This is only valid if the discharge does not decrease significantly. In Figure B.3, the instantaneous discharge is plotted for the considered nourishments. It can be observed that for all 4 nourishments the discharge decreases, although for case 1,2 and 3 the differences are in the order of 1-2 % while for case 4 the differences are in the order of 7-8 %. Case 4, required 2 times more sediment than the other 3 cases. This indicates that there is a relation between the nourished volume and the discharge in the channel. Considering the velocities in the Krabbenkreek channel as a result of the nourishment increased by 0.1-0.2 m/s, the reduction in discharge can be neglected.

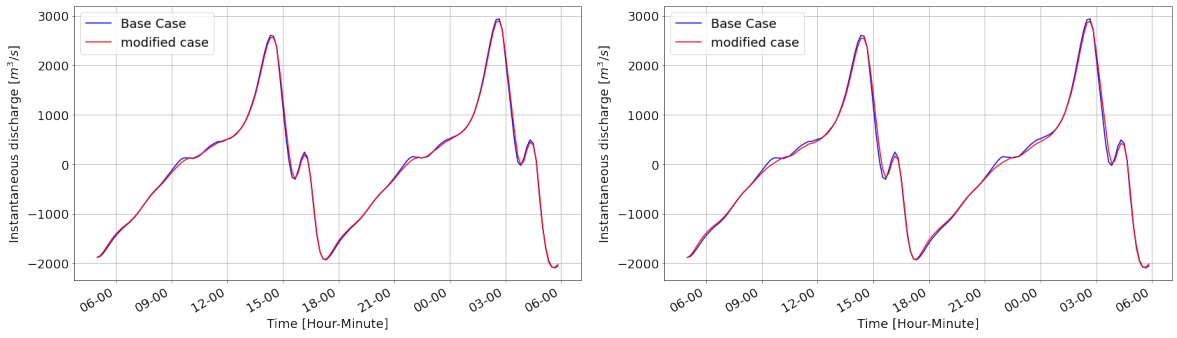

(a) base case compared to case 1

(b) base case compared to case 2

(c) base case compared to case 3

(d) base case compared to case 4

Figure B.3: Instantaneous discharge at the entrance of the Krabbenkreek channel for the base case in blue, compared to the four nourishment cases in red.

B.2.2. The Brabantsche Vaarwater

As with the Krabbenkreek, reducing the cross sectional area of the channel exerts additional friction on the flow. This might cause part of the discharge to be deflected towards another channel with less friction. The base case discharge is plotted in blue in Figure B.4, the discharge when nourished is plotted in red. Firstly, it can be observed that the discharge is significantly larger compared to the Krabbenkreek, 8000 m^3/s compared to 2500 m^3/s. The effect of the first nourishment can hardly be observed and is estimated to be smaller than 1%. The second nourishment causes a reduction in discharge of 3%. Considering these results, the effect on the discharge can be neglected.

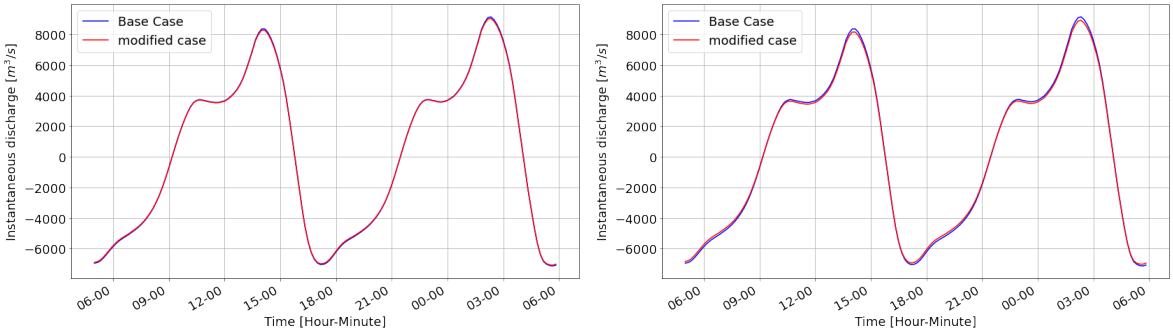

(a) base case compared to nourishing first bend

(b) base case compared to nourishing second bend

Figure B.4: Instantaneous discharge at the entrance of the Brabantsche Vaarwater channel for the base case in blue, compared to the 2 nourishment cases in red.